Spring 1999

Cracking in cycloaliphatic epoxy/aluminum composite electrical bushings

Keith Alan Parker
Louisiana Tech University

INFORMATION TO USERS

This manuscript has been reproduced from the microfilm master. UMI films the text directly from the original or copy submitted. Thus, some thesis and dissertation copies are in typewriter face, while others may be from any type of computer printer.

The quality of this reproduction is dependent upon the quality of the copy submitted. Broken or indistinct print, colored or poor quality illustrations and photographs, print bleedthrough, substandard margins, and improper alignment can adversely affect reproduction.

In the unlikely event that the author did not send UMI a complete manuscript and there are missing pages, these will be noted. Also, if unauthorized copyright material had to be removed, a note will indicate the deletion.

Oversize materials (e.g., maps, drawings, charts) are reproduced by sectioning the original, beginning at the upper left-hand corner and continuing from left to right in equal sections with small overlaps. Each original is also photographed in one exposure and is included in reduced form at the back of the book.

Photographs included in the original manuscript have been reproduced xerographically in this copy. Higher quality 6" x 9" black and white photographic prints are available for any photographs or illustrations appearing in this copy for an additional charge. Contact UMI directly to order.

UMI

A Bell & Howell Information Company
300 North Zeeb Road, Ann Arbor MI 48106-1346 USA
313/761-4700 800/521-0600

CRACKING IN CYCLOALIPHATIC EPOXY / ALUMINUM COMPOSITE ELECTRICAL BUSHINGS

by

Keith Alan Parker, B.S., M.S., M.S.

A Dissertation Presented in Partial Fulfillment
of the Requirements for the Degree
Doctor of Engineering

COLLEGE OF ENGINEERING AND SCIENCE
LOUISIANA TECH UNIVERSITY

May 1999

LOUISIANA TECH UNIVERSITY

THE GRADUATE SCHOOL

5/10/99
Date

We hereby recommend that the thesis prepared under our supervision by

Keith Alan Parker entitled Cracking in Cycloaliphatic Epoxy/Aluminum Composite Electrical Bushings

be accepted in partial fulfillment of the requirements for the Degree of Doctorate of Engineering

Marion E Council (Marion Earl Council)
Supervisor of Thesis Research

Head of Department
Electrical Engineering
Department

Recommendation concurred in:

Louis Roemer
Dr. Louis Roemer

James O. Lowther
Dr. Jim Lowther

Dr. David Hall

Advisory Committee

Approved:
Dick Greechie /VDN
Director of Graduate Studies

Approved:
Terry M McDonnell
Director of the Graduate School

Leslie K Guice
Dean of the College

GS Form 13
2/97

ABSTRACT

The problem of cracking in electrical apparatus bushings as a result of thermal stresses was investigated. The bushings were composed of cycloaliphatic epoxy insulators with embedded aluminum conductors. The problem is due to the difference in coefficients of thermal expansion of the two materials. A solution to the problem had been to coat the conductors before they were formed together with the epoxy insulators. The coating was assumed to prevent cracking by allowing movement between the two materials as their dimensions changed during thermal expansion and contraction. The contribution of the coating was to be established.

The hypothesis was that the coating, above a given thickness, would prevent cracking and would fail to prevent cracking below that thickness. Inherent in this hypothesis was that the thickness of the coating was a controlling factor in its ability to prevent cracking during thermal changes.

A method of applying a controlled coating in an economically feasible manner was developed. Coatings of various thickness were then applied to a set of conductors. Those coated conductors along with non-coated conductors were then formed into bushings. The bushings were cycled from 250°F (121.1°C) to -300°F (-184.4°C) in cycles which began at -50°F (-45.6°C) and reduced -50°F (-45.6°C) until -300°F (-184.4°C) was reached.

The bushings with non-coated conductors exhibited a 50% failure rate. Those with coatings of any thickness failed to crack. A theoretical analysis of the bushings under thermal conditions indicated that the coatings prevented cracking by allowing relative movement between the conductor and insulator. It was concluded that the contribution of the conductor coating was not relative to its thickness but was due to its ability to separate the insulator from the conductor.

TABLE OF CONTENTS

LIST OF TABLES

Table

Table

LIST OF FIGURES

Figure

Figure

Figure

ACKNOWLEDGEMENTS

Many people contributed to the success of this research and development effort. Mr. Ken Elliott, III and the employees of Elliott Industries provided the facilities and cooperation needed to run the thermal cycle tests. Dr. M. E. Council provided guidance and leadership as committee chairman. Dr. Louis Roemer, Dr. Jim Lowther, and Dr. David Hall provided assistance as committee members. Jimmy Cook consulted on the development of the coating sleeves and performed the precision machining of the sleeves.

CHAPTER 1

INTRODUCTION

In 1980, EMC was formed with the purpose of producing high quality electrical components [7,10,11]. Among other components, EMC produced "air terminated" electrical bushings.

One of their components, a 600 Amp bushing, while appearing to provide good field service had a number of cracked bushings reported. This bushing consisted of a 1.25 inches (31.75 mm) diameter aluminum conductor embedded in an insulating material of cycloaliphatic epoxy. Investigation of each report led EMC to believe that the failures were due to excessive cantilever loading, impact, or improper removal from the mold during manufacture.

In late 1983, EMC began molding special 600 and 1250 Amp bushings which contained 1.25 inches (31.75 mm) diameter copper conductors in place of the usual 1.25 inches (31.75 mm) diameter aluminum conductors. After one and a half years, a customer reported a bushing failure as a result of cracking. Again, investigation led EMC to believe the crack was due to impact or excessive cantilever loading. After additional failures were reported from the same location, further investigation showed the bushings to be serving a highly cyclic load. The highly cyclic loading suggested that thermal fatigue could be the cause of the cracks [7].

A paper published in IEEE Transactions entitled "Thermal Fatigue Strength of Epoxy Supporting Insulators with Embedded Electrodes" pointed out that copper and aluminum cast in epoxy have an inherent mismatch of thermal expansion coefficients which cause thermal stresses in the epoxy when the temperature fluctuates [17]. EMC had already taken steps to compensate for the thermal expansion mismatch of aluminum and epoxy by coating the aluminum conductors with a material called Flexcoat-I. This same coating was then used on the copper conductors. Because of the greater mismatch in thermal expansion between copper and epoxy as compared to aluminum and epoxy, it was suggested that Flexcoat-I was not a sufficient coating for the copper conductors. A method was needed to test the bushings to determine their reaction to thermal cycling [7].

Cryogenic Tests

The paper, entitled "Thermal Fatigue Strength of Epoxy Supporting Insulators with Embedded Electrodes", suggested using cryogenic temperatures as a possible proof test [17]. The low temperature would produce maximum thermal stresses and accelerate any failure. EMC began the test by placing bushings in an insulated container filled with methanol and lowering the temperature of the bath to -100°F (-73.3°C) within 60 minutes. The test bushings cracked in the same manner as the field failures [7].

Flexcoat-I was replaced by a new coating called Flexcoat-II. While Flexcoat-II showed improvement over Flexcoat-I, it also proved to be inadequate. A final coating, called Flexcoat-S, was developed. Seven bushings were cycled from 80°F (26.7°C) to -100°F (-73.3°C) for two cycles. Subsequent mechanical and electrical tests performed

on those bushings found no problems. At this point, all the original bushings were replaced with bushings formed using Flexcoat-S, and the failures were eliminated.

As failures had been found in the bushings with copper conductors, EMC was no longer certain that the bushings with aluminum conductors would not eventually crack. These bushings had Flexcoat-I coatings. A Blue-M "Stabil Therm" liquid nitrogen thermal shock chamber was purchased [15]. It had a temperature range of 600°F (315.6°C) to -300°F (-184.4°C). Thermal shock tests were then run on a variety of EMC products using various conductor coatings.

The EMC 1201-625B2, 600 Amp, 35 kV bushing [8], which is a focus of this dissertation work, showed failures in the range of -100°F (-73.3°C) to -150°F (-101.1°C) in bushings with Flexcoat-I coated conductors. Bushings with Flexcoat-II had failures from -150°F (-101.1°C) to -300°F (-184.4°C). Bushings with Flexcoat-S were cycled to -300°F (-101.1°C) with no failures.

Although Flexcoat-S seemingly solved the cracking problem, questions about the coating and its contribution remained. The coating was applied to the conductors by hand wiping the coating onto the conductor. This method, while able to ensure complete coating of the conductor, produced a coating which varied greatly in thickness.

Research Objectives

The work of this dissertation was (1) to develop a method of applying the coating with control over thickness and consistency and (2) to determine the contribution of coating thickness when applied within a controlled range. In terms of the contribution of coating thickness, EMC hypothesized that within the range of coating

thickness to be tested, there would be a thickness below which the coating would fail to prevent cracking.

In developing a method of applying the coating with control over thickness and consistency, EMC applied certain constraints. First, the coating method had to coat the conductors without changing the existing masking operation. Parts of the conductors were masked to prevent adherence of the coating. Fixtures had been designed to hold both the masking tape and the conductors in such a manner that the masking operation was performed with precision repetitiveness. Second, the coating method had to be developed before any tests were performed to determine coating thickness contribution. In the early stages of this work, it was suggested that the hand coatings could be machined to controlled thickness, and after an optimal thickness was determined, a method of applying that specific coating could be developed. EMC rejected this because the coating thickness may need to be altered for other applications. Third, the coating method, once developed, could be routinely performed by EMC shop personnel.

In the following chapters, the development of the coating operation is described, the physical thermal tests are described, and a theoretical analysis of the bushing under thermal conditions is presented.

Proprietary Concerns

The exact composition of the bushing is proprietary. To analyze the bushing under thermal conditions and respect the proprietary nature of the project, properties of similar materials were used in the analysis. For the three materials which make up the bushings, the material properties used are given in Table 1-1 [3,5,6].

Table 1-1

Selected Material Properties

Property	Material		
	Aluminum	Flexcoat-S	Epoxy
Modulus of Elasticity (MPa)	70	1.0	9.0
Tensile Strength (MPa)	240	19	56
Coefficient of Thermal Expansion (/°C)	0.000023	0.000162	0.000036

CHAPTER 2

COATING APPLICATOR

The design of the coating applicator was a trial and error procedure. Initially, several observations were made. First, it was noted that the object to be coated was a solid cylinder which was symmetrical along its entire length. Next, the coating was very thin when compared to the thickness of the cylinder. Finally, Flexcoat-S, in its pre-applied state, was a viscous, semi-liquid. Upon contact with moist air, it began to solidify reaching a tacky state in approximately one minute.

The objective of designing a coating applicator was to devise a method of applying a smooth, consistent coating of Flexcoat-S with control over thickness and repeatability. A study of applications which performed similar tasks discovered wire coating processes, electroplating operations, extrusion processes, and taping operations [4]. The wire coating process was eliminated because it did not function well with a small number of discrete pieces instead of a continuous feed of wire. The electroplating operation was deemed too expensive and could also have had problems with the fast curing time of the coating. The taping operation was rejected by EMC because of the overlap required for complete coverage.

While the coating of the conductors was not necessarily an extrusion process, its basic operation gave some ideas. In the extrusion process, a workable substance is forced through a set of dies, and the substance takes on the shape imposed by the dies. When tubing is extruded, material is basically forced through a set of concentric rings. This results in a continuous tube which has an inner diameter proportional to the outer diameter of the inner ring and an outer diameter which is proportional to the inner diameter of the outer ring. Once again, a major difference is that the tubing extrusion process works best with a continuous feed of material, and the actual material to be coated came in discrete lengths. Additionally, only small batches of the conductors were coated at any one given time.

Another observation made was that the coating, once applied, modeled that of a thin-walled cylinder covering a solid cylinder. This observation, along with those made of the tube extrusion process, gave rise to the possibility that the coating could be extruded like tubing, allowed to cure, and somehow placed over the conductor. After discussing this possibility with a major manufacturer of extrusion equipment, this avenue, while possible, was deemed cost prohibitive by EMC.

The next try at solving this problem also involved the concentric ring concept. The conductor itself would be the inner ring. A second ring whose inner diameter was slightly larger than that of the conductor outer diameter would be used for the outer ring. The conductor could be given a rough but continuous coating of Flexcoat-S. While the Flexcoat-S was still in a viscous state, the conductor could be forced through the outer ring. The outer ring would remove all excess coating leaving a smooth consistent coat. The coating thickness could be regulated by controlling the inner diameter of the

outer ring. This idea, while showing promise, had a major problem. How do you maintain the relative alignment of the conductor and the outer ring?

Initial Design

The problem was attacked in stages. First, a length of 1.250 inches (31.75 mm) diameter cold roll steel was obtained from the university machine shop. This material was initially used because of its availability and consistency in dimension. Additionally, EMC had a coating thickness gauge which operated on a magnetic principle and was useless on a non-ferrous substrate. An outer ring with an inner diameter of 1.500 inches (38.10 mm) was also machined. The conductor was stood on one end, and the ring was held on the conductor at the top end. Flexcoat-S was injected in the annulus and applied thickly below the outer ring. This process took about 30 seconds. Next the ring was rotated around the conductor several times to ensure a complete coating in the annulus. Finally, the outer ring was forced down the length of the conductor. The process yielded a visibly smooth coating for approximately 3.000 inches (76.2 mm) and then tapered into an inconsistent coat. It should be noted that several unsuccessful attempts were made before a smooth, consistent coating of any length was obtained. This coating was taken to EMC and measured for thickness. Although smooth and consistent in appearance, the coating thickness varied from 17.0 mils (432 microns) to 6.0 mils (152 microns) at a single circumference location. The coating was smooth and consistent but there was no control over thickness. Part of the objective had been accomplished.

Next, a hand-coated aluminum conductor was checked with a set of dial calipers, and the coating thickness (assuming even thickness on both sides of the conductor) was determined to be approximately 6.0 mils (152 microns). As the

conductor was a typical hand coated conductor, it was determined that 6.0 mils (152 microns) would be an upper limit of coating thickness to be tested. From this information, a new outer ring with an inner diameter of 1.252 inches (31.80 mm) was made. Seemingly, this outer ring would leave a clearance of 1.0 mil (25 microns) between the conductor and the outer ring. The end of a second steel conductor was smeared with Flexcoat-S and before the material could cure, the new ring was forced over the coated conductor end and down the length of the conductor. The coating which resulted was smooth and consistent. However, it was so thin that it ruptured when touched. Although the clearance between the conductor and the outer ring was very small and the resulting coating was extremely fragile, it was now evident that Flexcoat-S would fill the annulus regardless of the clearance and would leave some thickness of coating. This fact would be important at a later time.

The process to this point had merely taken the existing hand application and smoothed the surface of the coating with the outer ring. No control over thickness was yet in place. However, if a method of controlling the alignment of the outer ring with the conductor could be devised, rings of varying inner diameter could be used to apply coatings of varying thickness.

The first idea came while working with the lathe. A fixture which would hold rings of the same outer diameter could be placed and aligned on the lathe track. That the inner diameter of the rings vary is the thing of importance. Next, lathe points could engage the conductor from both ends with one lathe point being initially positioned through the ring. The conductor could then be hand coated with Flexcoat-S. Once the hand coat had been applied, the lathe points with the conductor fixed between them,

would be moved down the track forcing the conductor through the outer ring and leaving only the thickness desired. The major problem with this idea came from the alignment aspect. As the conductor was 13.250 inches (336.55 mm) in length, the track would have to be at least 26.500 inches (673.10) in length for the conductor to completely run through the sleeve. Alignment for this length of travel would be difficult. Also, any curvature along the length of the conductor would shift the conductor relative to the outer ring. The size and bulk of such a device along with its long term alignment problems doomed the idea.

Alignment Sleeve

A new idea, which led to the final solution, came from the earlier use of the tight fitting ring. In trying to determine the thickness of the thin coat left by the ring, the observation was made that the coating would have to be less than the maximum clearance between the conductor and the outer ring. If the conductor were placed in contact with a side of the ring, the clearance on the opposite side would be the difference in the outer diameter of the conductor and the inner diameter of the outer ring. In this case the clearance would be 0.002 inches (0.05 mm) or 2.0 mils (51 microns).

Actually the clearance would be less than 2.0 mils (51 microns) because a film had been left completely around the conductor which meant that the conductor had never been completely in contact with the outer ring.

A new concept was examined. A second ring could be machined to lock into near perfect alignment with the tight fitting ring. This second ring could be machined to have inner diameters larger than the tight fitting ring. The tight fitting ring could be

used as an alignment tool while the second ring would control the coating thickness. The alignment ring would have to lead in order for the ring combination to work. Otherwise, the alignment sleeve would wipe off the coating left by the other ring. Additionally, the second ring would have to have a reservoir of sufficient capacity to coat the conductor, and the reservoir would have to be between the two rings. A second ring was machined, and the tight fitting ring was adapted such that the two rings locked together. The ring combination was placed on a steel conductor, the reservoir was filled, and the ring combination forced down the length of the conductor. What was left was a smooth, consistent coating which varied between 1.5 mils (38 microns) and 3.0 mils (76 microns). Although the ring copmbination appeared to be a solution to the problem of applying acceptable coatings, a new problem arose.

The design of the bushing as a whole required that certain areas of the conductor not be coated. To facilitate this, EMC had designed fixtures that placed masking tape in the areas not to be coated. The masking tape was approximately 3.0 mils (76 microns) in thickness, and when overlapped, produced a hump of 6.0 mils (152 microns) on the conductor. The ring combination would not work with this type of masking operation. Suggestions that the conductors could be coated first and then have the coating removed from certain areas were unacceptable to EMC.

Because of the initial success with the two-ring method, it was not immediately abandoned. Two things had to be considered. First, EMC wanted to keep their masking tape operation intact. Second, the two-ring system worked only if the alignment ring was able to minimize the lateral movement of the coating ring. Close examination showed that by increasing the length of the alignment ring, its inner diameter could be

increased while still maintaining the same alignment capability. This, however, had limitations also. Finally, it was concluded that if a very thin (thickness) tape could be found which could be substituted for the present masking tape and the length and inner diameter of the alignment ring were increased, the combined effect would produce a coating process of acceptable nature.

A tape was found which came in the proper width and was readily available. It was a 3M 3690 which had a thickness of 1.3 mils (33 microns). The length of the alignment ring was increased from 0.500 inches (12.70 mm) to 1.000 inch (25.40 mm), and its inner diameter increased from 1.252 inches (31.80 mm) to 1.256 inches (31.90 mm). Because of the new dimension ratio, the alignment ring was then referred to as the alignment sleeve At this point, a steel conductor was taped with the new tape, Flexcoat-S was applied to the conductor and the alignment sleeve was tested by itself. The resulting coating ranged from 0.5 mils (13 microns) to 2.0 mils (51 microns). As plus or minus 2.0 mils (51 microns) was in the range acceptable to EMC, the method was approved, and the conversion to coating aluminum conductors was begun.

Conversion to Aluminum Conductors

The aluminum conductors presented additional problems. First, the steel conductor was actually 1.248 inches (31.70 mm) in diameter, and the aluminum conductor was actually 1.252 inches (31.80 mm) in diameter. The alignment sleeve would not clear the masked areas of the aluminum conductor. The inner diameter of the alignment sleeve had to be bored to 1.260 inches (32.00 mm) to accommodate the larger diameter of the aluminum conductor. Next, a check was made of the diameter at various lengths along three aluminum conductors. The diameter varied from 1.252 inches

(31.80 mm) to 1.250 inches (31.75 mm). Variation in the diameter of the conductor would cause variation in the final coating thickness. The three aluminum conductors were masked in the appropriate areas with the new masking tape. All three were then coated using only the alignment sleeve. By visual inspection, the coatings were all smooth and consistent (figure 2-1). The three coated conductors were then taken to EMC for inspection. The thickness gauge utilized by EMC could not test the thickness of the coatings on the aluminum conductors. EMC arranged for the use of an Elcometer 300 coating thickness tester. The three aluminum conductors coated with the alignment sleeve (designated A, B, C) and a typical hand-coated conductor (designated E) were all tested at 36 points each (figure 2-2). The results obtained are given in tables 2-1, 2-2, 2-3, and 2-4.

Final Solution

At this stage, plans were drawn for six coating sleeves which would lock onto the alignment sleeve (figures 2-3, 2-4, 2-5). Additionally, EMC purchased an Elcometer 345 which would test coating thickness on either ferrous or non-ferrous substrates. The new sleeves were made and the process of coating the test conductors was begun.

The alignment sleeve had an inner diameter of 1.260 inches (32.00 mm) and would hence be referred to as sleeve 1.260. The new coating sleeves had inner diameters of 1.262 inches (32.05 mm), 1.264 inches (32.10 mm), 1.266 inches (32.16 mm), 1.268 inches (32.20 mm), 1.270 inches (32.26 mm), and 1.272 inches (32.31 mm). Each of these sleeves would also be referred to by their diameter.

The original bushing tests called for 24 bushings: 3 with non-coated conductors, 3 with conductors coated using only the alignment sleeve, and 3 each with conductor

coated by each of the coating sleeves. After sleeve 1.268, the design of the reservoir was not large enough to completely coat the conductors. However, after examining the coatings of the successful sleeves and comparing them to the hand coatings, EMC determined that it would not be necessary to use the largest sleeves. Each of the coatings were tested for thickness at 36 points. The overall coating thickness of each conductor is given in table 2-5. A more detailed analysis of the coating data can be found in Appendix A.

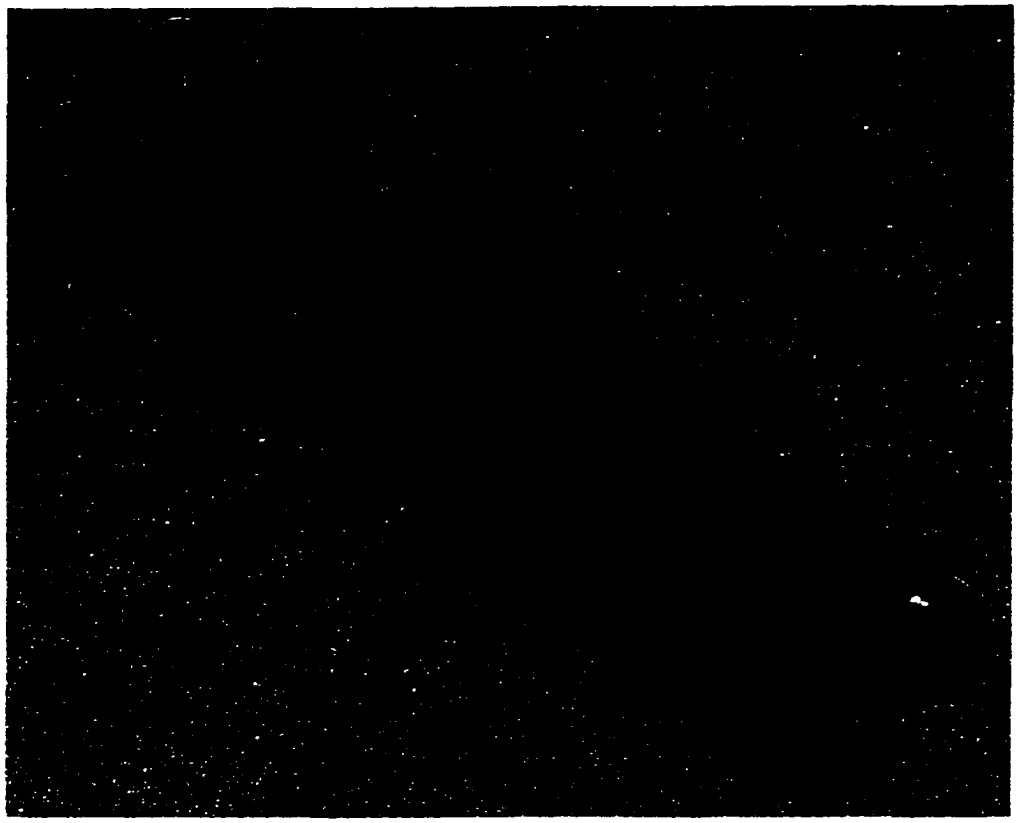

Figure 2-1. Sleeve Coated Conductor versus Hand Coated Conductor

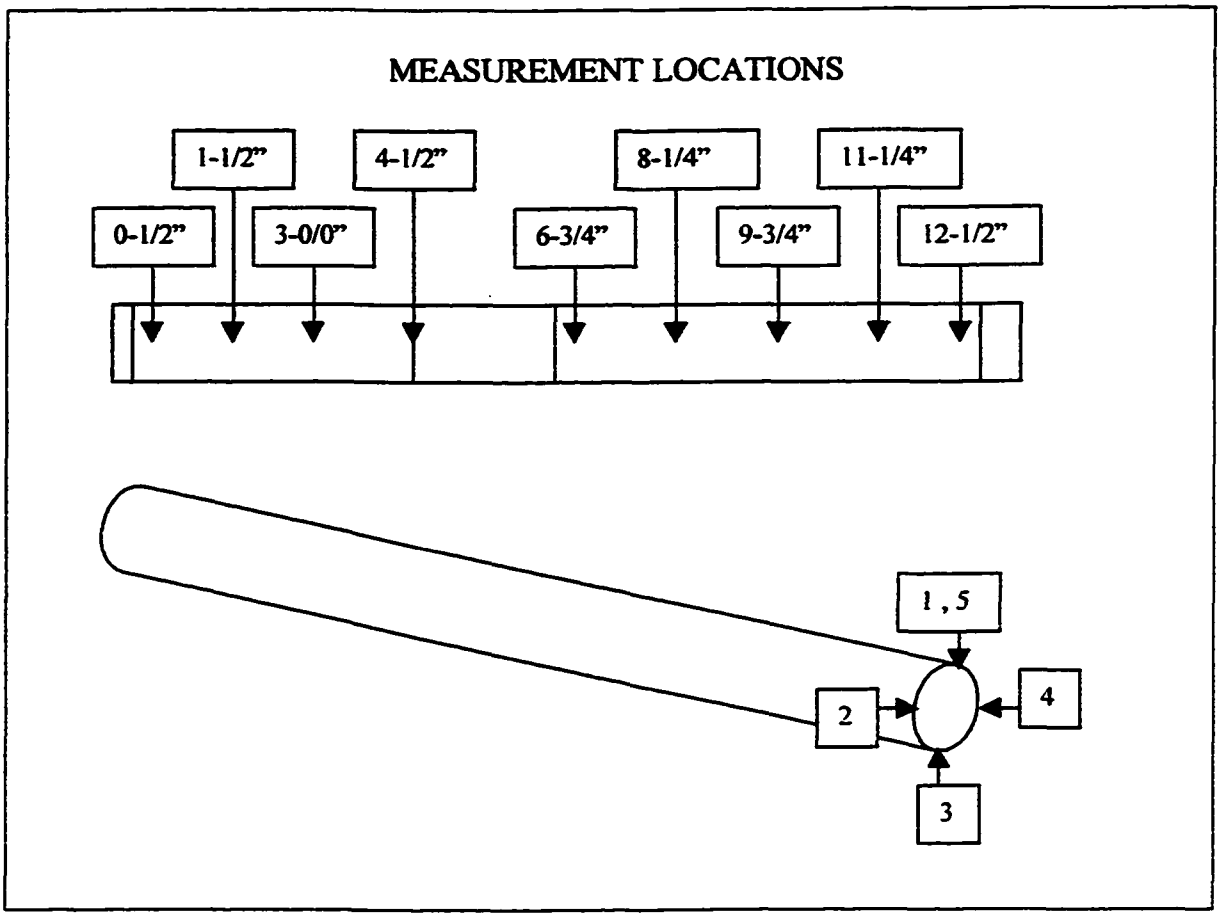

Figure 2-2. Locations for Coating Thickness Measurements

Table 2-1

Conductor E

Degrees	0	90	180	270	0
Location					
12-1/2	2.3	2.2	2.2	1.8	2.3
	57	55	56	45	57
11-1/4	4.2	4.7	4.2	2.8	4.2
	106	119	105	71	106
09-3/4	4.1	4.7	4.0	3.0	4.1
	103	119	101	76	103
08-1/4	4.1	10.6	6.2	4.4	4.1
	105	269	157	110	105
06-3/4	5.7	4.3	5.1	3.9	5.7
	144	109	130	98	144
04-1/2	6.9	2.6	3.8	4.1	6.9
	175	67	96	105	175
03-0/0	3.9	3.0	4.5	3.8	3.9
	99	75	114	96	99
01-1/2	2.3	4.5	5.0	4.3	2.3
	59	115	126	108	59
00-1/2	1.9	3.6	3.4	1.8	1.9
	49	91	86	44	49

Coating Thickness plus Plating Thickness (mils/microns)

Table 2-2

Conductor A

Degrees	0	90	180	270	0
Location					
12-1/2	2.3	2.0	2.1	2.5	2.3
	57	50	52	63	57
11-1/4	2.5	1.4	1.8	2.3	2.5
	63	36	45	59	63
09-3/4	2.0	1.2	2.0	2.1	2.0
	51	31	51	52	51
08-1/4	1.9	1.6	1.9	2.1	1.9
	49	41	48	53	49
06-3/4	2.1	1.7	2.0	2.0	2.1
	53	44	50	51	53
04-1/2	1.6	1.5	1.6	2.0	1.6
	40	38	41	50	40
03-0/0	2.1	1.9	1.9	2.0	2.1
	54	49	49	50	54
01-1/2	2.0	2.0	2.0	2.3	2.0
	51	50	50	59	51
00-1/2	2.4	2.5	2.2	2.1	2.4
	60	65	55	52	60

Coating Thickness plus Plating Thickness (mils/microns)

Table 2-3

Conductor B

Degrees	0	90	180	270	0
Location					
12-1/2	1.8	1.6	2.9	3.0	1.8
	45	40	73	75	45
11-1/4	2.0	2.0	2.7	2.5	2.0
	50	51	69	65	50
09-3/4	2.6	2.1	2.1	2.3	2.6
	65	54	53	59	65
08-1/4	2.5	2.4	2.3	2.2	2.5
	64	60	58	55	64
06-3/4	2.5	3.1	2.5	1.9	2.5
	64	79	63	47	64
04-1/2	1.8	2.0	2.1	2.3	1.8
	44	50	52	57	44
03-0/0	2.5	2.0	1.9	2.4	2.5
	64	50	49	61	64
01-1/2	2.7	2.1	2.0	2.4	2.7
	68	54	52	60	68
00-1/2	2.6	2.3	2.1	3.1	2.6
	67	58	53	79	67

Coating Thickness plus Plating Thickness (mils/microns)

Table 2-4

Conductor C

Degrees	0	90	180	270	0
Location					
12-1/2	1.8	1.2	1.8	1.6	1.8
	46	29	46	41	46
11-1/4	2.0	2.0	1.9	2.3	2.0
	52	52	47	57	52
09-3/4	2.5	1.9	2.2	2.3	2.5
	62	48	57	58	62
08-1/4	2.2	1.9	2.3	2.5	2.2
	55	48	57	63	55
06-3/4	2.7	2.2	2.4	2.7	2.7
	68	56	61	70	68
04-1/2	1.9	2.0	2.3	1.8	1.9
	48	52	59	46	48
03-0/0	2.3	2.3	2.5	2.1	2.3
	58	59	64	54	58
01-1/2	2.1	2.4	2.3	2.2	2.1
	54	60	58	57	54
00-1/2	3.0	2.9	3.2	2.7	3.0
	76	74	82	68	76

Coating Thickness plus Plating Thickness (mils/microns)

Figure 2-3. Sleeves in Relative Position on Conductor

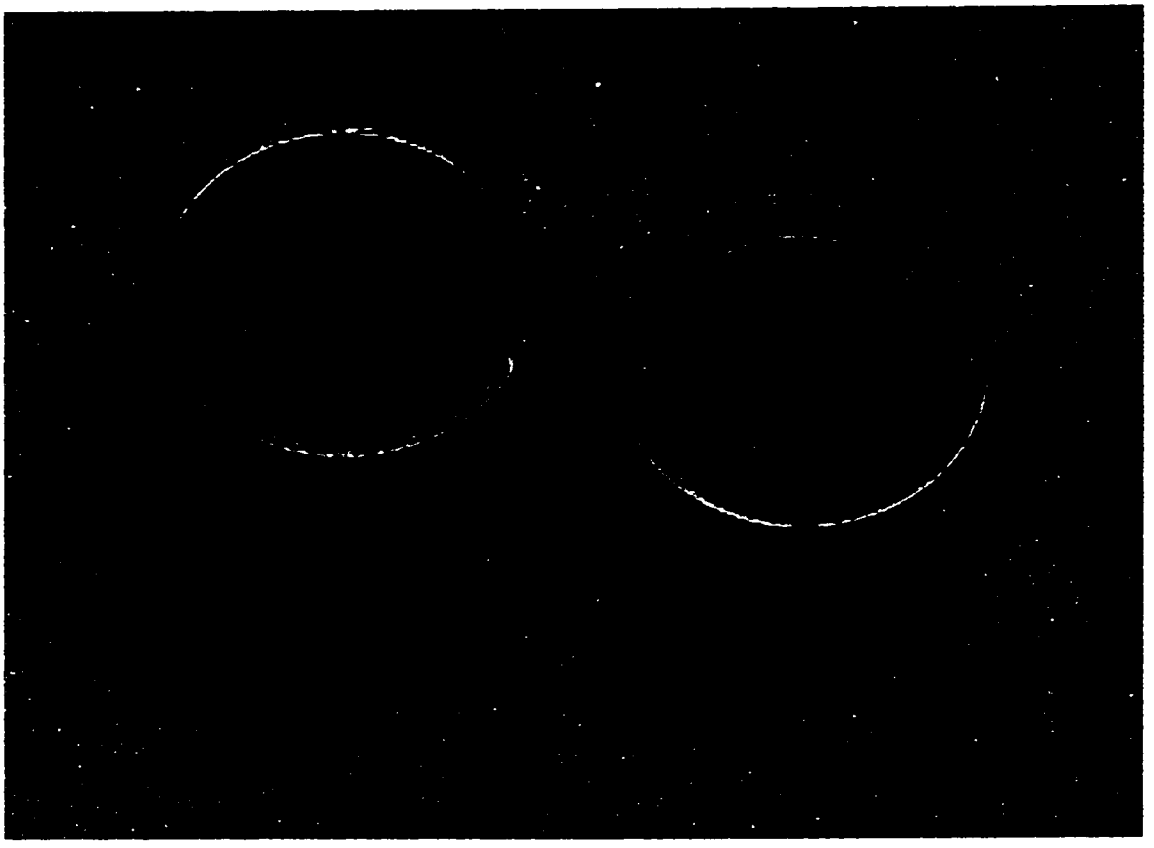

Figure 2-4. Leading Edge View of Coating Sleeves

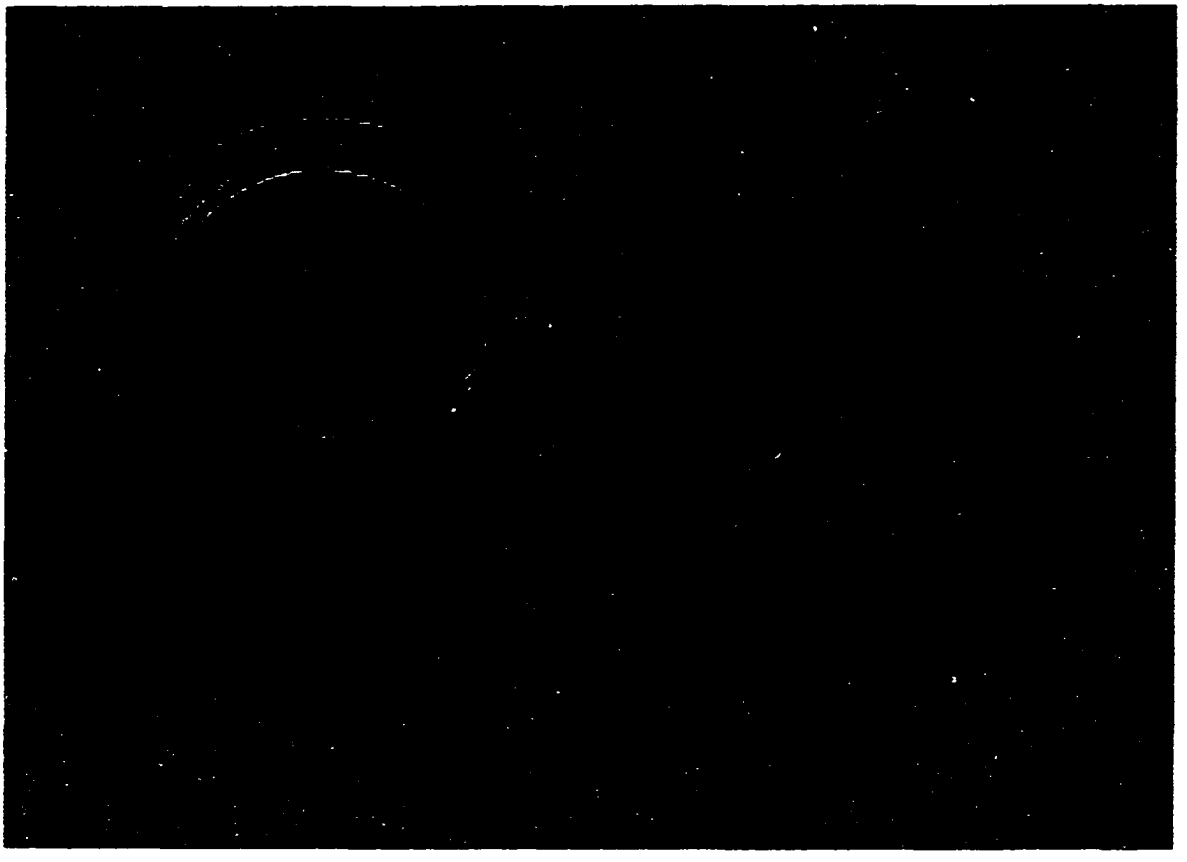

Figure 2-5. Mating End View of Coating Sleeves

Table 2-5

Summary of Conductor Coating Thickness

	Mean (mils / microns)	Standard Deviation (mils / microns)
Conductor		
1.260 (1)	1.7 (42)	0.6 (15)
1.260 (2)	1.9 (47)	0.5 (13)
1.260 (3)	1.7 (42)	0.4 (10)
1.262 (1)	2.0 (50)	0.4 (10)
1.262 (2)	2.1 (54)	0.8 (20)
1.262 (3)	2.2 (56)	0.4 (10)
1.264 (1)	2.5 (63)	0.5 (13)
1.264 (2)	2.5 (65)	0.3 (8)
1.264 (3)	2.6 (65)	0.5 (13)
1.266 (1)	2.9 (75)	0.4 (10)
1.266 (2)	3.1 (80)	0.7 (18)
1.266 (3)	2.8 (71)	0.4 (10)
1.268 (1)	3.0 (77)	0.7 (18)
1.268 (2)	3.2 (82)	0.8 (20)
1.268 (3)	3.3 (84)	0.7 (18)

CHAPTER 3

THERMAL CYCLE TESTS

After the design and the manufacture of the coating sleeves were completed, the research was moved to EMC. The following chapter documents the thermal cycle tests. Exact thermal cycle times and other related information can be found in Appendix B.

Prior to beginning the thermal cycle tests, eighteen 1201-625B2 bushings were formed. Three bushings were formed with conductors which had no coating. These bushings were designated NC (1), (2), and (3). Three bushings each were formed with conductors coated by sleeves 1.260, 1.262, 1.264, 1.266, and 1.268. They were designated 1.260 (1), (2), (3); 1.262 (1), (2), (3); 1.264 (1), (2), (3); 1.266 (1), (2), (3); and 1.268 (1), (2), (3). Information on the coatings themselves can be found in Chapter 2 and Appendix A.

Initial Tests

The 18 bushings were loaded into the Blue-M "Stabil Therm" liquid nitrogen thermal shock chamber [15]. The chamber was heated to 250°F (121.1°C) and allowed to sit at this temperature for one hour (the heat source was an electric coil). Next, liquid nitrogen supplied from an L3 bottle was used to drop the chamber temperature to –50°F (-45.6°C). The chamber sat at this temperature for one hour. Next, the chamber was heated to 250°F (121.1°C) and allowed to sit for another hour. The bushings were then

inspected. Although discoloration was found on all bushings, no cracks were found. Next, the chamber was cooled to –100°F (-73.3°C), allowed to sit for one hour, heated to 250°F (121.1°C), allowed to sit for one hour, and then the bushings were inspected. No cracks were found. EMC was informed that there were no failures during the first two cycles. Previous research indicated that there should have been some cracking of the bushings without coated conductors during those cycles.

The chamber was again heated to 250°F (121.1°C), lowered to –150°F (-101.1°C), and held for one hour. The heat cycle was then engaged, and the chamber was held at 250°F (121.1°C) for an hour. The bushings were then inspected. No cracks were found.

As no cracked parts were found, the thermal tests were not verifying previous test results. Questions arose as to the mass of material being loaded into the chamber. All parties involved agreed to repeat the –100°F (-73.3°C) cycle with only one bushing of each coating level (6 bushings total) to reduce the total mass in the chamber. All but six bushings were removed from the chamber.

Reduced Mass Tests

The chamber with the six bushings [NC (3), 1.260(1), 1.262(1), 1.264(1), 1.266(3), 1.268(1)] was heated to 250°F (121.1°C), left for an hour, cooled to –100°F (-73.3°C), left for an hour, heated to 250°F (121.1°C), and left for an hour. The bushings were inspected. No cracks were found. The chamber was then cooled to –150°F (-101.1°C), left for one hour, heated to 250°F (121.1°C), and left for one hour. Again, the bushings were inspected. No cracks were found.

The chamber was dropped to –200°F (-128.9°C), left for one hour, heated to 250°F (121.1°C), and left for one hour. The bushings were then inspected. No cracks were found. The chamber was cooled to -250°F (-156.7°C), held for one hour, heated to 250°F (121.1°C), and held for one hour. The bushings were then inspected. No cracks were found.

The chamber was brought up to 250°F (121.1°C), held for one hour and dropped to –300°F (-184.4°C). The chamber was then heated to 250°F (121.1°C) and held for one hour. When the bushings were inspected, no cracks were found.

Additional Testing of Bushings with Non-Coated Conductors

After the –300°F (184.4°C) cycle failed to result in the cracking of any of the bushings, it was discussed that the tests were not verifying previous tests. Further research disclosed that during earlier tests, not all 1201-625B2's had failed, and it was possible that the one 1201-625B2 (NC3) in these tests was not a sufficient sample. Additionally, it was discussed that there had been more problems with cracking in the 1203-1225B2's (silver-plated copper conductors) than with the 1201-625B2's (tin-plated aluminum conductors). Also, there was a material change in the composition of the epoxy mixture since the earlier tests had been performed. It was possible that this change had a significant affect on the epoxy mixture strength. After some discussion, it was decided to run tests on 6 non-coated 1201-625B2's and 2 non-coated 1203-1225B2's to determine if bushings with non-coated conductors would indeed crack in the chamber environment.

Four new 1201-625B2's with no conductor coatings and two 1203-1225B2's with no conductor coatings were also formed. The new 1201-625B2's were designated

NC (4), NC (5), NC (6), and NC (7). The two 1203-1225B2's were designated NCC (1) and NCC (2) [8]. Bushings NC (1) and NC (2) were added to those newly formed. The observation was made that bushings NC (1) and NC (2) had been cycled through the –150°F (-101.1°C) cycle when the original 18 bushings were run through the –150°F (-101.1°C) cycle and could show results related to previous thermal history. NC (3) was omitted from these tests because it was run through the entire thermal cycle with the six bushings in the previous tests.

Tests were begun on the eight bushings with no conductor coatings. NCC (1) (1203-1225B2) cracked during the –100°F (-73.3°C) cycle. The crack extended the circumference of the bushing beginning in valley #1 (behind flange) and propagated into valley #2. This crack was approximately at a 45 degree angle to its longitudinal axis. From valley #2, the crack extends the remaining length of the bushing in a line approximately parallel to the conductor. It terminates at the rear (opposite to the interface end). There was no crack in the interface. NCC (1) was removed after the –100°F (-73.3°C) cycle.

Tests were run on the 7 remaining bushings. The chamber was cooled to -150°F (-101.1°C), left for one hour, heated to 250°F (121.1°C), and left for one hour. The bushings were then inspected. No cracks were found. The chamber was cooled to –200°F (-128.9°C), held for one hour, heated to 250°F (121.1°C), and held for one hour. No cracks were found.

The chamber was heated to 250°F (121.1°C), held for one hour, cooled to –250°F (-156.7°C), held for one hour, heated to 250°F (121.1°C), and held for one hour. The bushings were then inspected. Two bushings, NC (2) and NC (7) cracked during the

–250°F (-156.7°C) cycle. Both cracked in the ANSI interface [13]. NC (2) cracked in the interface at a 45 degree angle, then propagated under the flange parallel to the conductor and continued, parallel to the conductor, the entire length of the bushing (figures 3-1, 3-2). NC (7) cracked the entire length of the bushing except for the flange. The crack propagated under the flange and ran parallel to the conductor the entire length (figures 3-3, 3-4). These bushings were then removed from the chamber. The chamber was then cooled to –300°F (-184.4°C), held for one hour, heated to 250°F (121.1°C), and held for one hour. The bushings were then inspected. A single bushing (NC5) cracked during the –300°F (-184.4°C) cycle (figures 3-5, 3-6). NC (5) cracked in an identical manner to NC (7).

These tests confirmed that some of the bushings with non-coated conductors do indeed crack. The failure rate for both the 1201-625B2's and the 1203-1225B2's was 50%. These results were discussed with EMC. It was decided to load the remainder of the original 1201-625B2's back into the chamber and complete the thermal cycle tests [(-200°F (-128.9°C), -250°F (-156.7°C), -300°F (-184.4°C)]. The bushings which passed the –300°F (-184.4°C) cycle were to be cycled to –300°F (-184.4°C) a total of 3 times. No further tests would be necessary after that point.

Final Tests of Bushings with Coated Conductors

The chamber was loaded with bushings 1.260 (2), (3); 1.262 (2), (3); 1.264 (2), (3); 1.266 (1), (2); and 1.268 (2), (3). All had been previously cycled through the -150°F (-101.1°C) cycle.

The chamber was heated to 250°F (121.1°C), held for one hour, cooled to –200°F (-128.9°C), held for one hour, heated to 250°F (121.1°C), and held for one hour.

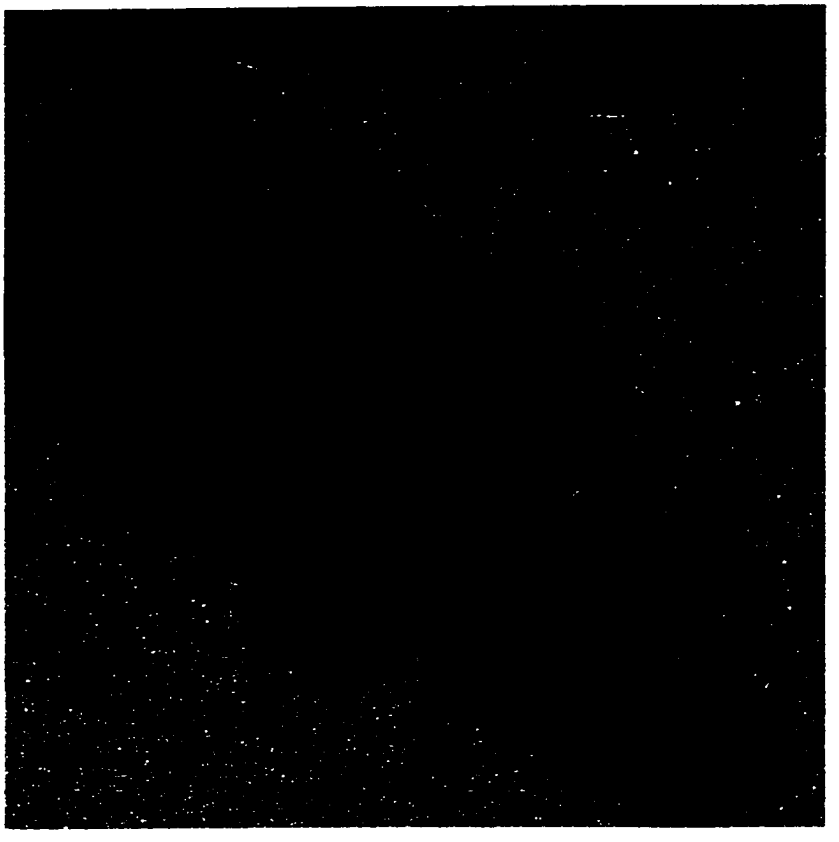

Figure 3-1. Bushing NC (2)

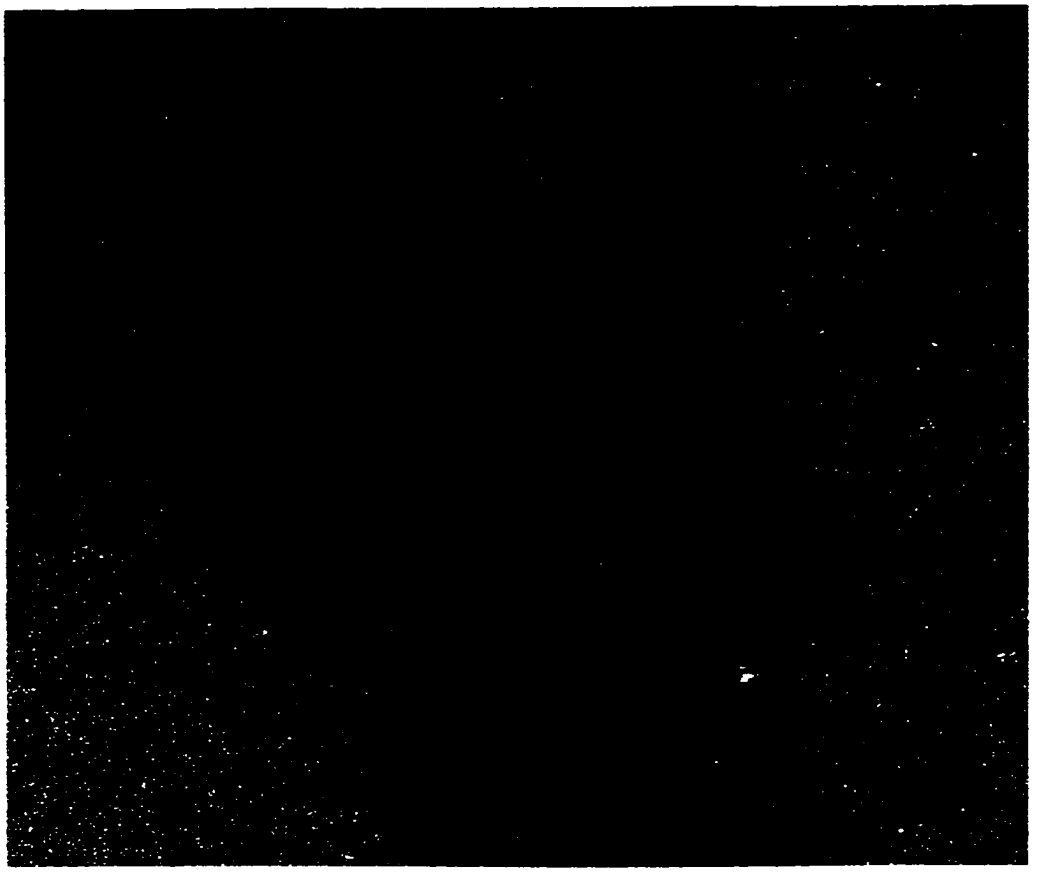

Figure 3-2. Bushing NC (2) End View

Figure 3-3. Bushing NC (7)

Figure 3-4. Bushing NC (7) End View

Figure 3-5. Bushing NC (5)

Figure 3-6. Bushing NC (5) End View

No cracks were found. The chamber was cooled to –250°F (-156.7°C), held for one hour, heated to 250°F (121.1°C), and held for one hour. The bushings were then inspected. No cracks were found. Finally, the chamber was cooled to –300°F (-184.4°C), held for one hour, heated to 250°F (121.1°C), and held for one hour. The bushings were then inspected. No cracks were found. All 10 bushings had passed the –300°F (-184.4°C) cycle.

As no cracking had occurred in any of the bushings being presently tested, it was decided to remove those with the thickest coatings and replace them for the final -300°F (-184.4°C) tests. The new batch consisted of bushings 1.260 (1), (2), (3); 1.262 (1), (2), (3); 1.264 (2), (3); and 1.266 (1), (2). The chamber was heated to 250°F (121.1°C), held for one hour, cooled to –300°F (-184.4°C), held for one hour, heated to 250°F (121.1°C), and held for one hour. The bushings were then inspected. No cracks were found. This thermal cycle constituted the second –300°F (-184.4°C) cycle.

The chamber was heated to 250°F (121.1°C), held for one hour, cooled to –300°F (-184.4°C), held for one hour, heated to 250°F (121.1°C), and held for one hour. The bushings were then inspected. No cracks were found. This thermal cycle constituted the third and final –300°F (-184.4°C) cycle.

Table 3-1 summarizes the results of the thermal cycle tests. More detailed information can be found in Appendix B.

Table 3-1

Summary of Thermal Cycle Tests

Temperature (°F/°C)	-50 -45.6	-100 -73.3	-150 -101.1	-200 -128.9	-250 -156.7	-300 -184.4	-300 -184.4	-300 -184.4
Bushing								
1.260 (1)	P	P*	P*	P	P	P	P	P
(2)	P	P	P	P	P	P	P	P
(3)	P	P	P	P	P	P	P	P
1.262 (1)	P	P*	P*	P	P	P	P	P
(2)	P	P	P	P	P	P	P	P
(3)	P	P	P	P	P	P	P	P
1.264 (1)	P	P*	P*	P	P	P	P	P
(2)	P	P	P	P	P	P	P	P
(3)	P	P	P	P	P	P	X	X
1.266 (1)	P	P	P	P	P	P	P	P
(2)	P	P	P	P	P	P	P	P
(3)	P	P*	P*	P	P	P	X	X
1.268 (1)	P	P*	P*	P	P	P	X	X
(2)	P	P	P	P	P	P	X	X
(3)	P	P	P	P	P	P	X	X
NC (1)	P*	P*	P*	P	P	P	X	X
(2)	P*	P*	P*	P	C			
(3)	P	P*	P*	P	P	P	X	X
(4)	P	P	P	P	P	P	X	X
(5)	P	P	P	P	P	C		
(6)	P	P	P	P	P	P	X	X
(7)	P	P	P	P	C			
NCC (1)	P	C						
(2)	P	P	P	P	P	P	X	X

P - Passed at the given temperature
P* - Passed twice at the given temperature
C - Bushing cracked at the given temperature
X - Was not included in the test at the given temperature
1.26(xxx) - Bushing with coated aluminum conductor
NC (x) - Bushing with non-coated aluminum conductor
NCC (x) - Bushing with non-coated copper conductor

CHAPTER 4

THEORETICAL ANALYSIS

The theoretical analysis examined the bushing without the Flexcoat-S coating and then examined it with the Flexcoat-S coating. As the cracking problem occurred in the ANSI interface region of the bushing, only this region was analyzed.

The region where the cracking began can be described as a solid cylinder of aluminum inside a hollow cylinder of epoxy [2]. When subjected to temperature change, each material attempts to expand or contract according to its own coefficient of expansion [6, 9, 12, 16].

In the first case (no Flexcoat-S coating), the materials are bonded together such that the dimensions of each material must remain the same at their interface. When the temperature is dropped on the bushing, both materials attempt to shrink at their own rate. Because of the mismatch in coefficients of thermal expansion and the fact that the two materials are bonded together, neither material reaches its natural dimension, and thermal stresses are developed in each of them. Because failure occurred in the epoxy portion of the bushing, the stresses developed in the epoxy are those of importance.

Description of Thermal Stresses

Both the aluminum and the epoxy were assumed to be isotropic and homogeneous materials with constant properties throughout the range of temperatures involved in the tests. While this assumption produced errors in the analysis, it provided a method of general analysis to examine the stresses which developed when the bushings were subjected to temperature change. These assumptions were made regarding the epoxy material because of the lack of available data.

The stress analysis was done using two planar cross-sections of the interface region of the bushings. The first section is an end view and was analyzed as an annulus. The second section is a side view and represented a quarter section of the interface.

In both sections, there are assumed to be no external forces. Thus, the only stresses encountered were those produced by thermal changes. For an unconstrained material, the change in dimension as a result of a change in temperature is proportional to its coefficient of thermal expansion and to its original dimension [14]. The relationship is given as:

$$DELTAL = (ALPHA)(DELTAT)(L) \qquad 4\text{-}1$$

where the equation variables are

DELTAL = the change in dimension

ALPHA = the coefficient of thermal expansion

DELTAT = the change in temperature

L = the original dimension.

Where the material is constrained from moving, stresses develop which are proportional to the change in temperature and the modulus of elasticity [12]. This relationship is given as:

$$SIGMA = (ALPHA)(DELTAT)(E) \qquad 4\text{-}2$$

where the equation variables are

SIGMA = stress

ALPHA = the coefficient of thermal expansion

DELTAT = the change in temperature

E = the modulus of elasticity.

For this study, ALPHA for the epoxy material was given as 0.000032 / °C and ALPHA for the aluminum was given as 0.000023 / °C [2]. The modulus of elasticity for aluminum was given as 70.0 GPa [5], and the modulus of elasticity for the epoxy was given as 9.0 GPa [6].

As the epoxy had the higher rate of thermal expansion and the aluminum had a much higher modulus of elasticity, it was assumed that the aluminum would reach its natural reduction in dimension and all stresses developed in the epoxy would be the result of the difference in the coefficients of thermal expansion. The temperature at which the pass/fail criteria was established was –300°F (-184.4°C). Stress analysis was done at this temperature only.

No Coating

In the first case (no Flexcoat-S coating), the materials were bonded together and stresses were developed in the epoxy as the result of the difference in coefficients of

thermal expansion. This difference of coefficients (ALPHAD) was 0.000009 / °C. The stresses developed, given by eq. 4-2 were

SIGMA = (0.000009 / °C)(305.5 °C)(9000 MPa)

SIGMA = 24.7 Mpa.

Analysis of the Annulus

The annulus, which was examined at the interface end was modeled as a thin walled cylinder [14]. With this model, the magnitude of the radial stresses are small when compared to the magnitude of the hoop (tangential stresses). The maximum stresses occur at the inner surface of the cylinder [5]. In this case, the inner surface of the cylinder coincides with the contact surface of the two materials. A finite element model [1] of the annulus (figure 4-1) resulted in maximum tangential stresses of 24.3 MPa. In this model, the annulus had an initial temperature of 250°F (121.1°C). It was then subjected to a uniform temperature drop which resulted in a final temperature of -300°F (-184.4°C).

Analysis of the Longitudinal Cross Section

For the longitudinal cross-section, thermal stresses at the surface in contact with the conductor were developed in a similar manner to those of the annulus. A major difference, however, was the lack of symmetry along its axis. In place of the simple stress expected at the contact surface, a finite element analysis (figure 4-2) showed a higher more complex state of stress. Figure 4-3 gives an expanded view of the area where failure occurred. The magnitude of the principal stress in the region of failure is 44.3 MPa. Additionally, a region of very high stress is shown in the shoulder of the

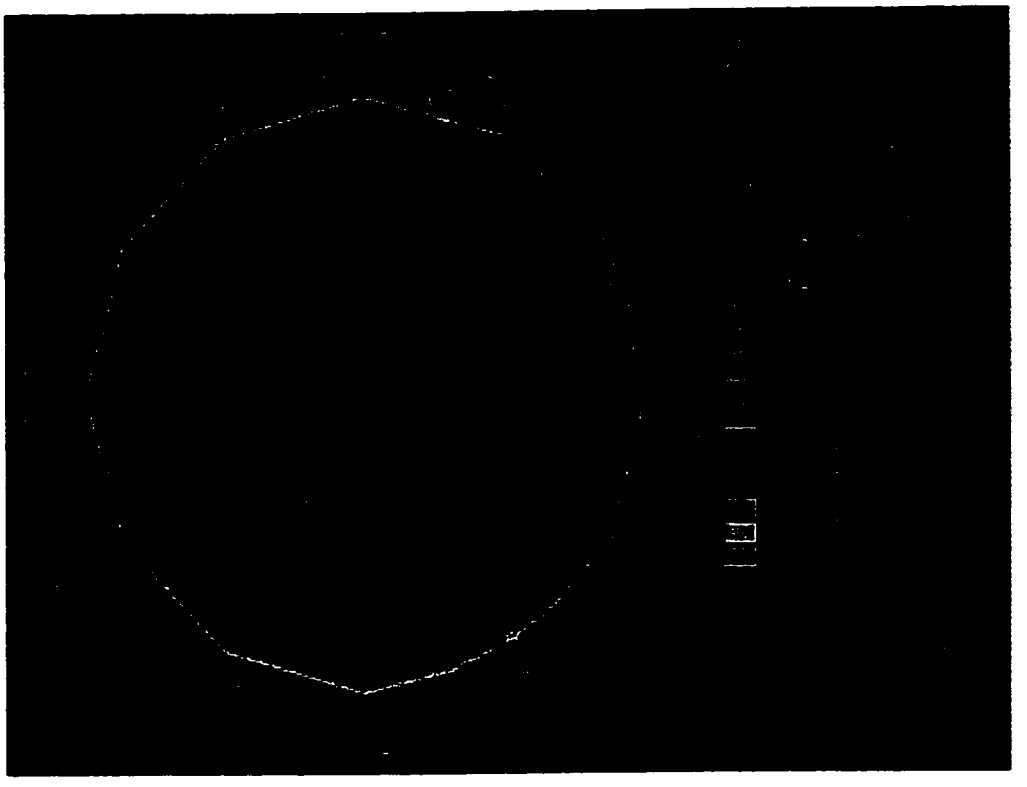

Figure 4-1. Annulus Stresses

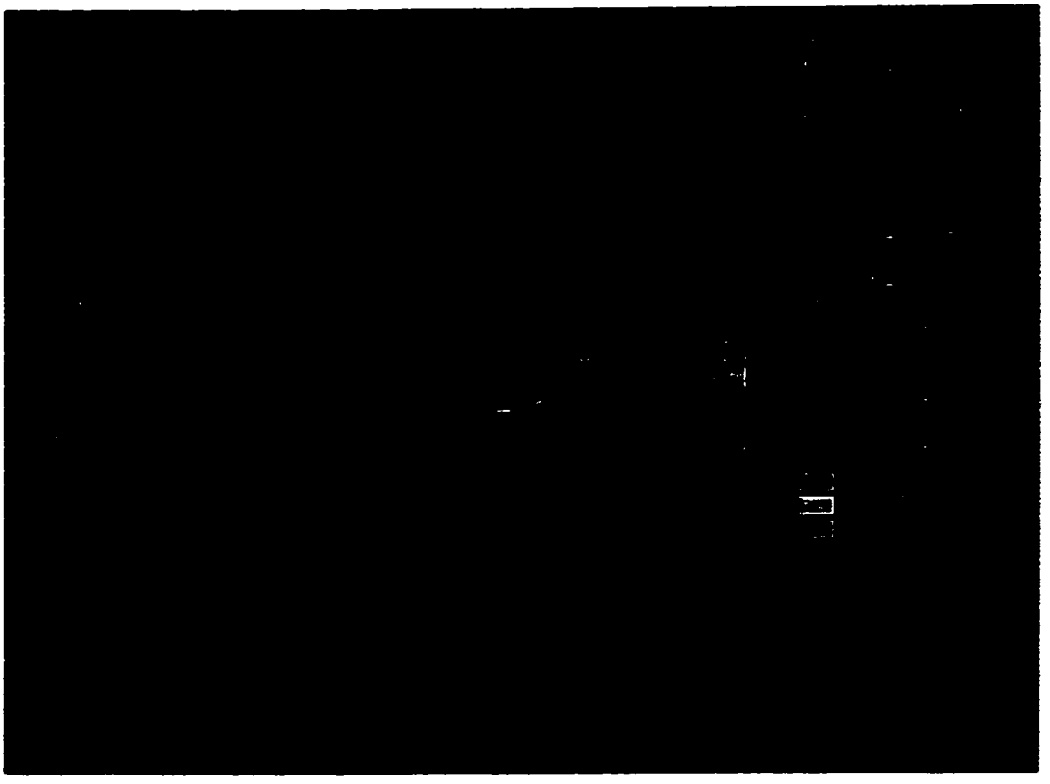

Figure 4-2. Longitudinal Stresses Developed with Fixed Boundaries

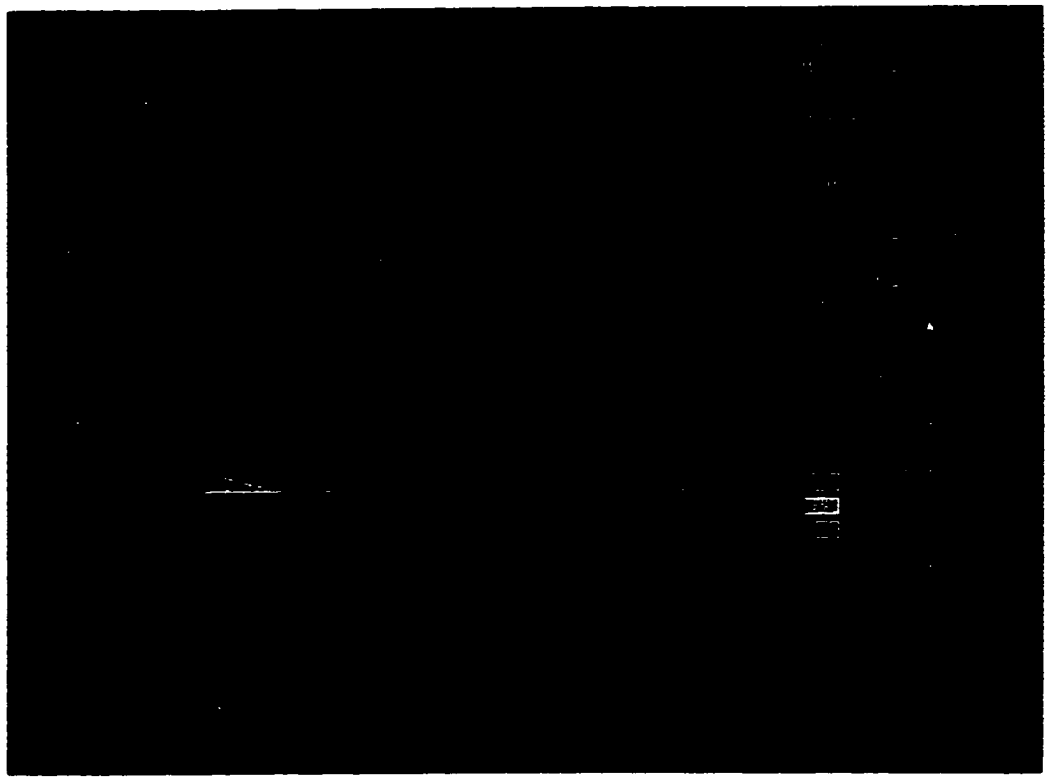

Figure 4-3. Expanded View of Region Subject to Cracking

interface. Although there were no failures in this region during the thermal cycle tests performed for this investigation, a previous bushing had failed in that particular region (figure 4-4). If the maximum principal stresses in both planes are combined, (assuming perpendicular stress at the inner surface of the epoxy, stress in the magnitude of 50 MPa is developed. The tensile strength of similar epoxy is given as 56 MPa. In addition to the stresses developed by the thermal contraction, residual stresses developed during manufacture are also present [2]. The combined affect of these stresses brings the epoxy into the range of failure. Any discontinuity in the material which produced stress concentrations could produce combined stresses which exceed the material strength.

Coated Conductors

When the conductor in a bushing was coated with Flexcoat-S, the Flexcoat-S separated the epoxy and the aluminum thus allowing relative movement between the two materials. Because the coating at any thickness level prevented failure of the epoxy, thickness of the coating was eliminated as a contributing factor to failure prevention. An analysis of the clearance provided by the coating showed no significant change in inner diameter of the epoxy when compared to a conductor with no coating.

The contribution of the coating in the longitudinal direction was significant. By allowing relative movement between the epoxy and the aluminum, the epoxy was allowed to contract, and the longitudinal stress was greatly reduced. A finite element analysis of the longitudinal cross section where relative movement is allowed in the longitudinal direction is given in figure 4-5. An examination of the model shows that stresses in that plane are nearly eliminated. The overall stress is then reduced to the hoop (tangential) stress plus any residual stress developed during the forming process.

The finite element model shows general stress levels when viewed as a planar cross-section. The model does not show the true stress levels which result from the three dimensional case.

Figure 4-4. Previous Bushing Failure

Figure 4-5. Stresses Developed when Longitudinal Constraint is Relaxed

CHAPTER 5

RESULTS AND CONCLUSIONS

Results

A method was developed that facilitated the application of Flexcoat-S to cylindrical conductors. Fifteen conductors were coated with Flexcoat-S which ranged in mean thickness from 1.7 mils (42 microns) to 3.3 mils (84 microns). Thermal shock tests were run on bushings formed with these conductors and with bushings formed with non-coated conductors. While bushings with coatings of any thickness passed all tests, bushings with non-coated conductors exhibited a 50% failure rate.

A theoretical analysis of the bushings formed without coated conductors indicated that under thermal change, both longitudinal and tangential stresses occurred in the region where the bushings cracked during the thermal shock tests. A finite element model verified those findings. The same type of analysis was done on bushings with coated conductors. While tangential stresses remained, the longitudinal stresses were relieved.

Conclusions

These test results lead to the conclusion that Flexcoat-S conductor coatings having a minimum mean thickness of 1.7 mils (42 microns) will prevent cracking of the bushing epoxy when the bushing is cycled to -300°F (-184.4°C). The Flexcoat-S coating

acted to allow relative movement between the conductor and insulator during thermal expansion and contraction. The relative movement between the conductor and insulator partially relieved stress which was developed in bushings with non-coated conductors. By relieving this stress, the overall stresses developed in the bushings were held below the level of stress required for the bushing insulation to fail.

APPENDIX A

CONDUCTOR COATING DATA

Appendix A gives detailed information on the Flexcoat-S coating of each conductor used in the initial coating development. These conductors are designated A, B, C, and E. Conductors A, B, and C were coated using coating sleeve 1.260, while conductor E was coated using the hand wiping method. Figures A-1 through A-36 compare the relative profiles of the sleeve coated conductors with that of the hand coated conductor. In each figure, orientation marks 1 and 5 represent the same location. Orientation mark 1 was repeated to complete the profile around the circumference of the conductor. Figure 2-2 identifies the location of each measurement.

Additionally, statistical data on the coatings of each aluminum conductor used to form bushings for the thermal shock tests are presented in tables A-1 through A-15. The coating sleeve used for each conductor is designated by the name of the conductor. As an example, conductor A1.260 (1) was coated with sleeve 1.260 (1) and was used to form bushing 1.260 (1).

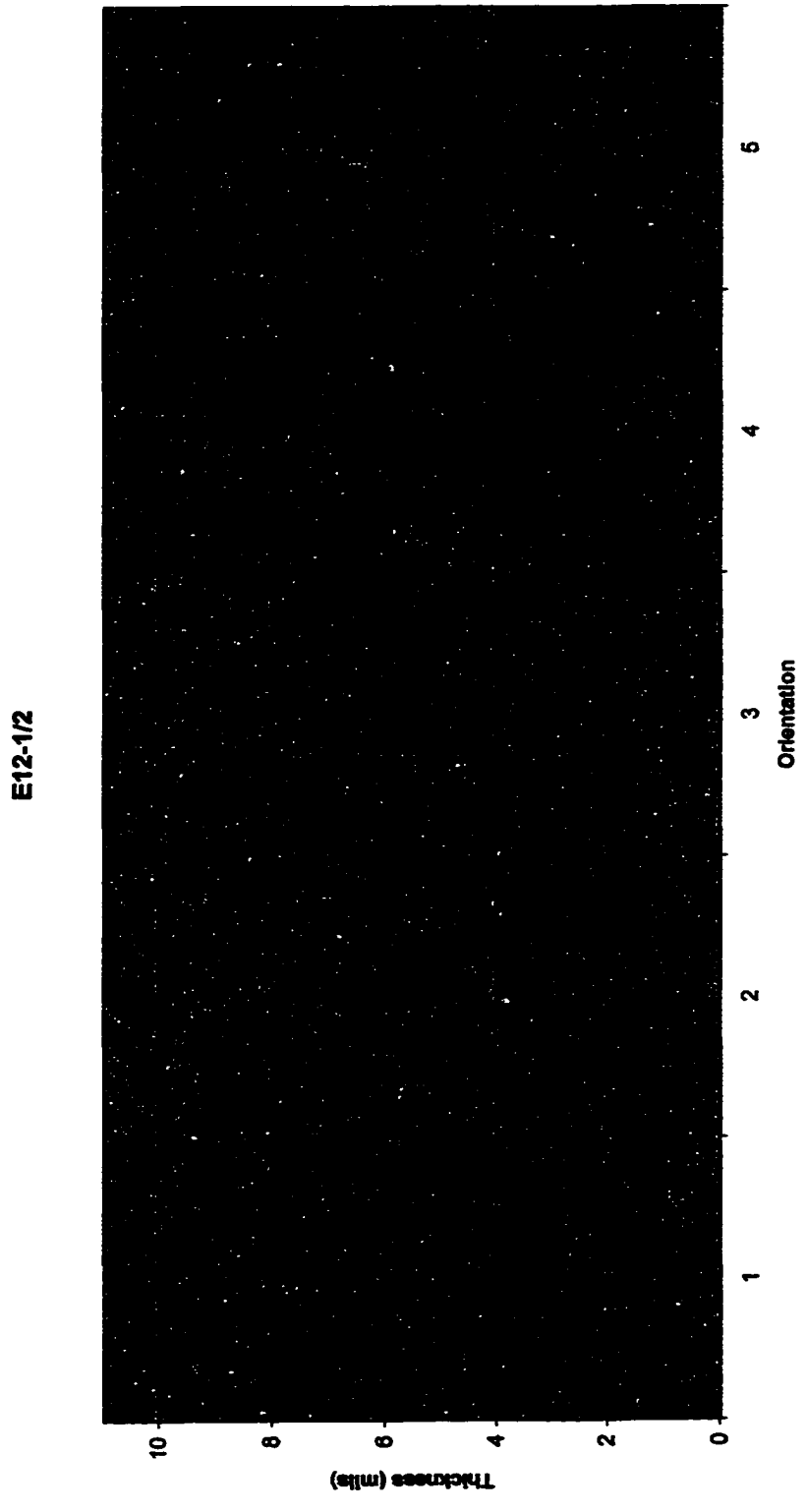

Figure A-1. Coating Thickness Profile of Conductor E at Location 12-1/2

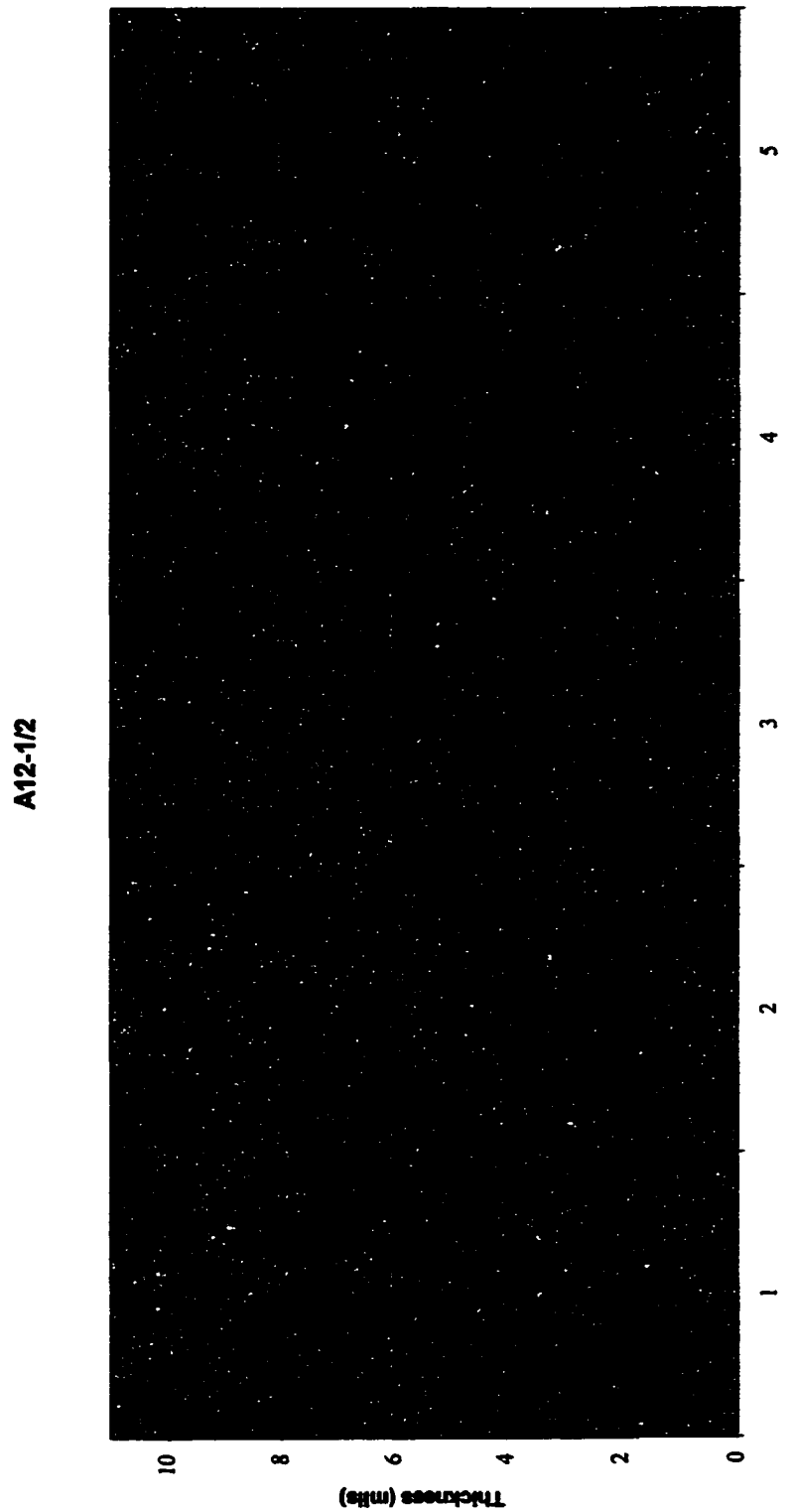

Figure A-2. Coating Thickness Profile of Conductor A at Location 12-1/2

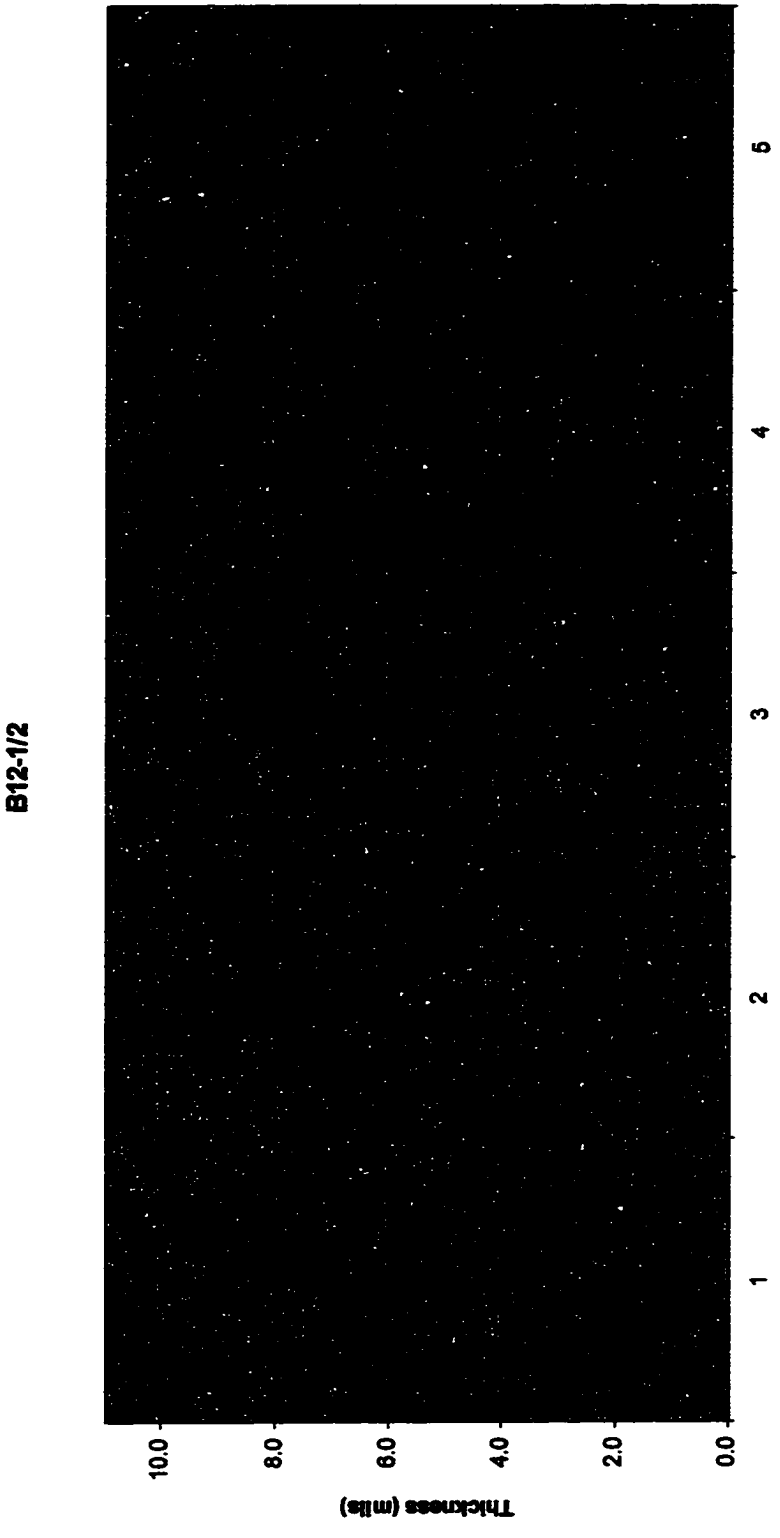

Figure A-3. Coating Thickness Profile of Conductor B at Location 12-1/2

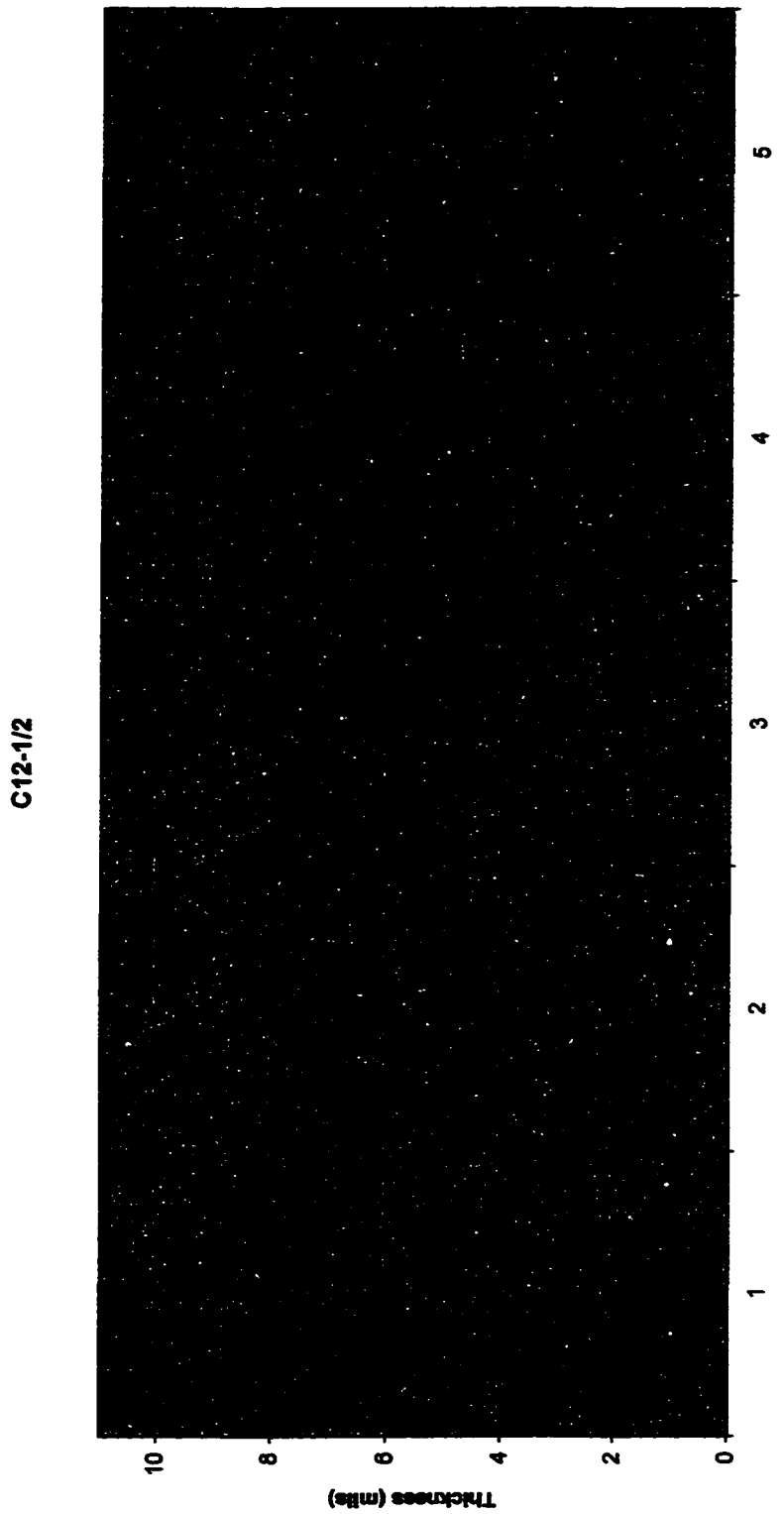

Figure A-4. Coating Thickness Profile of Conductor C at Location 12-1/2

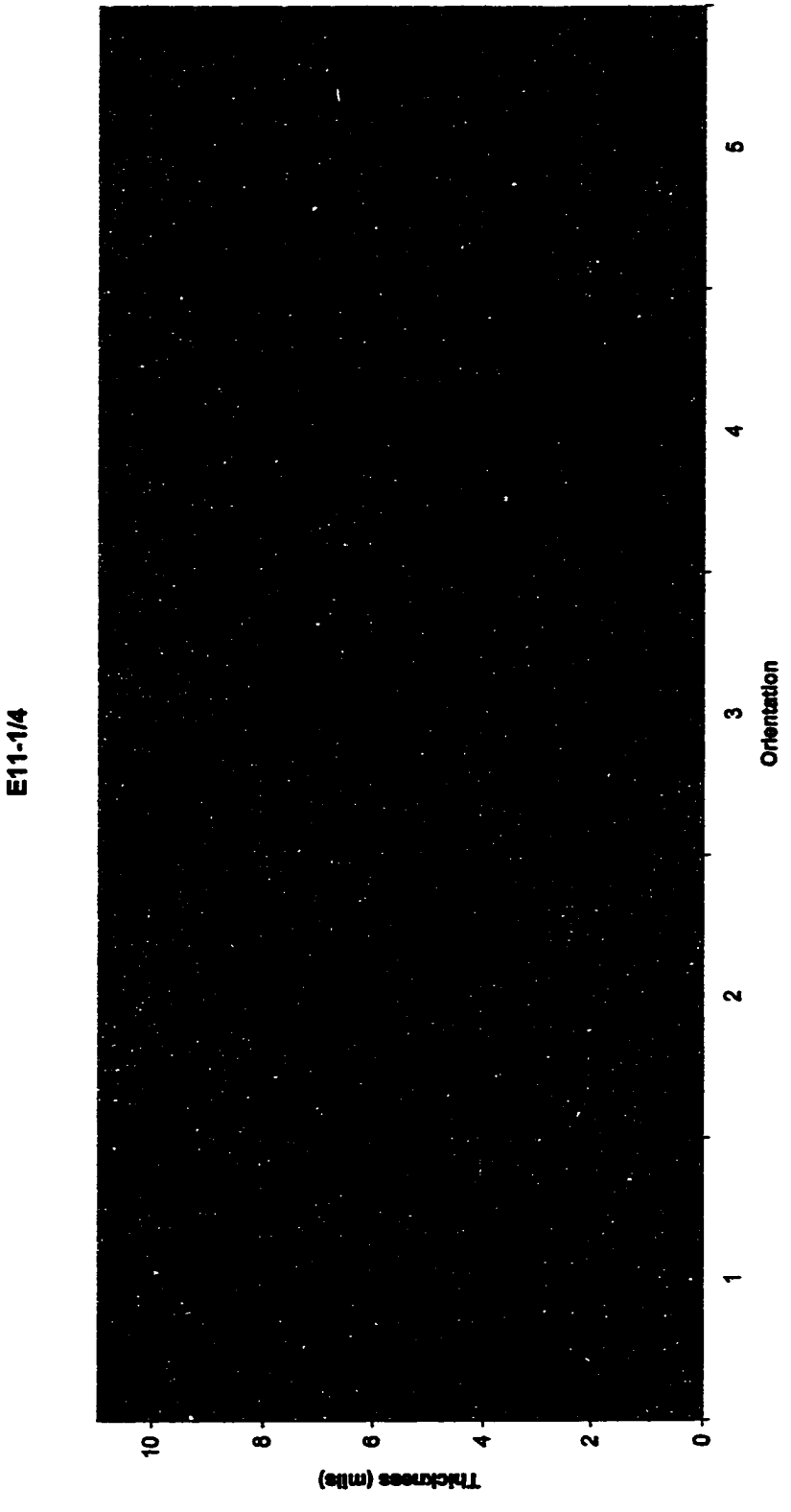

Figure A-5. Coating Thickness Profile of Conductor E at Location 11-1/4

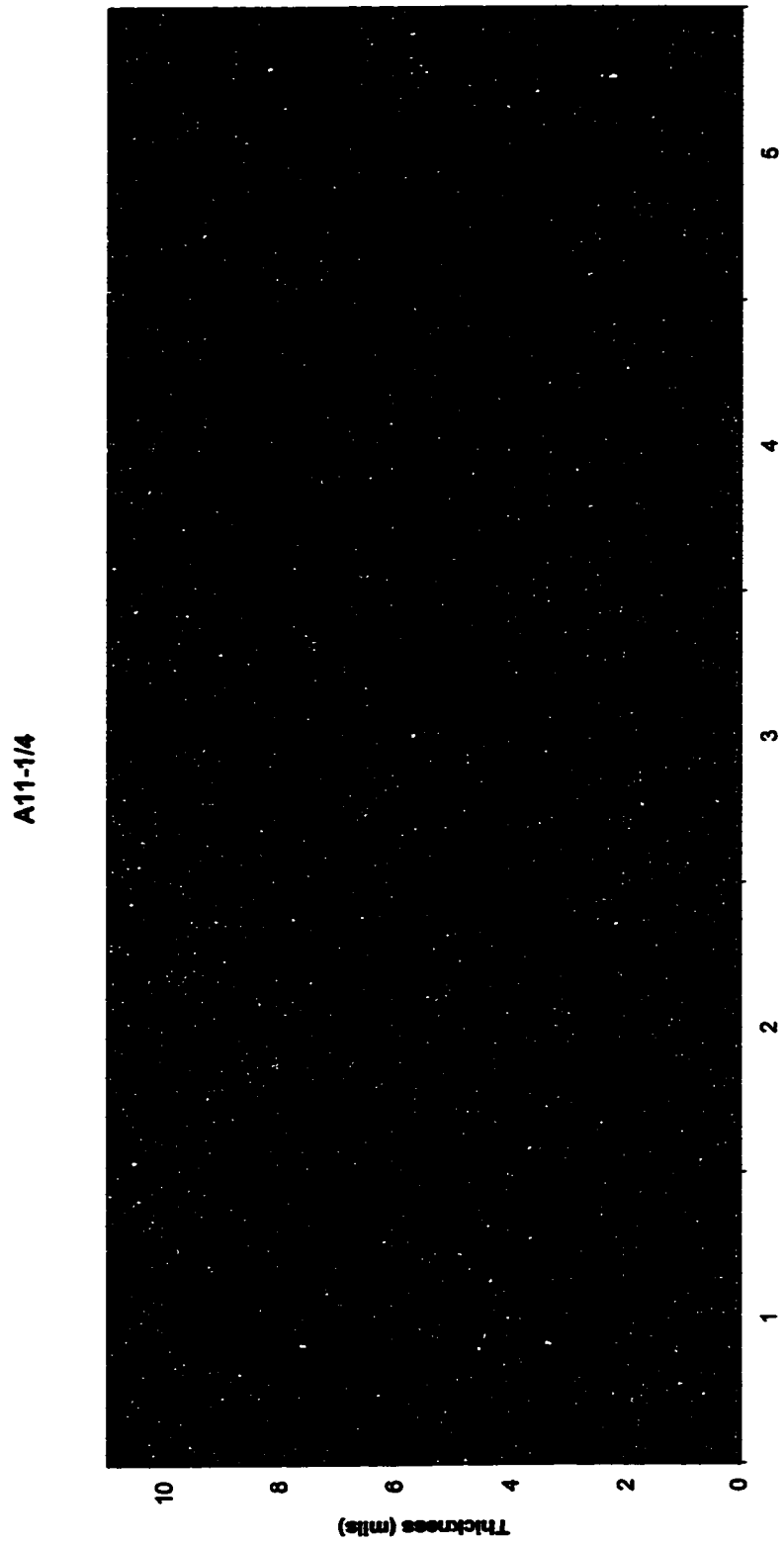

Figure A-6. Coating Thickness Profile of Conductor A at Location 11-1/4

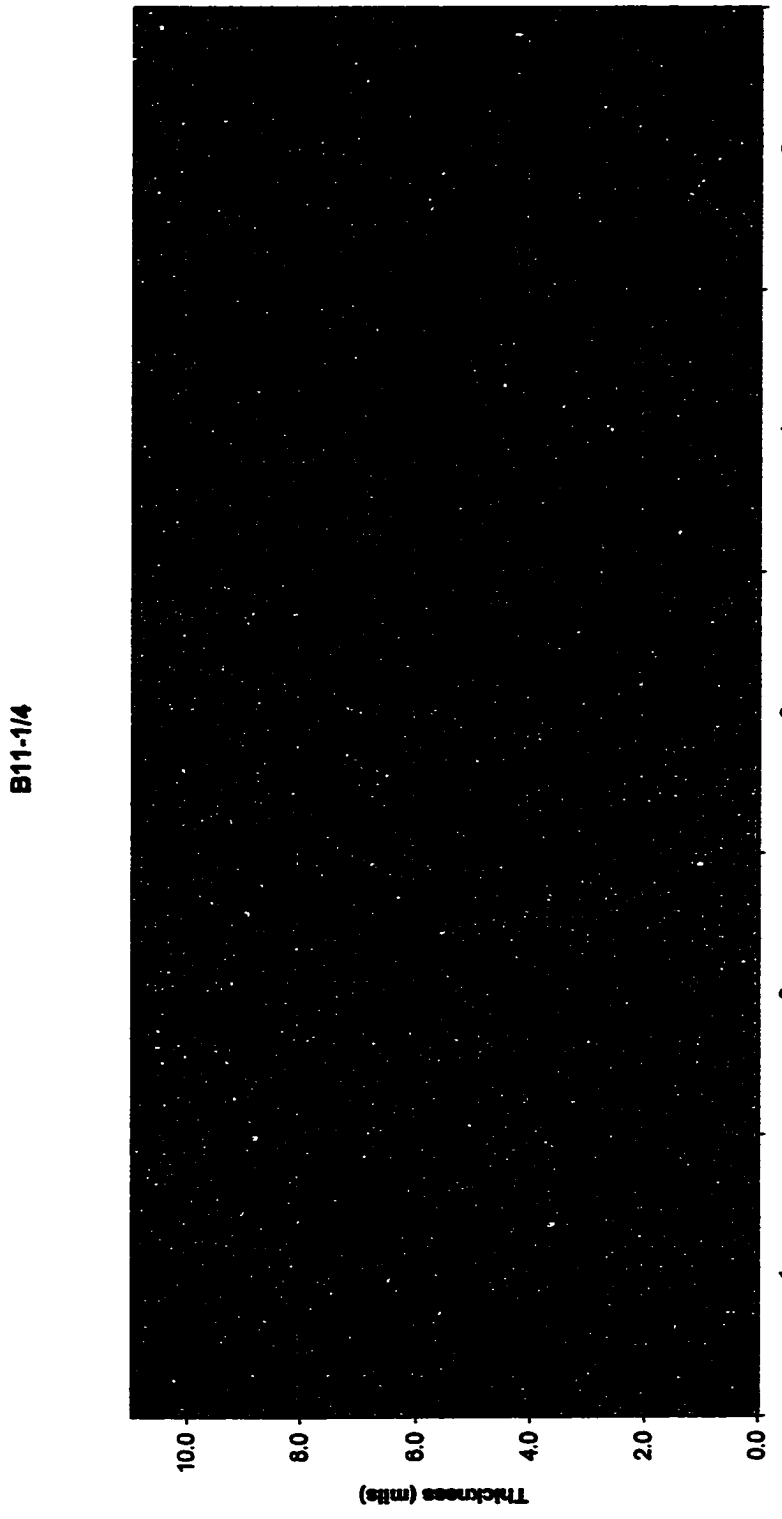

Figure A-7. Coating Thickness Profile of Conductor B at Location 11-1/4

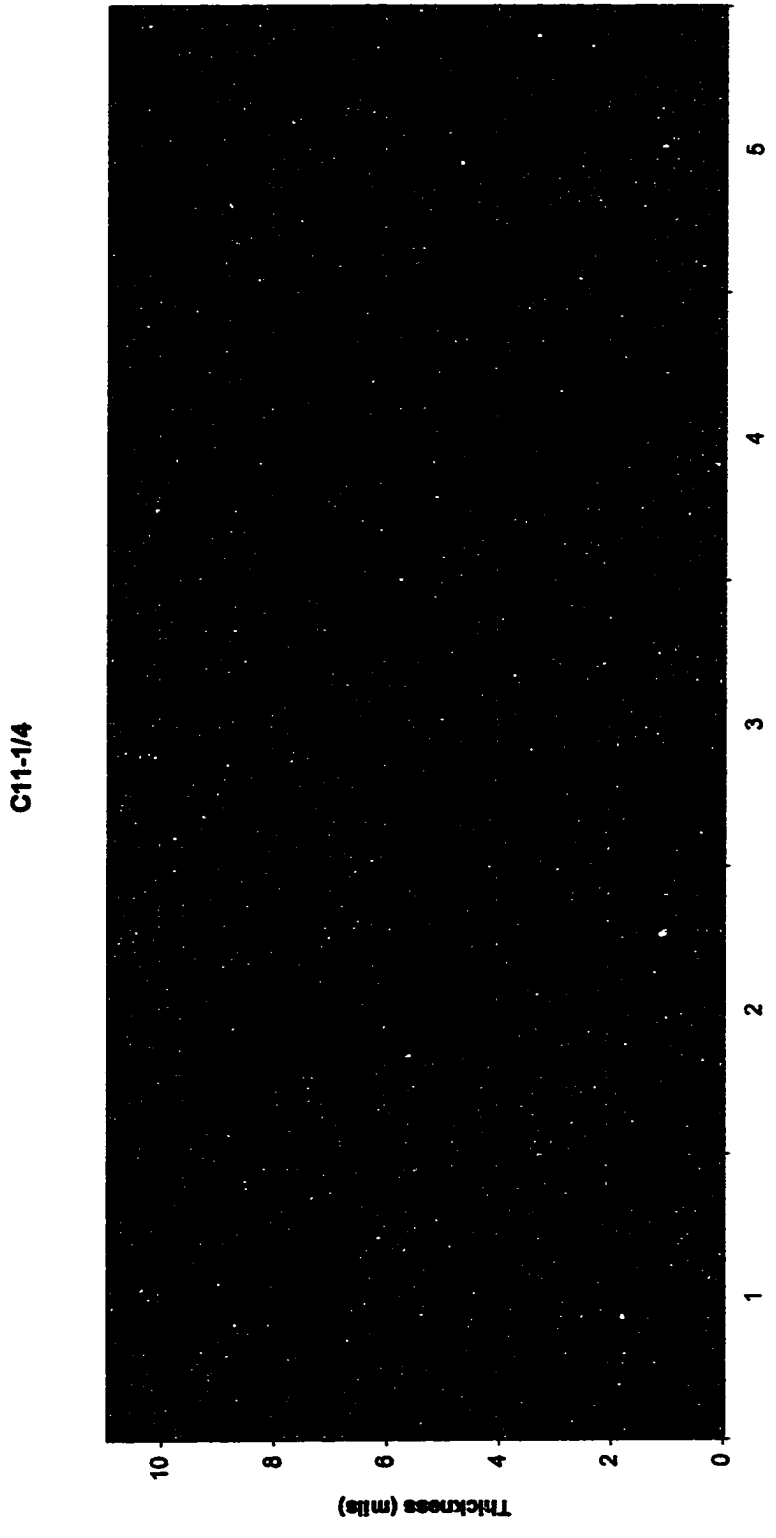

Figure A-8. Coating Thickness Profile of Conductor C at Location 11-1/4

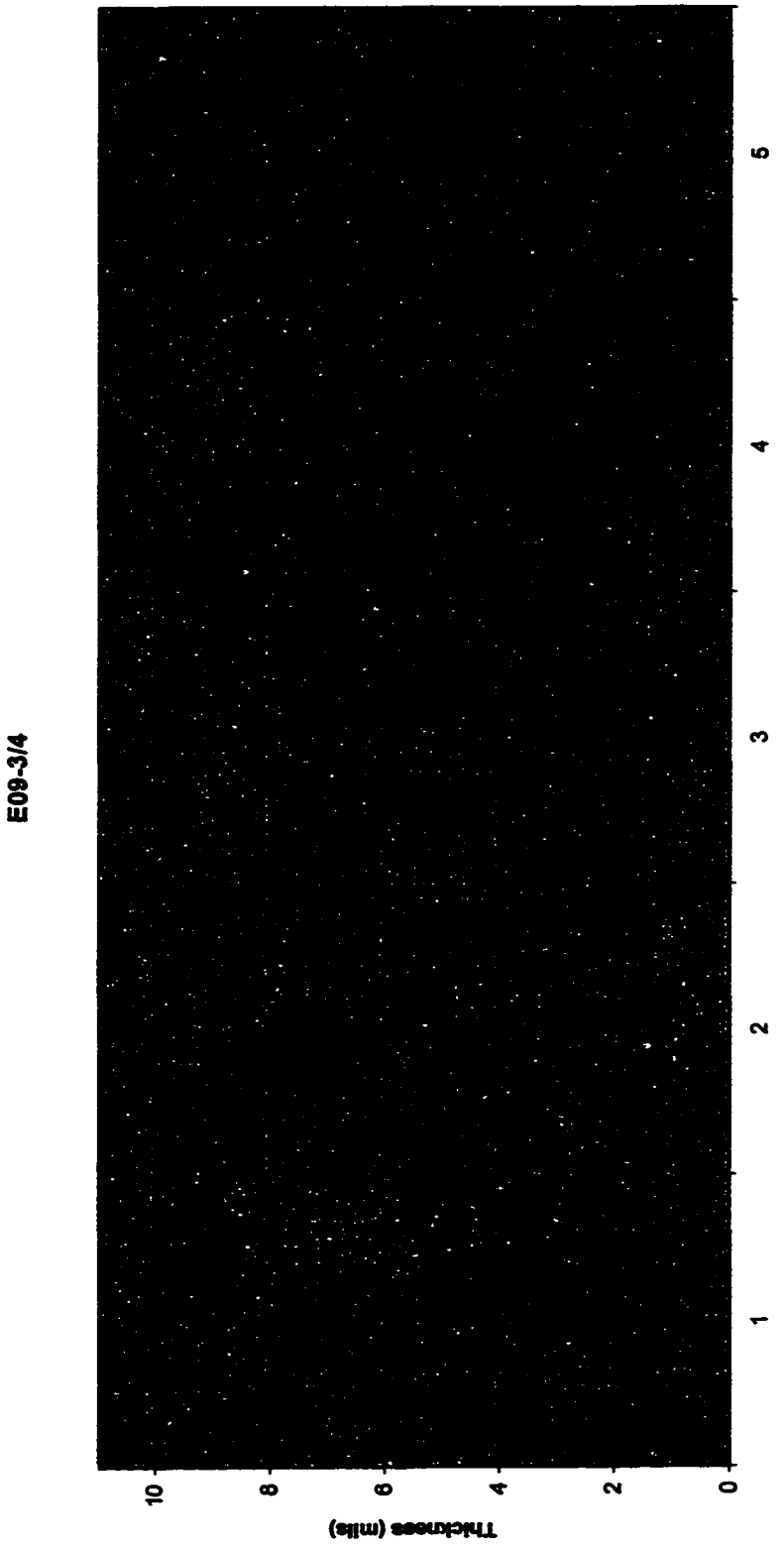

Figure A-9. Coating Thickness Profile of Conductor E at Location 09-3/4

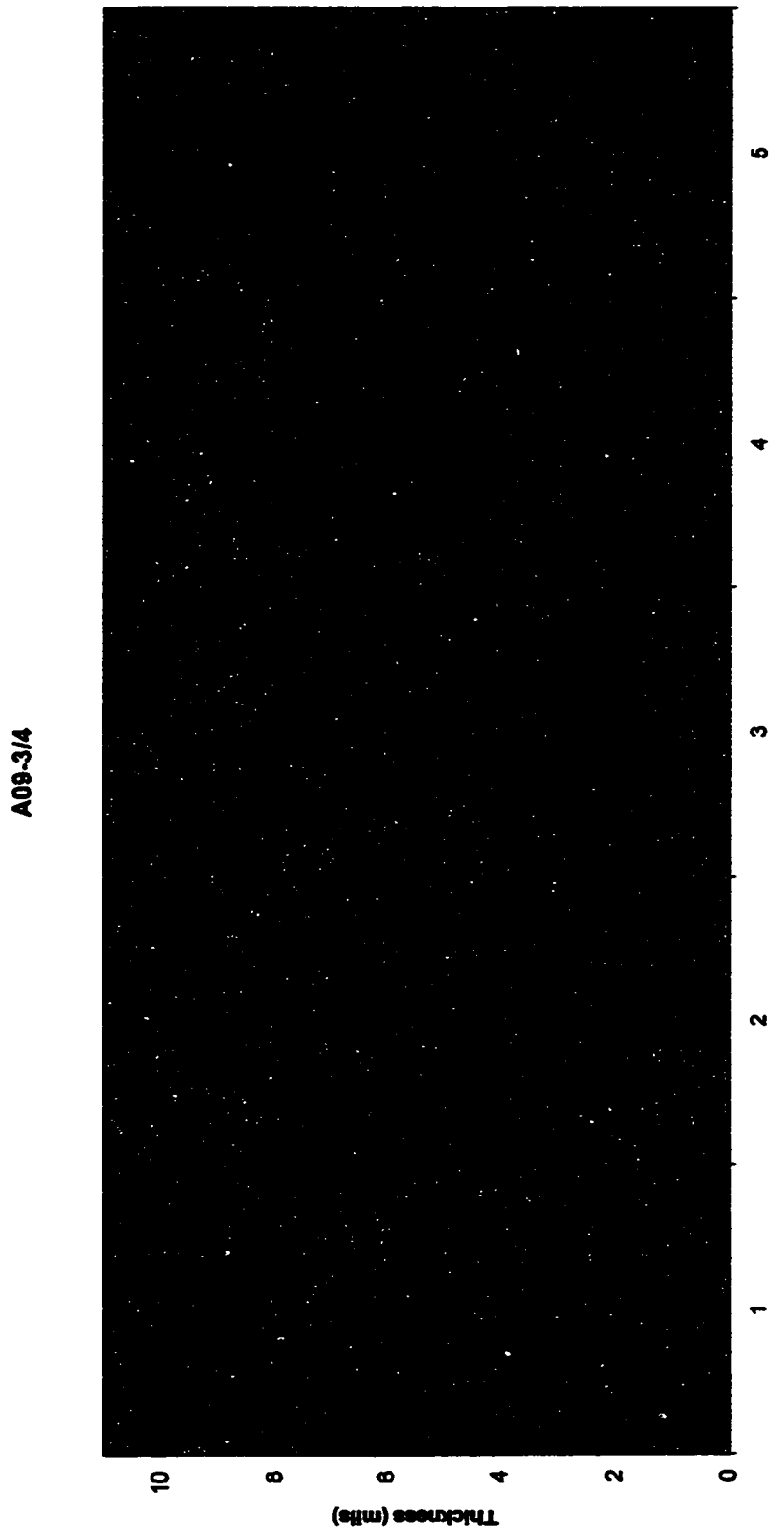

Figure A-10. Coating Thickness Profile of Conductor A at Location 09-3/4

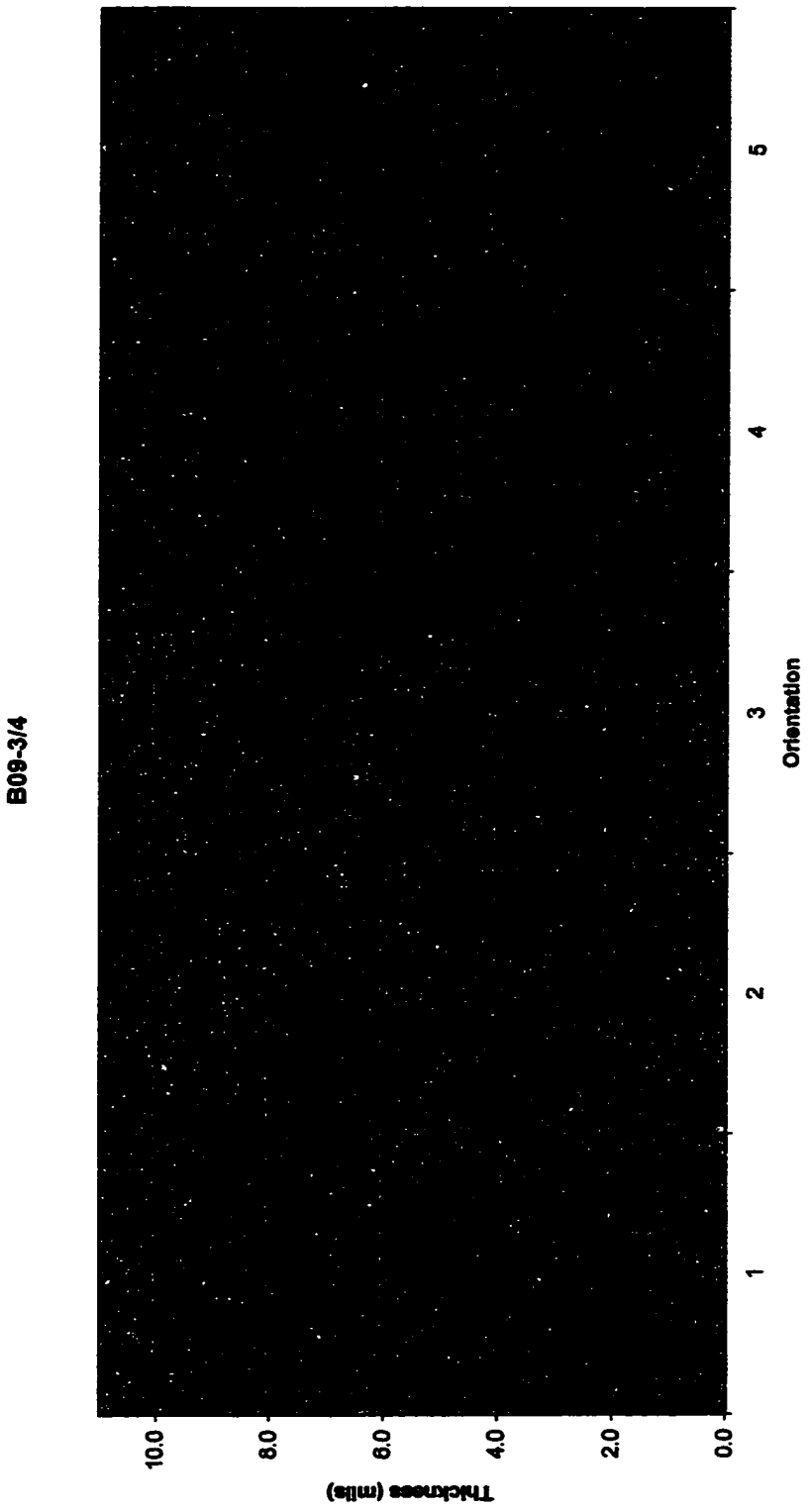

Figure A-11. Coating Thickness Profile of Conductor B at Location 09-3/4

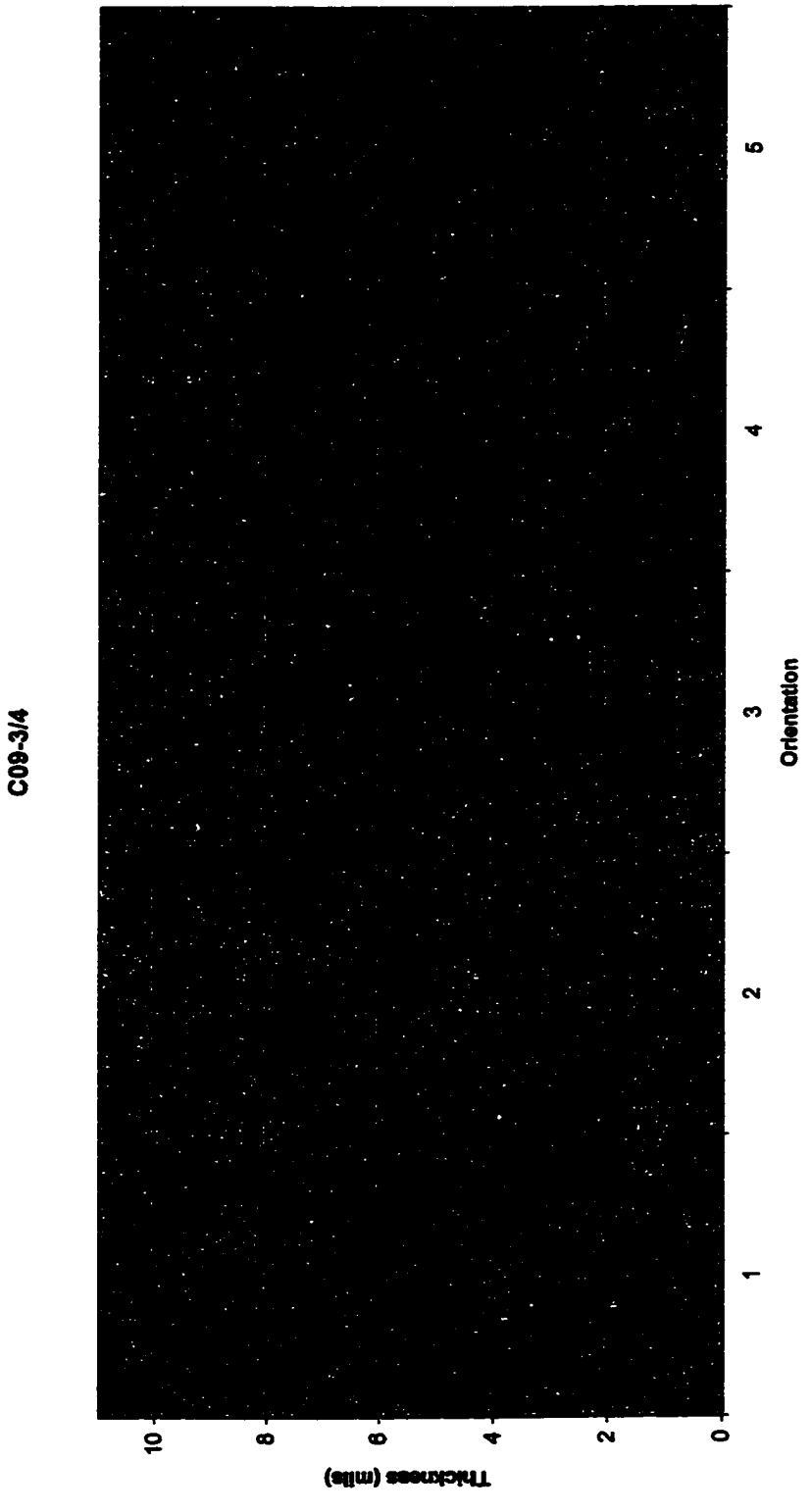

Figure A-12. Coating Thickness Profile of Conductor C at Location 09-3/4

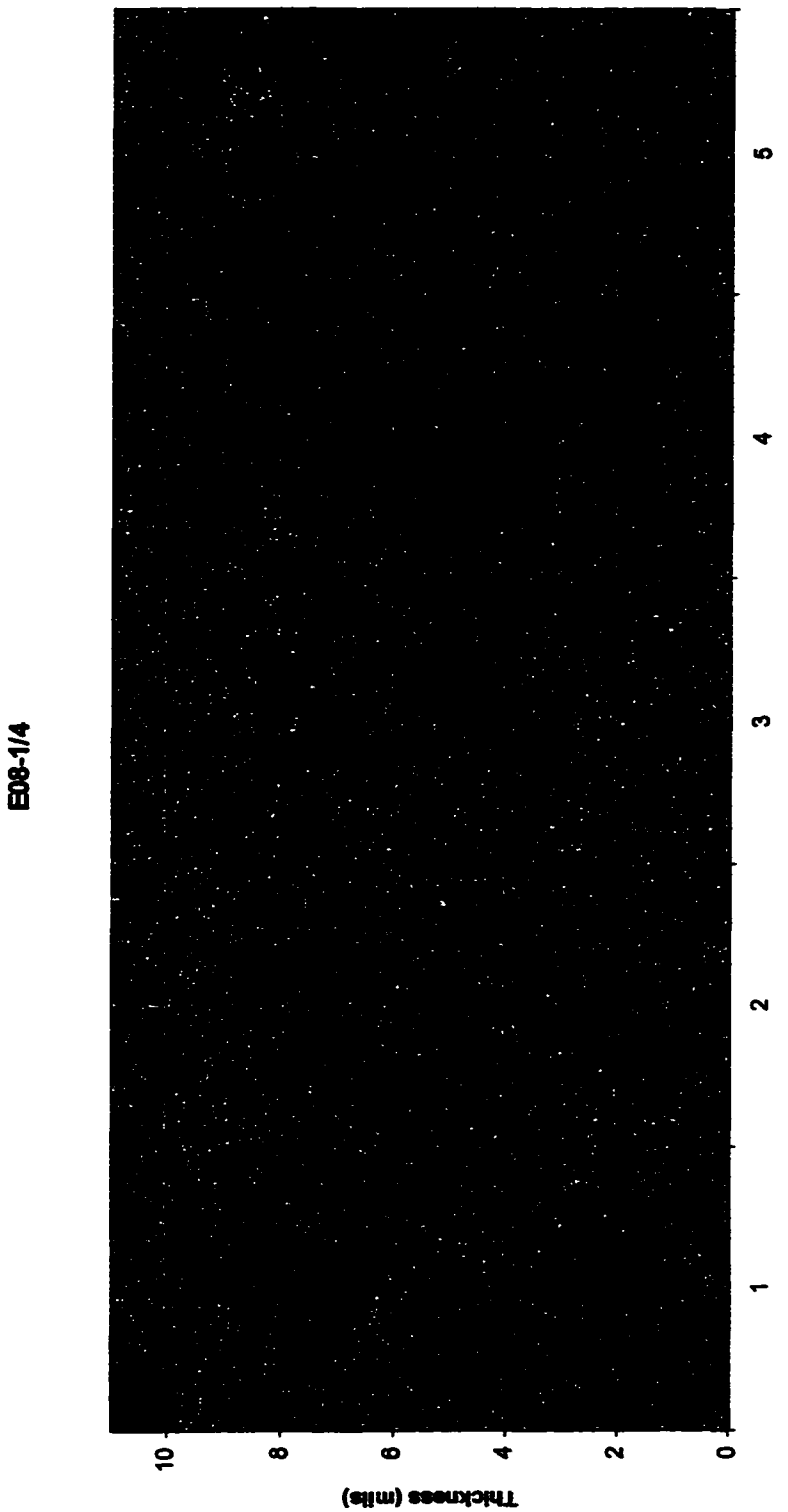

Figure A-13. Coating Thickness Profile of Conductor E at Location 08-1/4

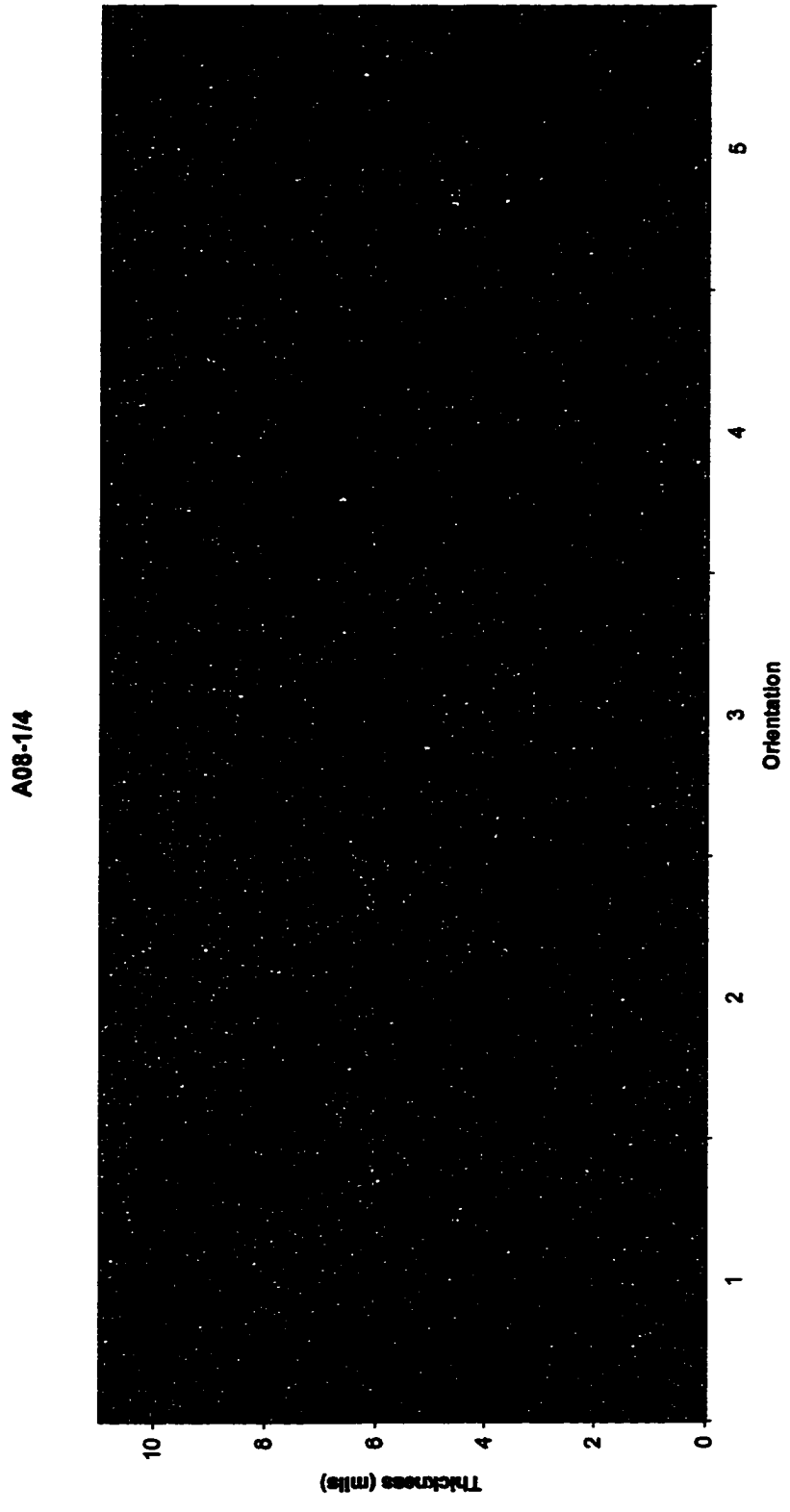

Figure A-14. Coating Thickness Profile of Conductor A at Location 08-1/4

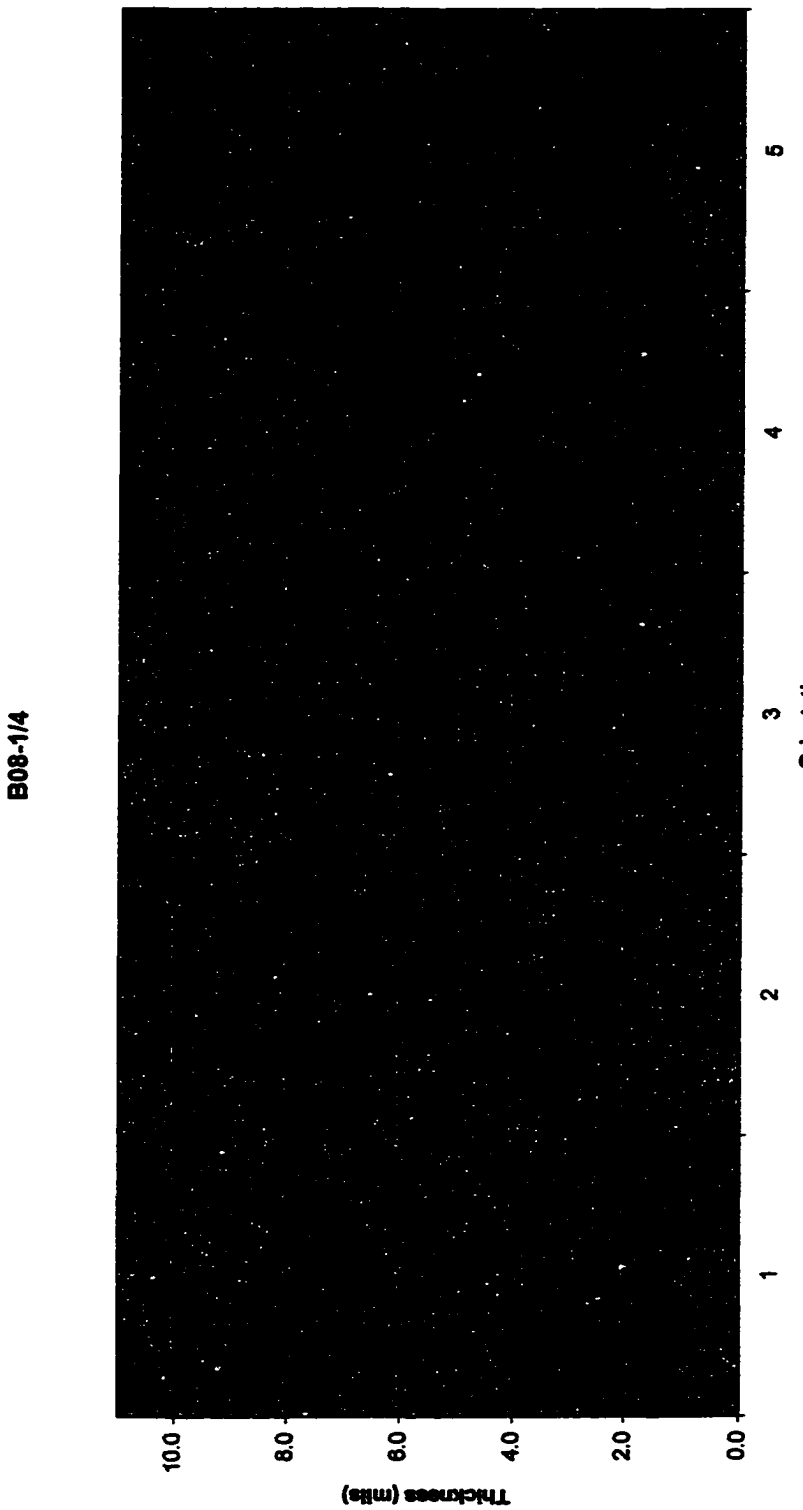

Figure A-15. Coating Thickness Profile of Conductor B at Location 08-1/4

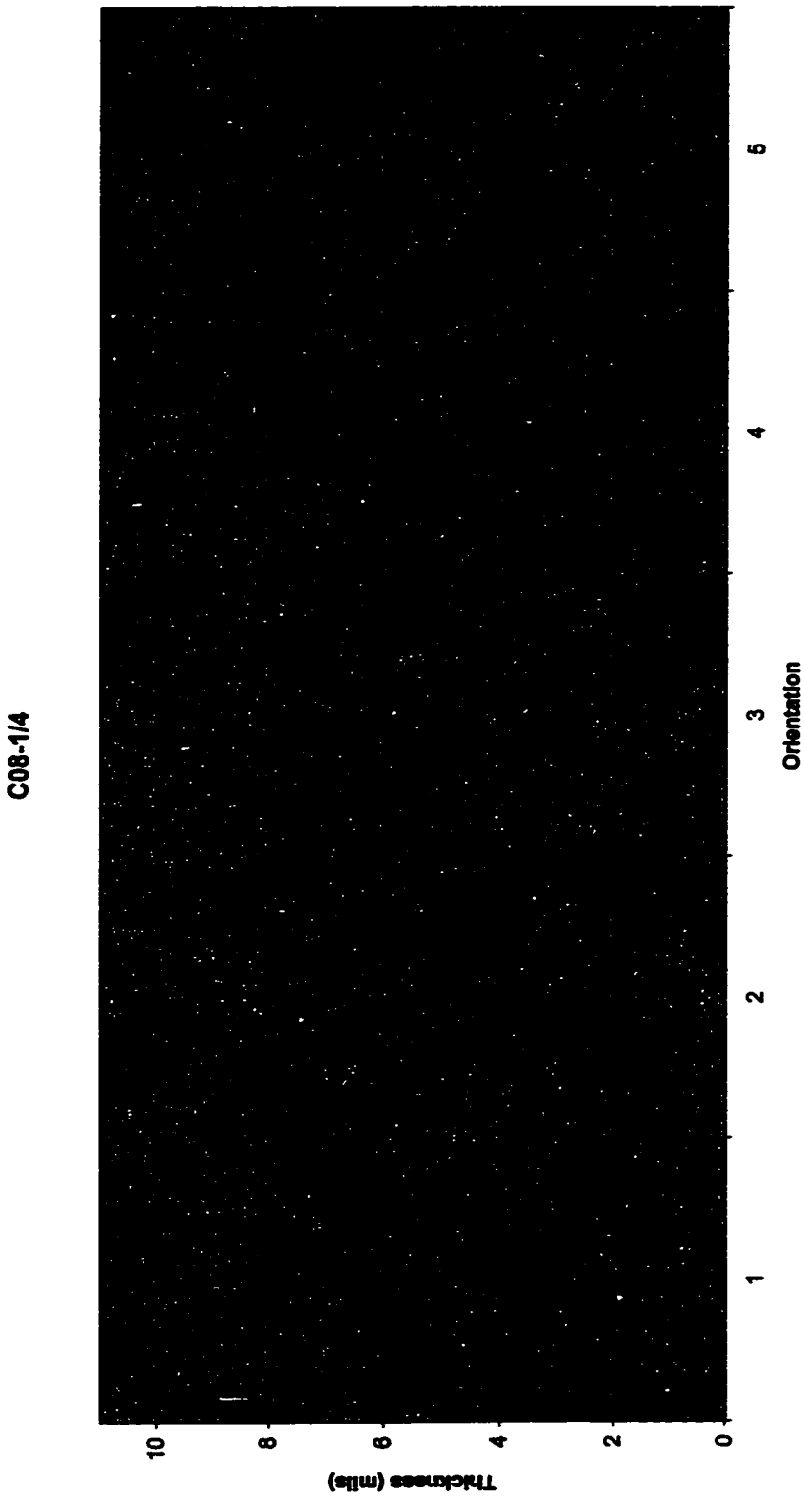

Figure A-16. Coating Thickness Profile of Conductor C at Location 08-1/4

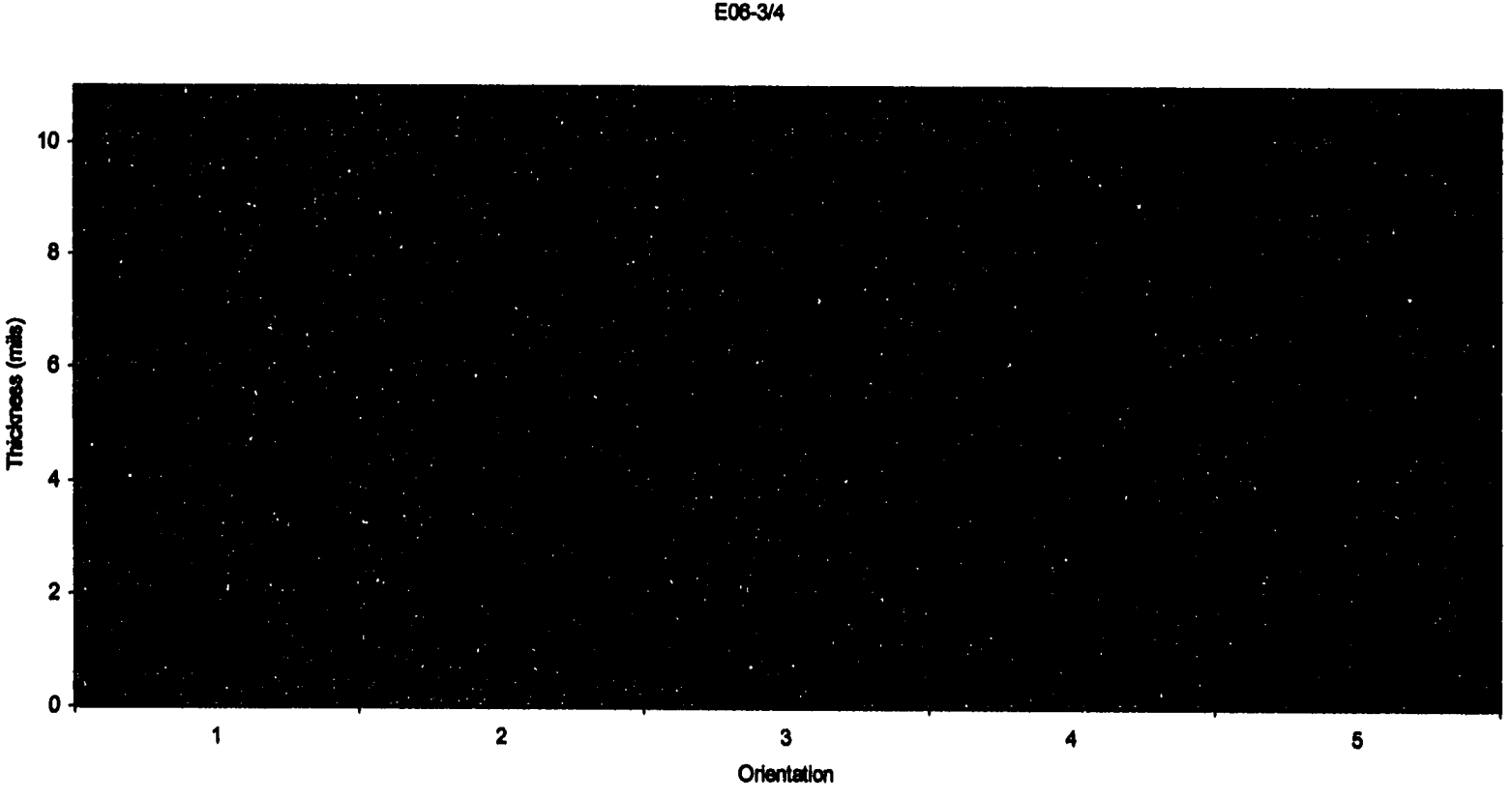

Figure A-17. Coating Thickness Profile of Conductor E at Location 06-3/4

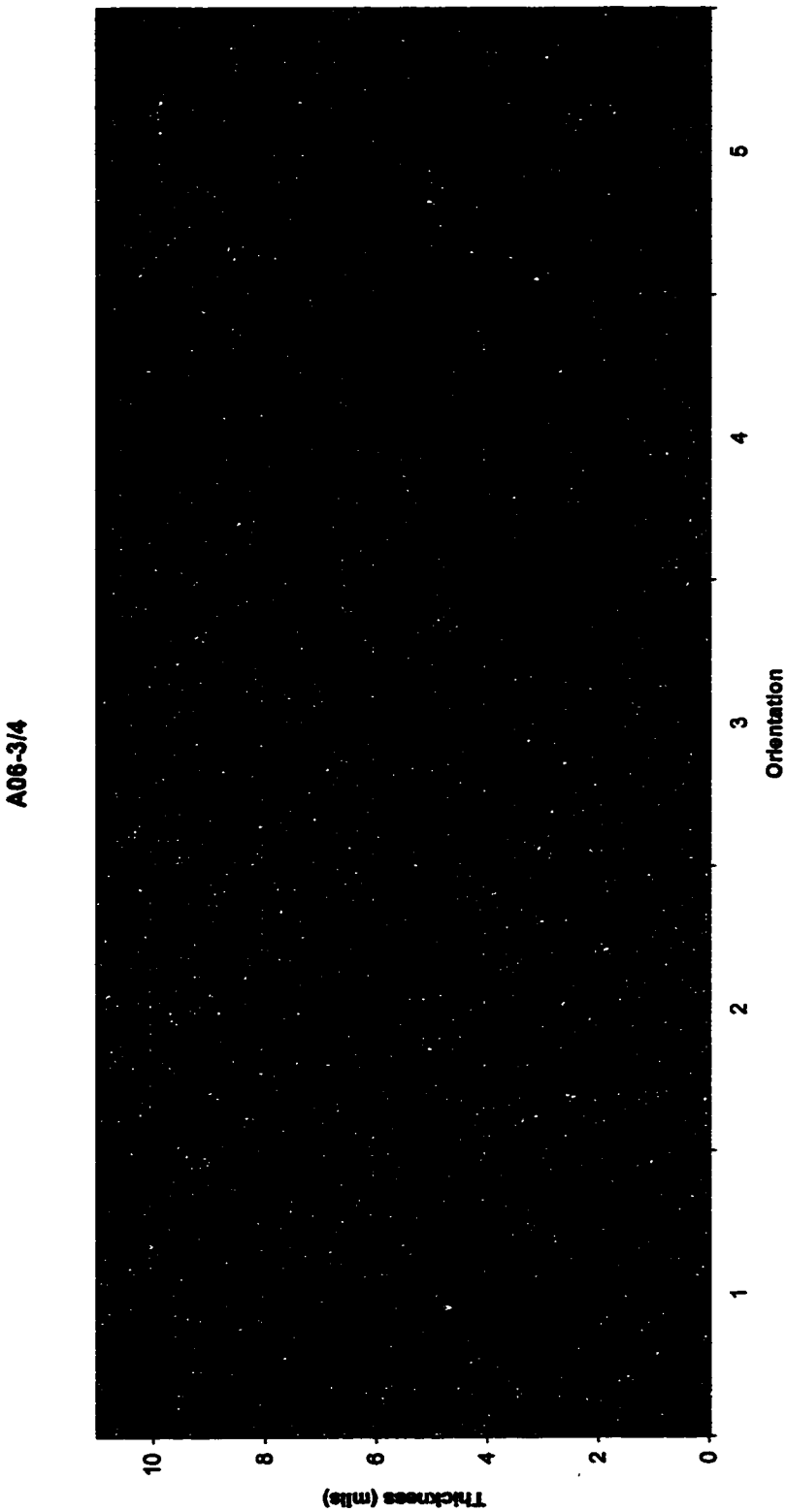

Figure A-18. Coating Thickness Profile of Conductor A at Location 06-3/4

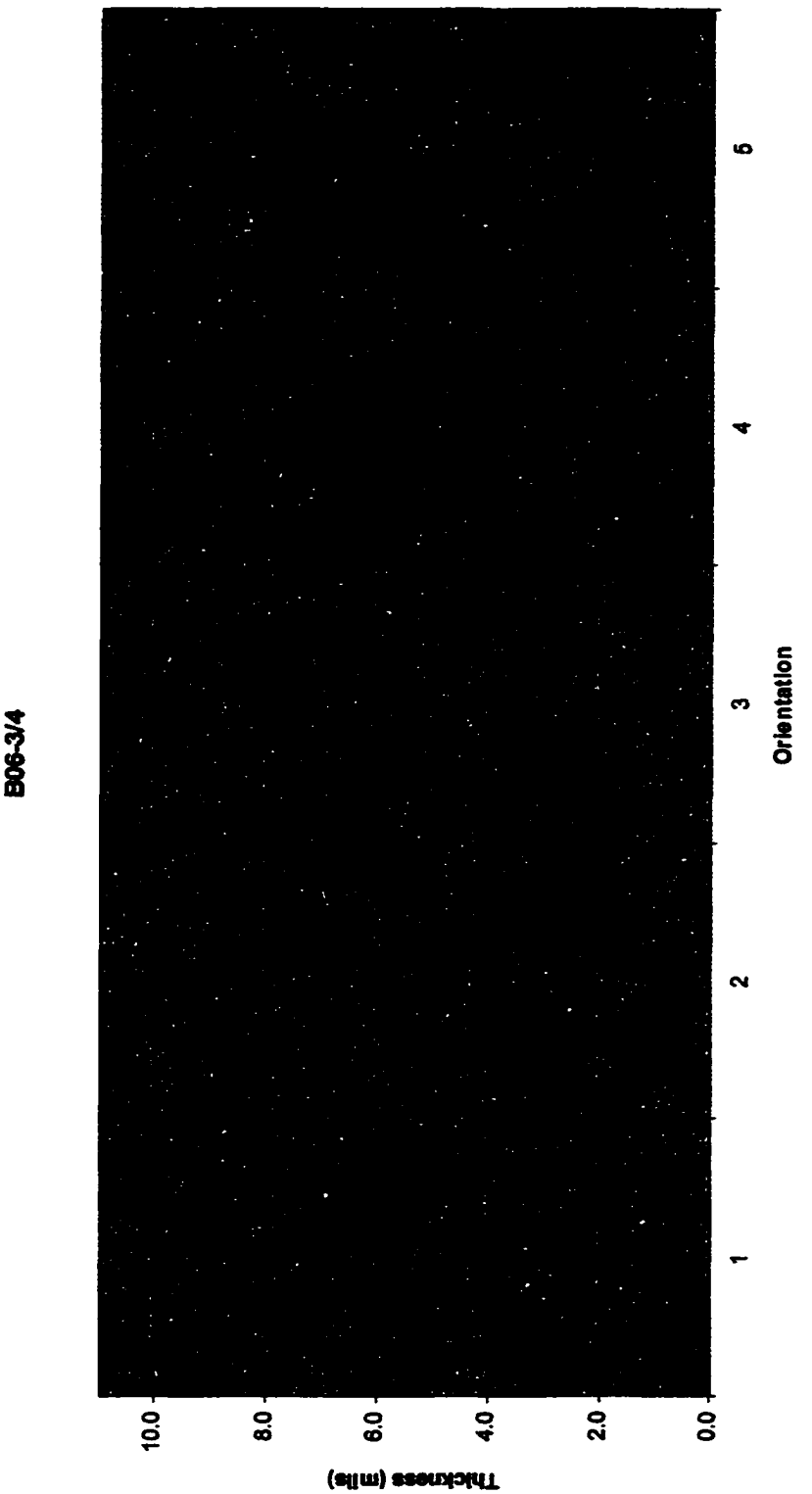

Figure A-19. Coating Thickness Profile of Conductor B at Location 06-3/4

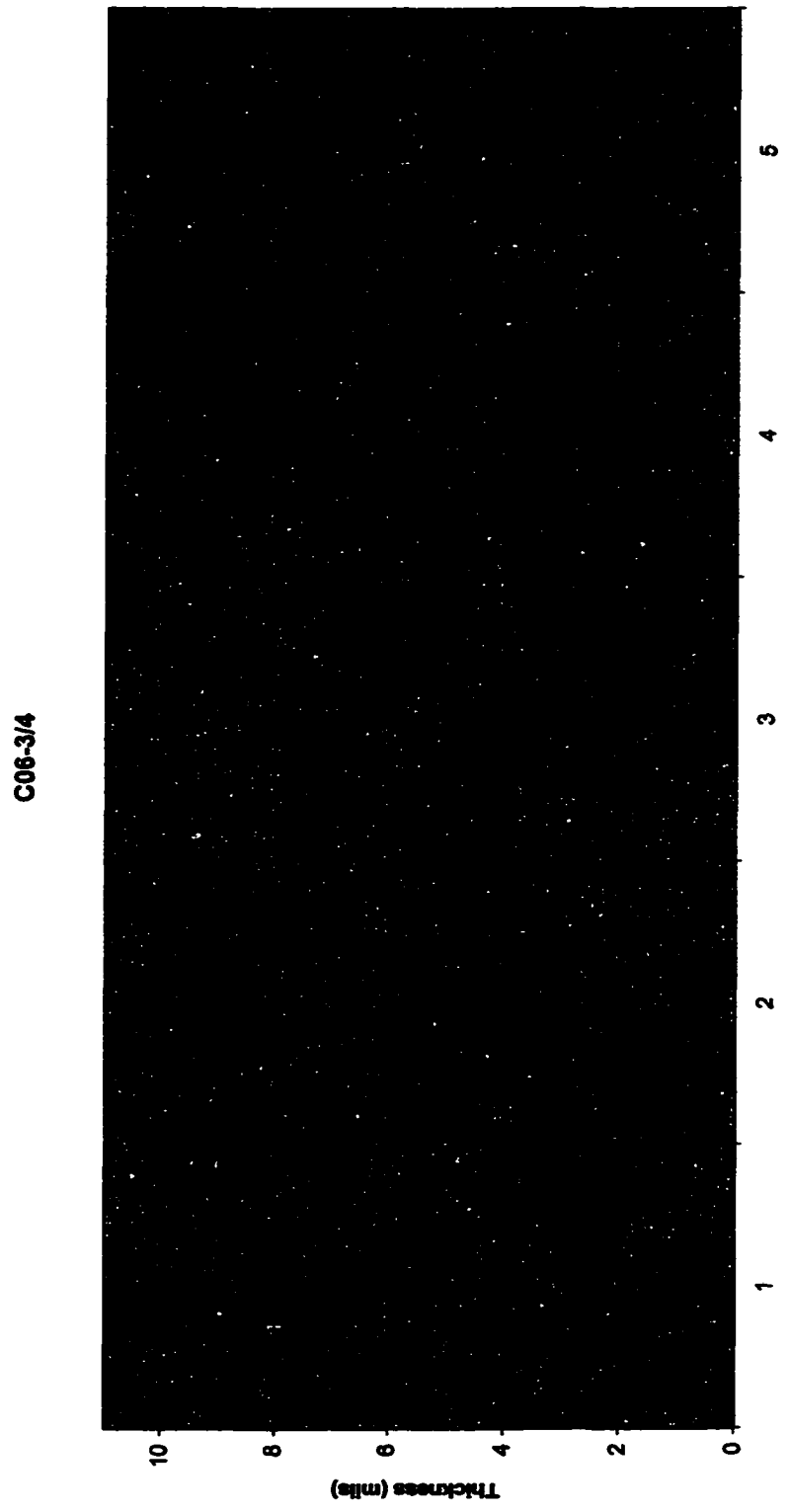

Figure A-20. Coating Thickness Profile of Conductor C at Location 06-3/4

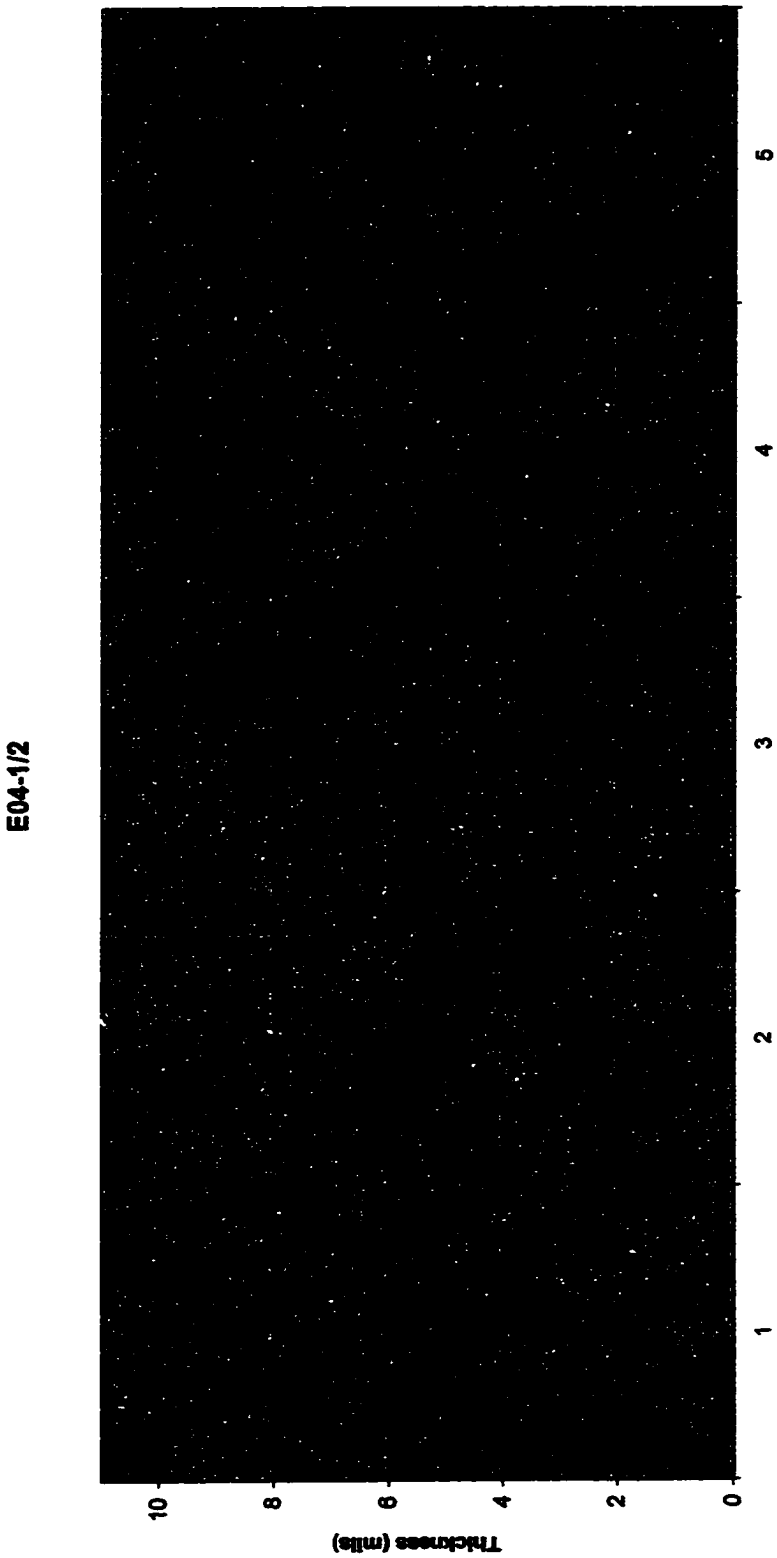

Figure A-21. Coating Thickness Profile of Conductor E at Location 04-1/2

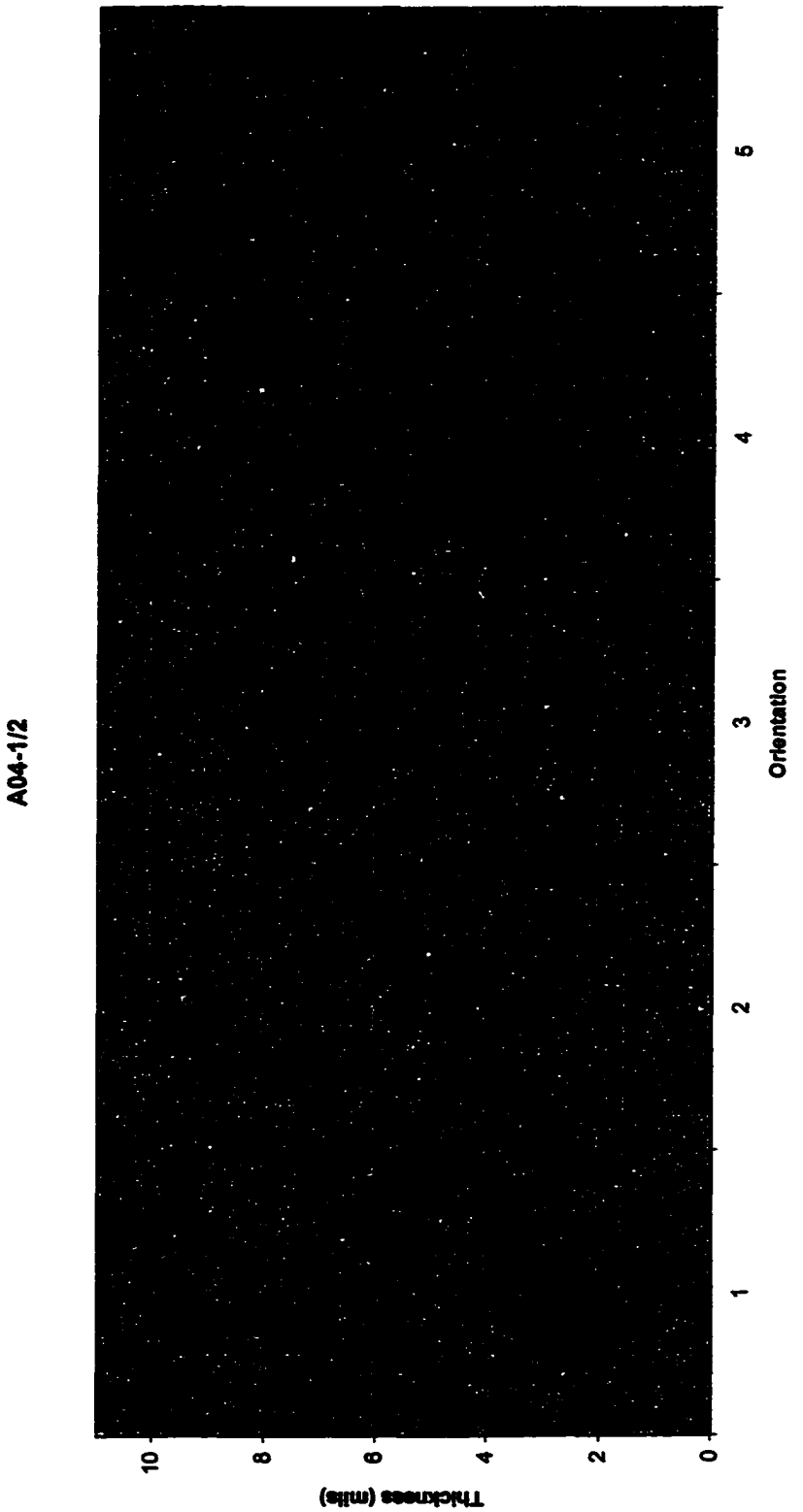

Figure A-22. Coating Thickness Profile of Conductor A at Location 04-1/2

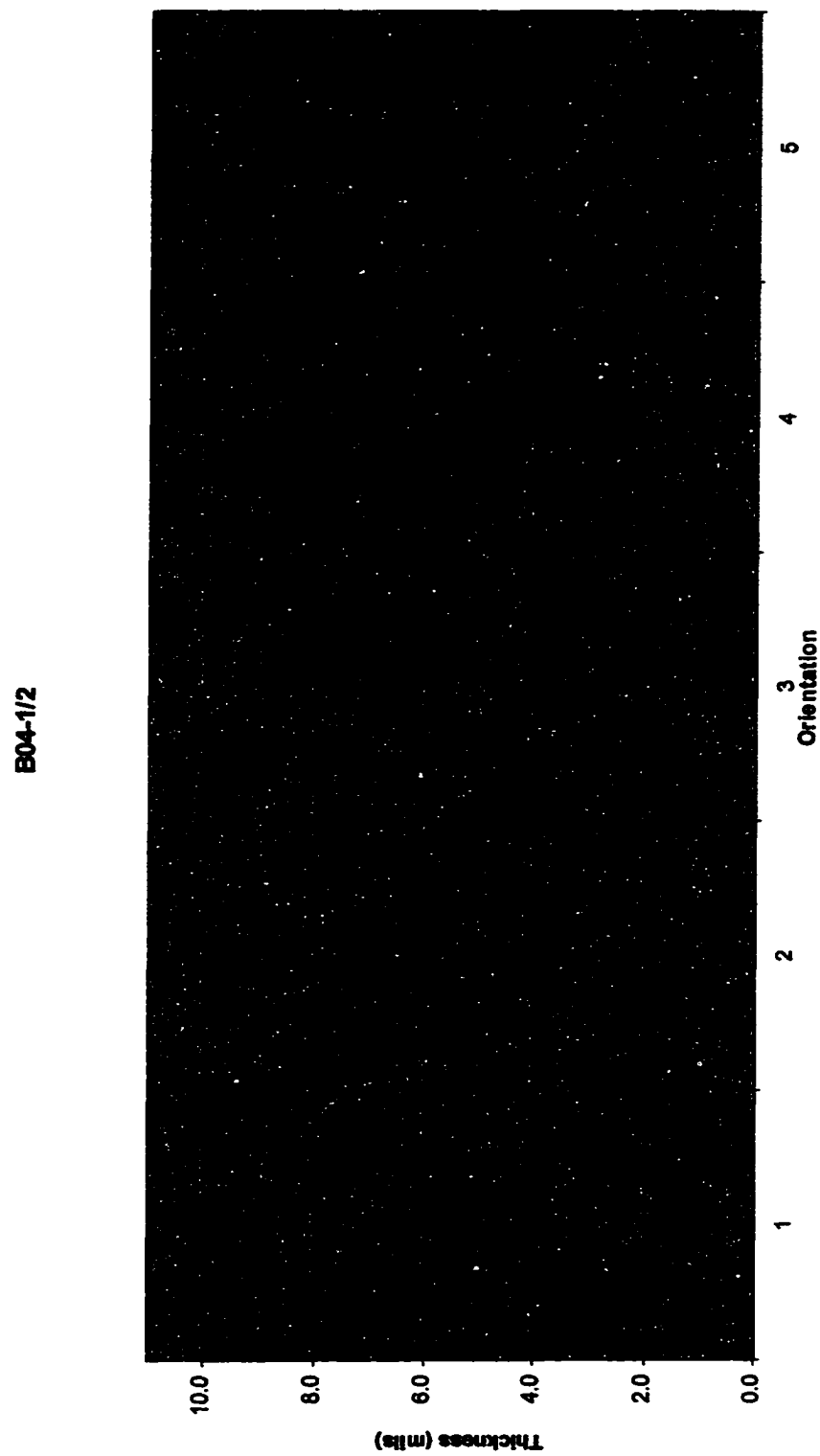

Figure A-23. Coating Thickness Profile of Conductor B at Location 04-1/2

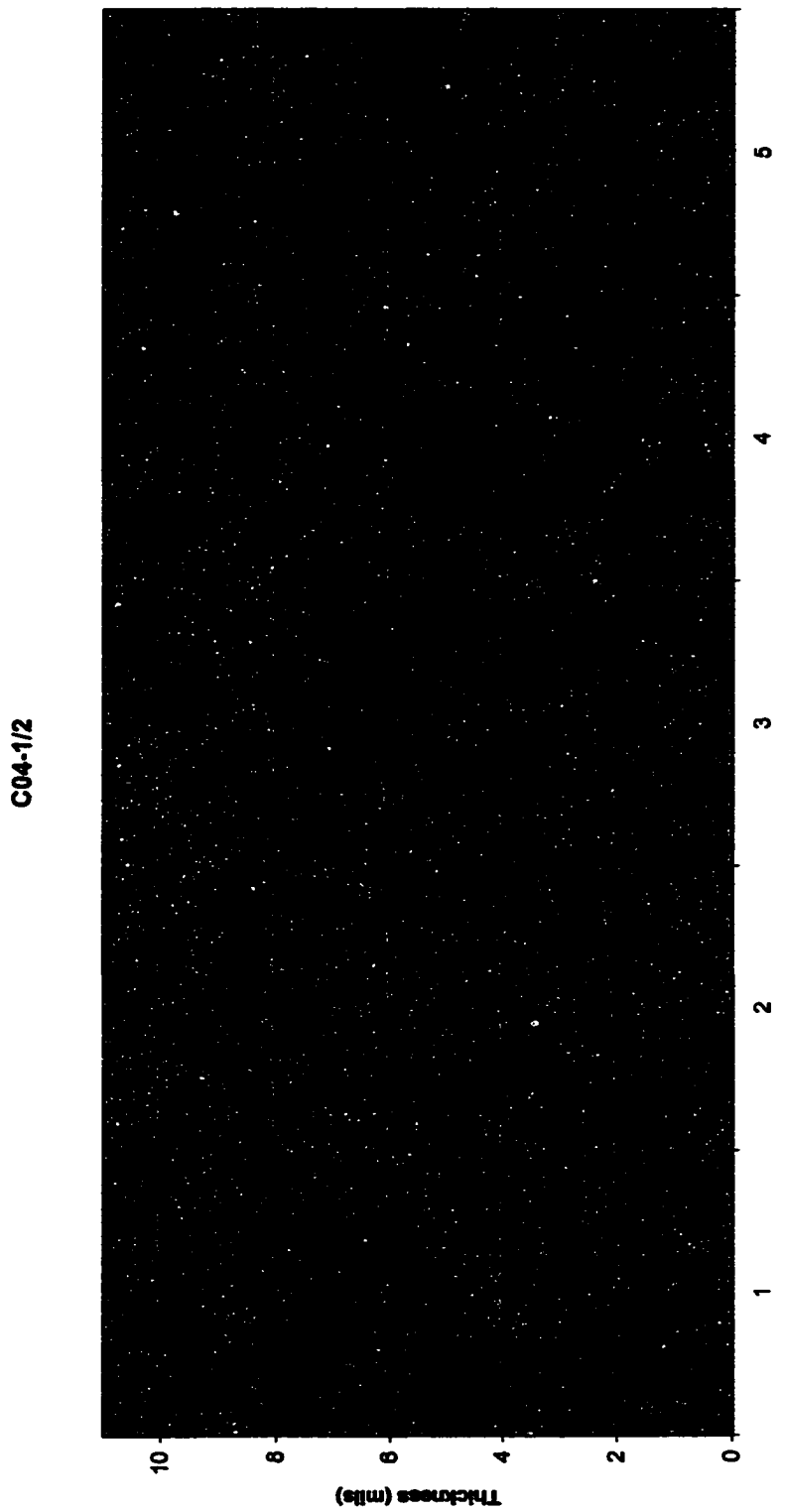

Figure A-24. Coating Thickness Profile of Conductor C at Location 04-1/2

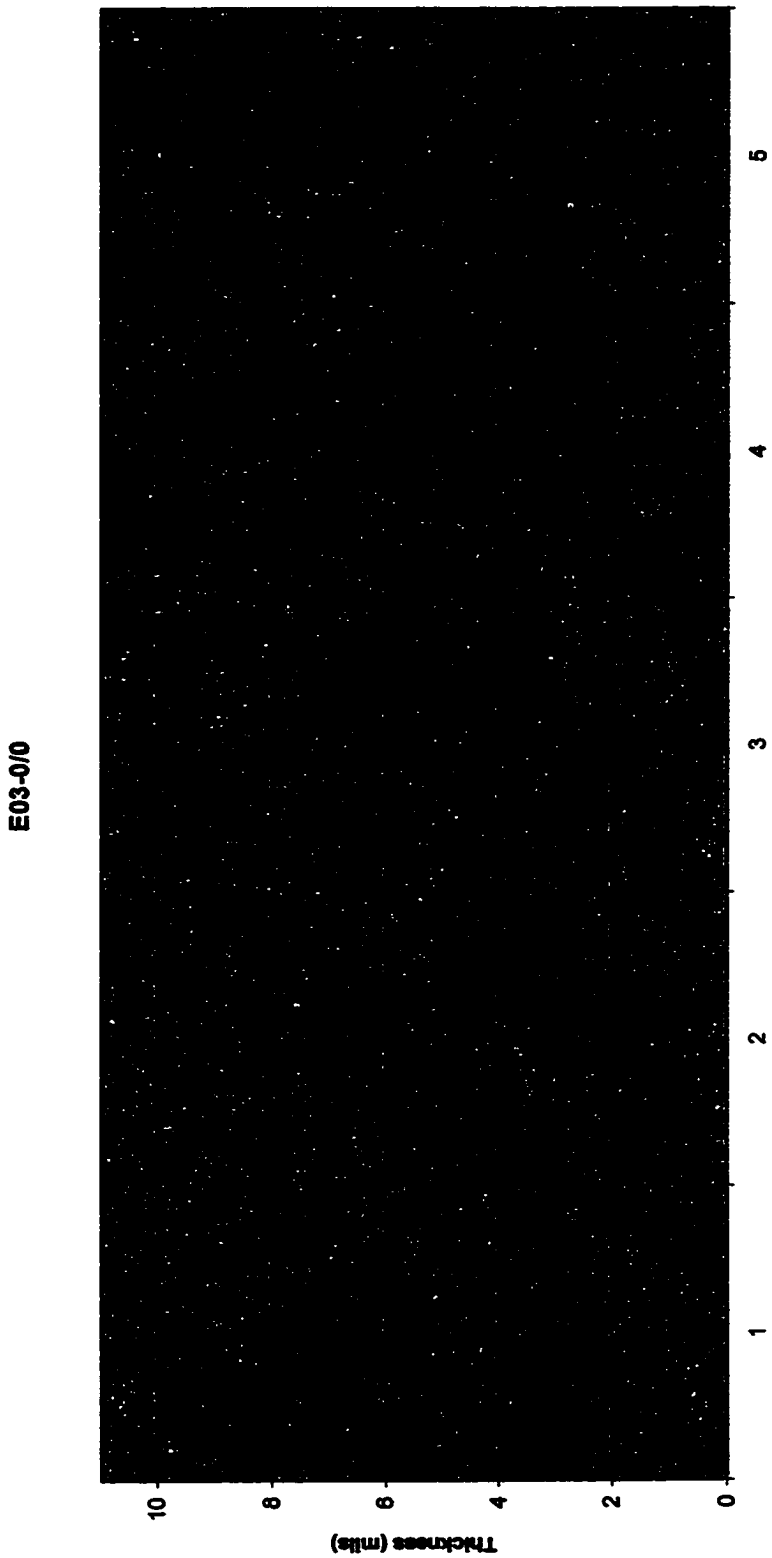

Figure A-25. Coating Thickness Profile of Conductor E at Location 03-0/0

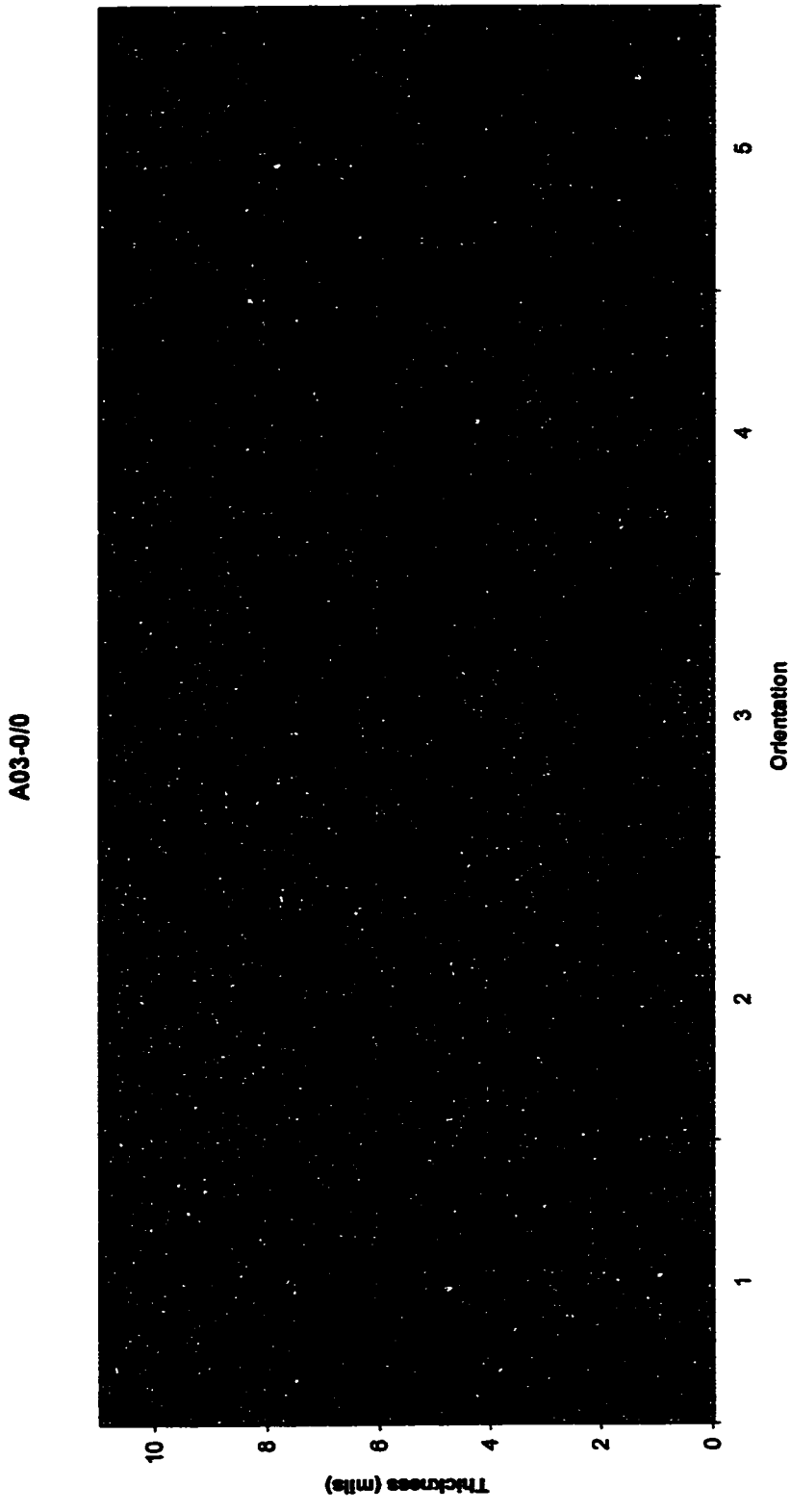

Figure A-26. Coating Thickness Profile of Conductor A at Location 03-0/0

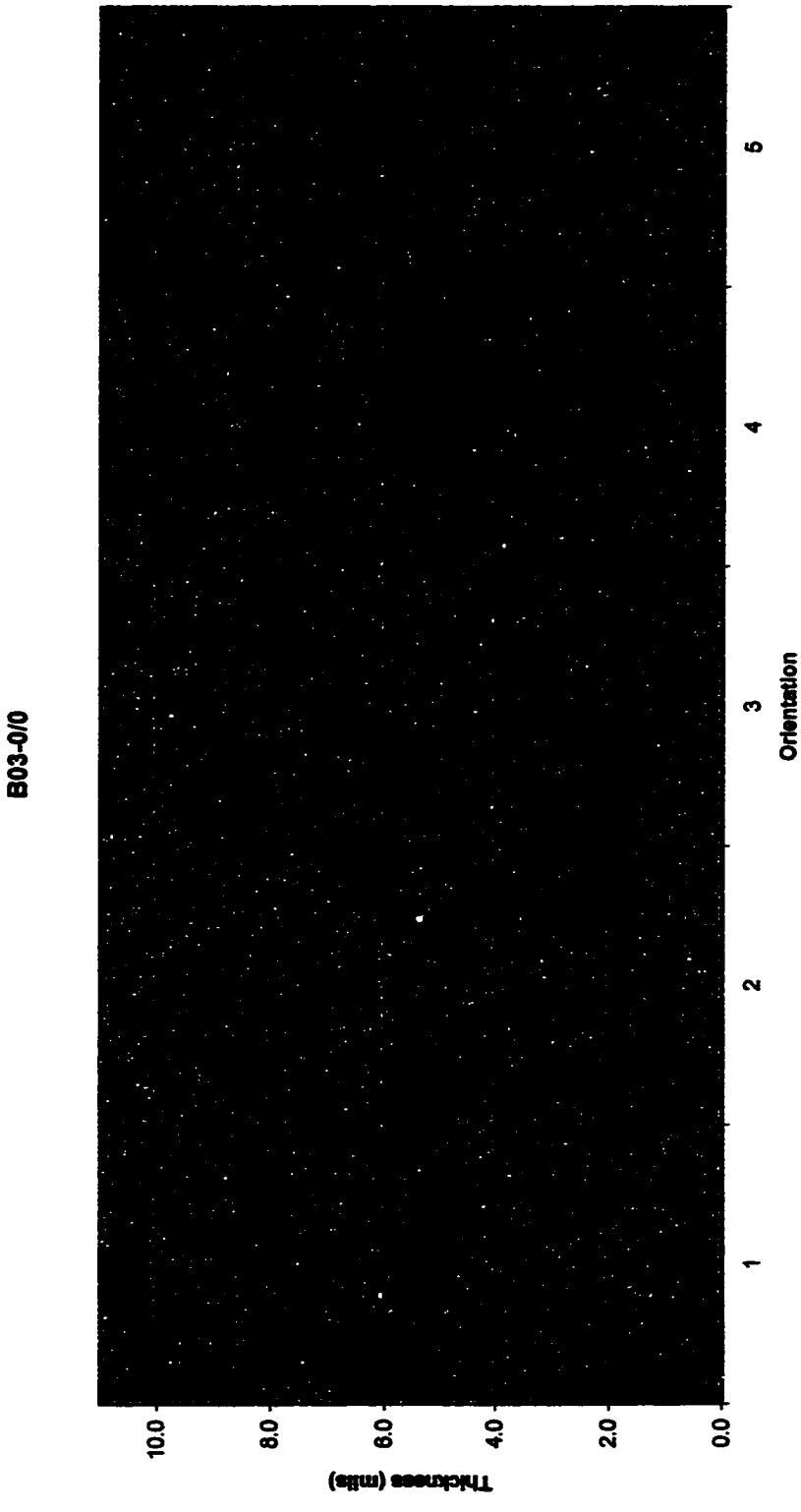

Figure A-27. Coating Thickness Profile of Conductor B at Location 03-0/0

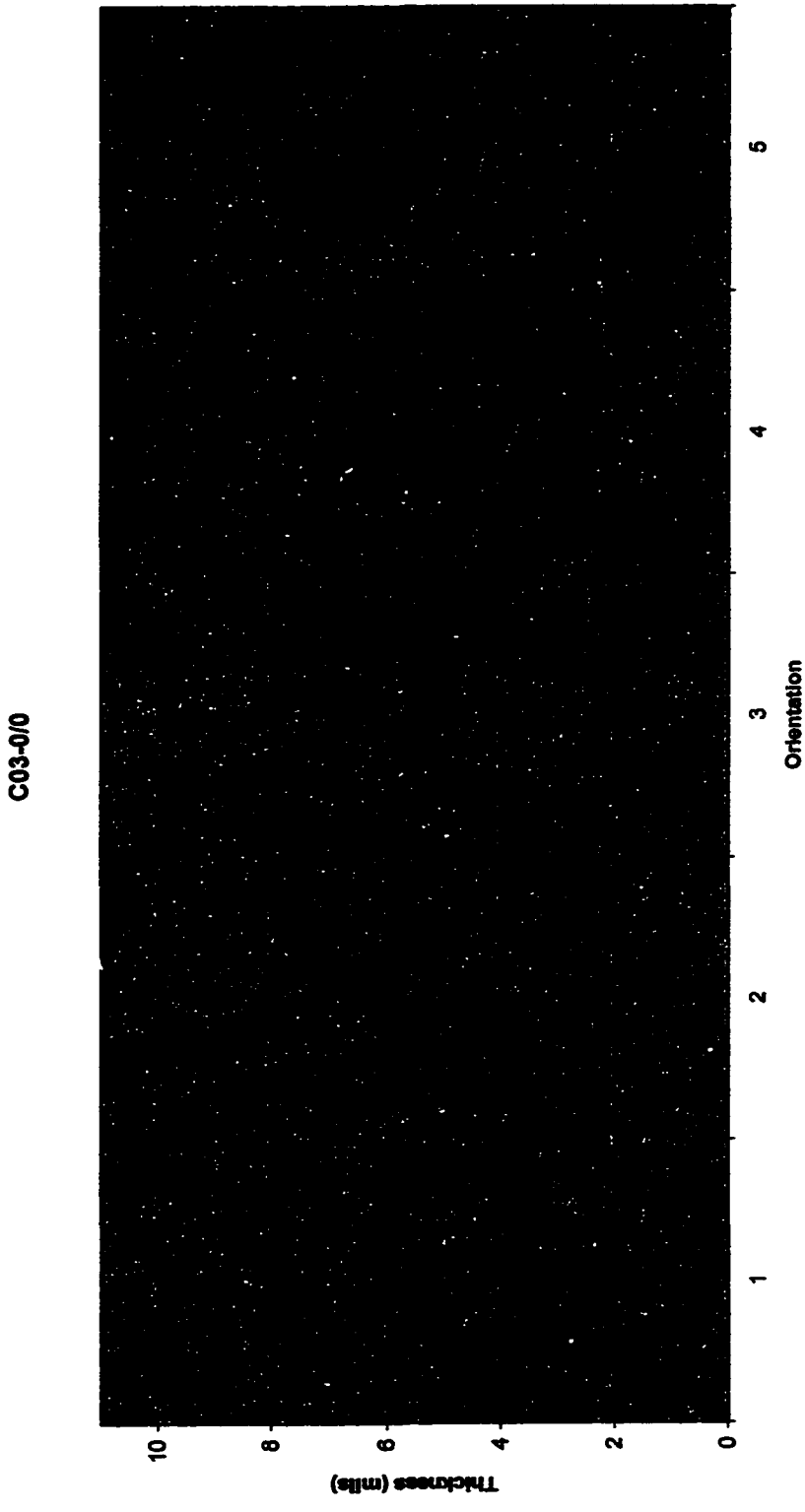

Figure A-28. Coating Thickness Profile of Conductor C at Location 03-0/0

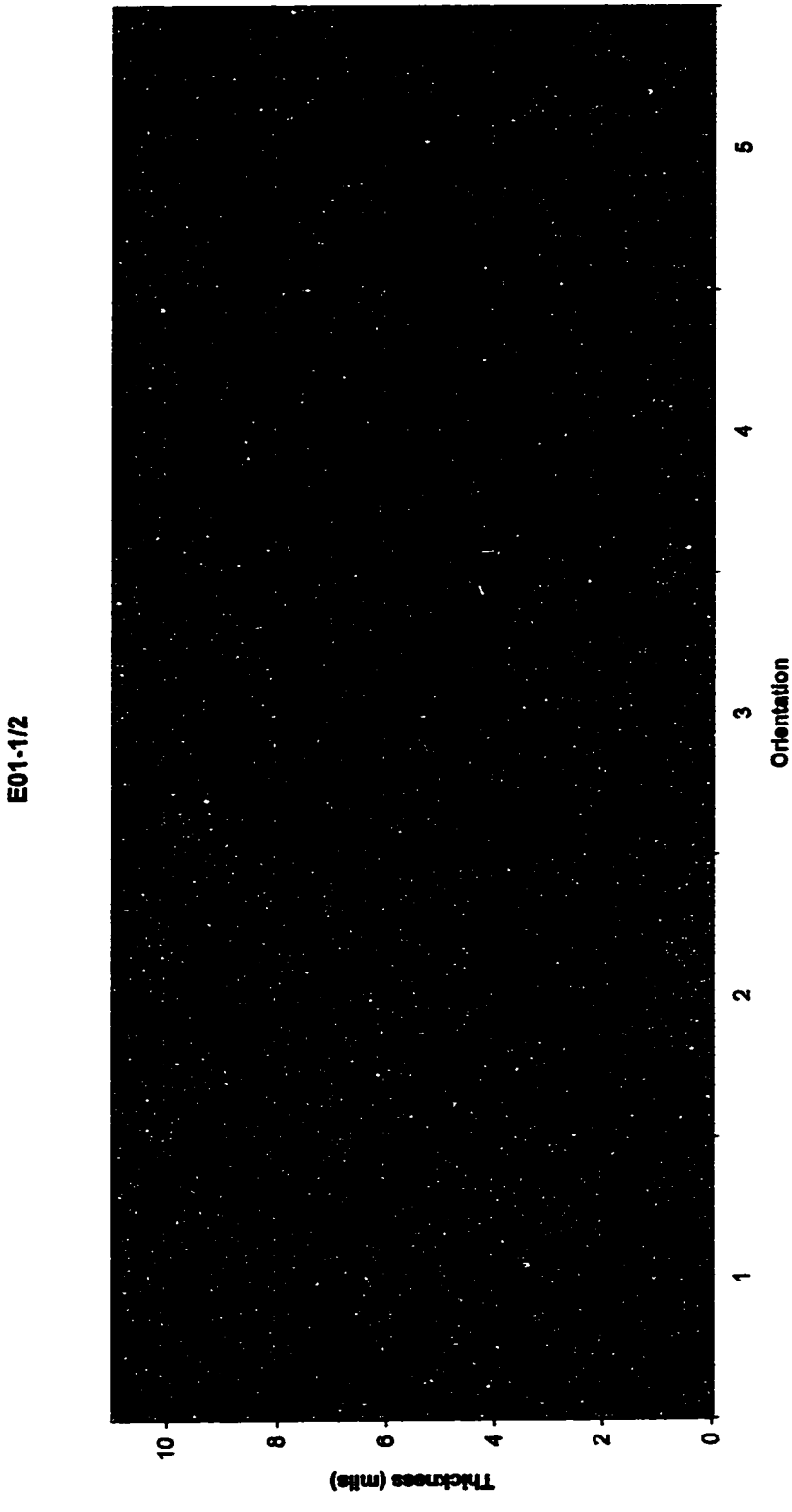

Figure A-29. Coating Thickness Profile of Conductor E at Location 01-1/2

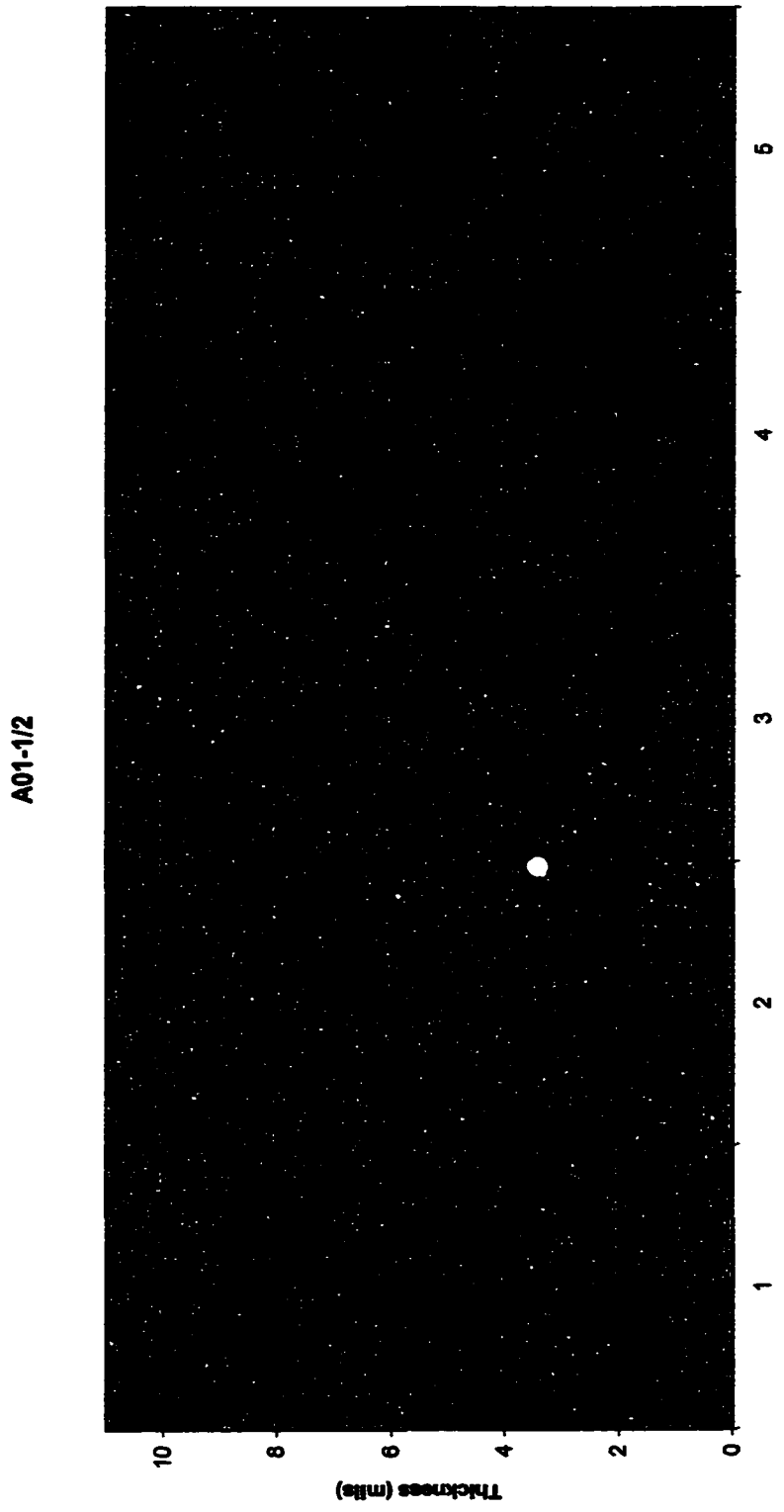

Figure A-30. Coating Thickness Profile of Conductor A at Location 01-1/2

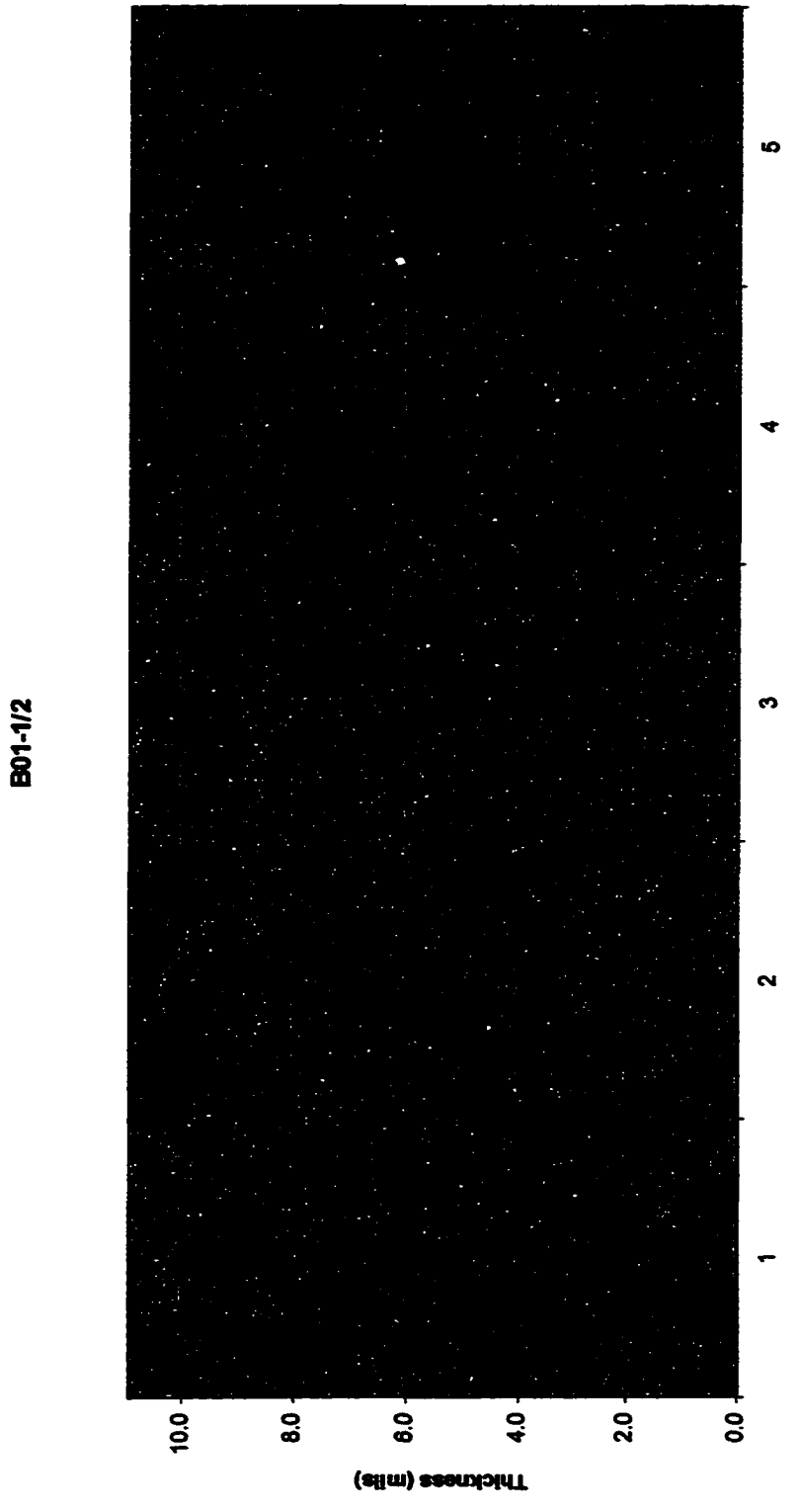

Figure A-31. Coating Thickness Profile of Conductor B at Location 01-1/2

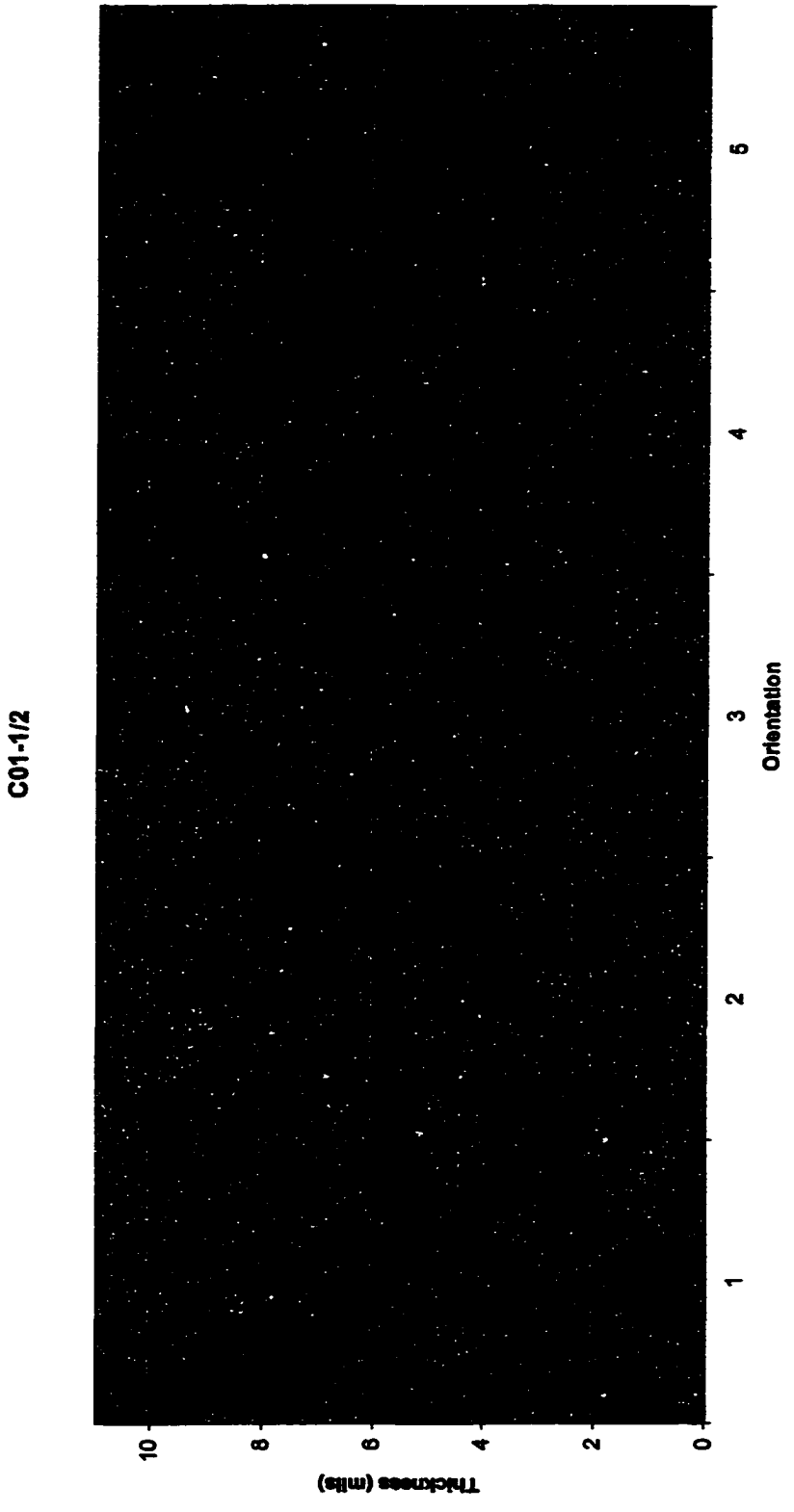

Figure A-32. Coating Thickness Profile of Conductor C at Location 01-1/2

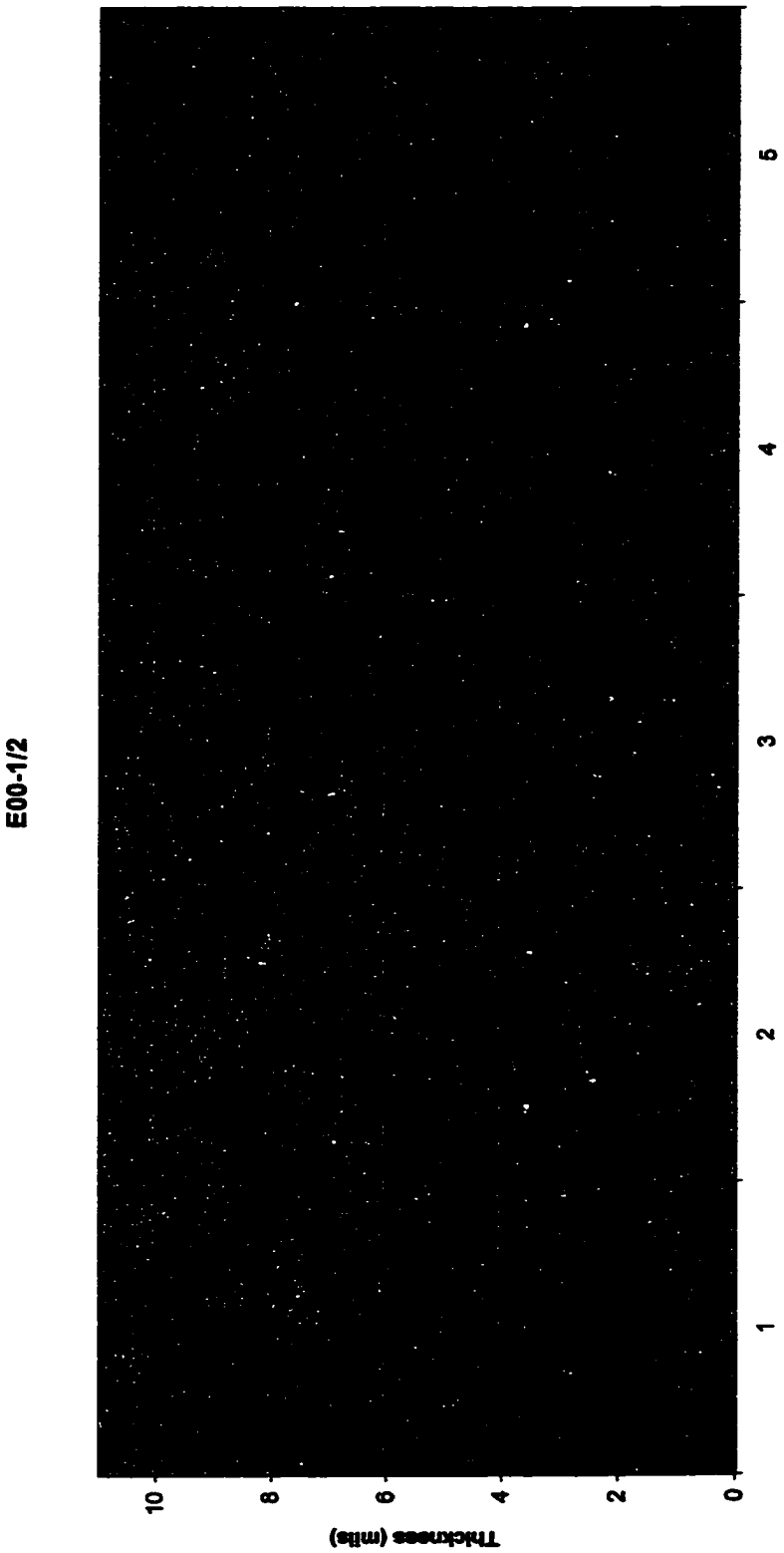

Figure A-33. Coating Thickness Profile of Conductor E at Location 00-1/2

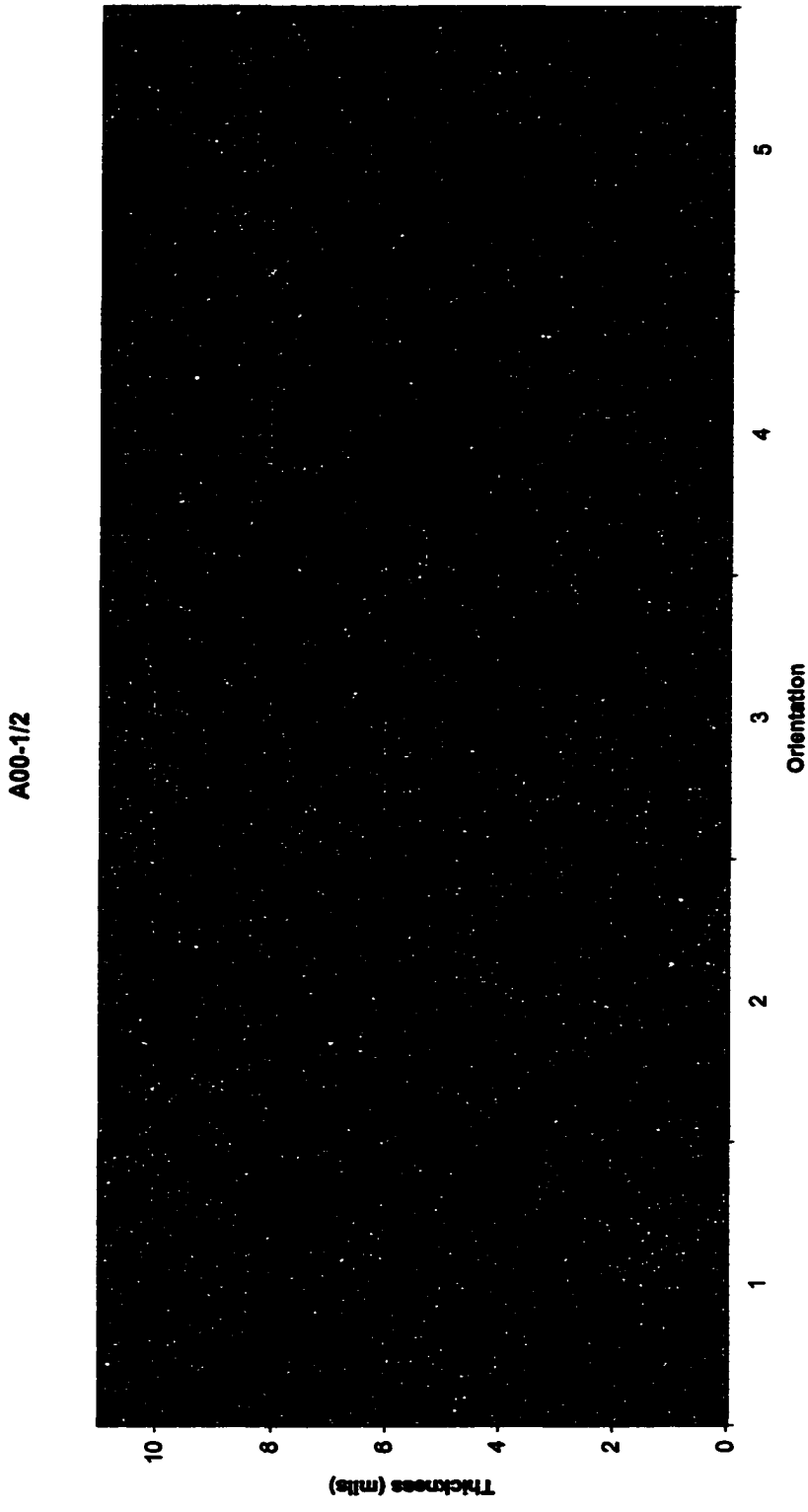

Figure A-34. Coating Thickness Profile of Conductor A at Location 00-1/2

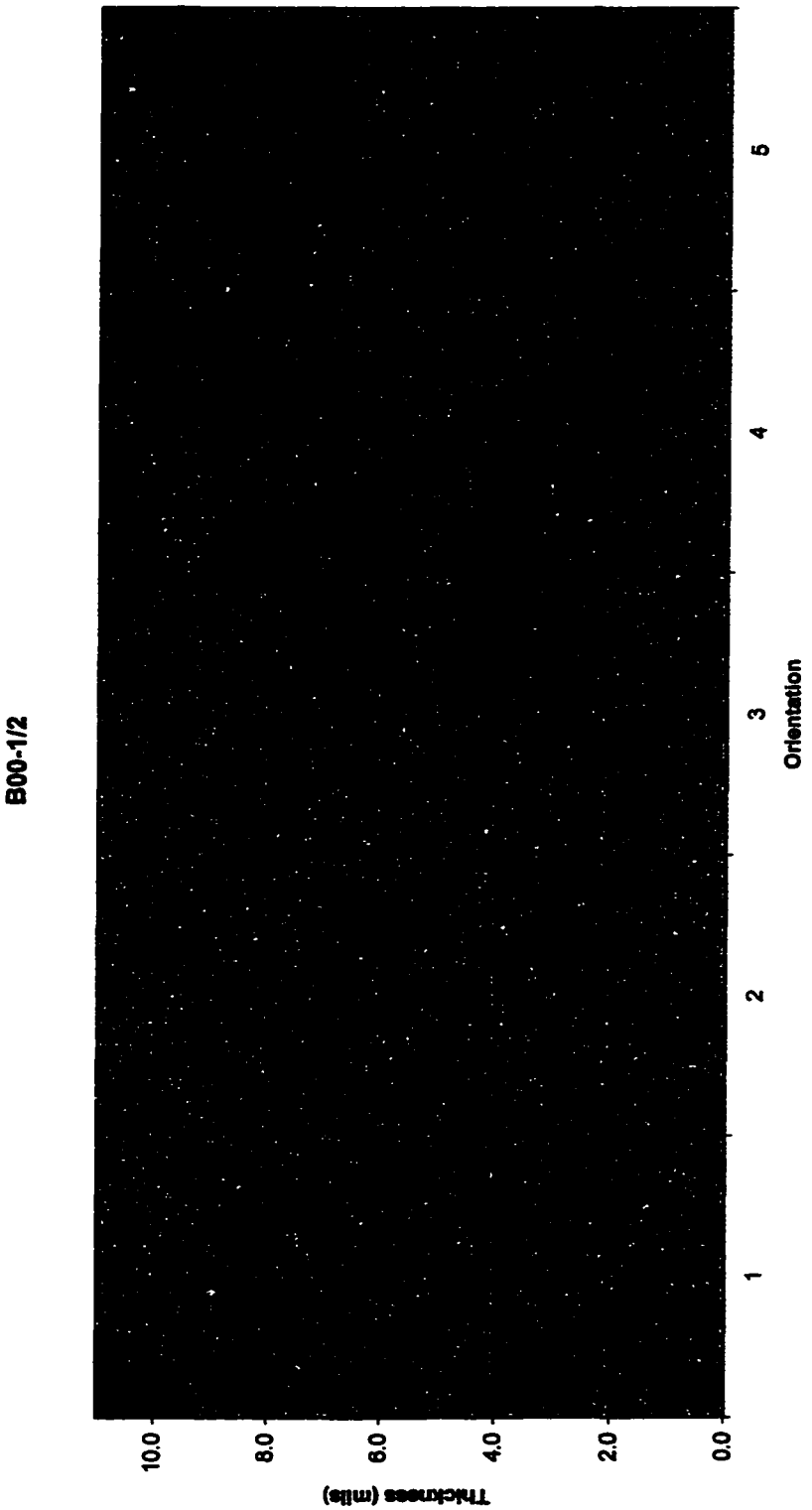

Figure A-35. Coating Thickness Profile of Conductor B at Location 00-1/2

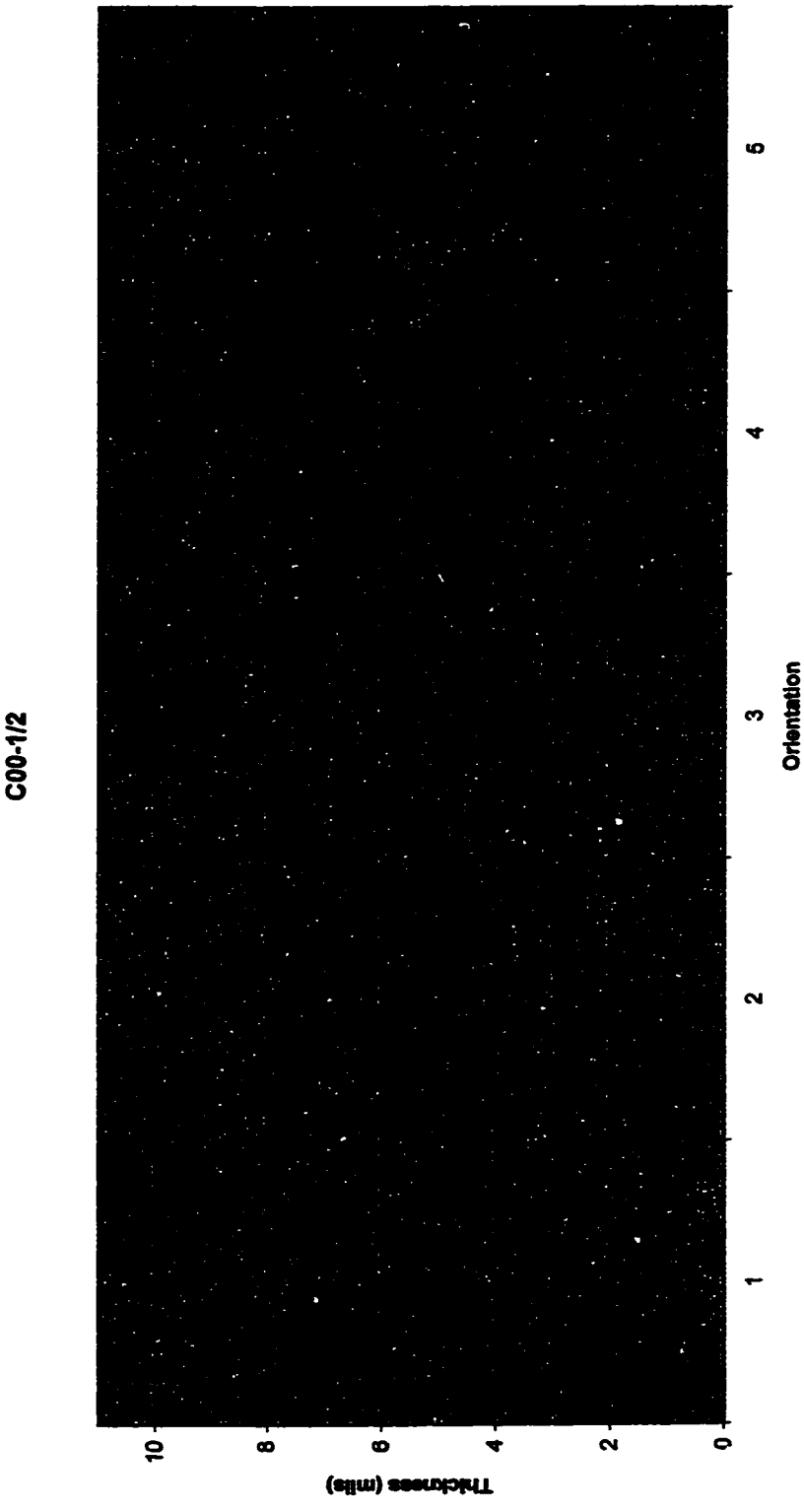

Figure A-36. Coating Thickness Profile of Conductor C at Location 00-1/2

Table A-1

Conductor Coating Thickness Data / Bushing 1.260 (1)
(mils / microns)

Degrees	0	90	180	270
Location				
12-1/2	1.1	0.8	1.2	1.8
	28	20	30	46
11-1/4	0.8	1.3	2.3	2.3
	20	33	58	58
09-3/4	1	1.8	2.3	1.8
	25	46	58	46
08-1/4	1.1	1.9	2.1	1.6
	28	48	53	41
06-3/4	1.5	1.9	2.6	1.6
	38	48	66	41
04-1/2	0.6	1.6	1.7	1.7
	15	41	43	43
03-0/0	0.9	1.8	2.3	1.4
	23	46	58	36
01-1/2	0.9	1.8	2.5	1.6
	23	46	64	41
00-1/2	1.4	2.2	2.5	1.9
	36	56	64	48

Mean (mils / microns) - 1.7 (42)
Standard Deviation (mils / microns) - 0.6 (15)

Table A-2

Conductor Coating Thickness Data / Bushing 1.260 (2)
(mils / microns)

Degrees	0	90	180	270
Location				
12-1/2	0.6	0.9	1.5	1
	15	23	38	25
11-1/4	1.6	1.5	2	2.2
	41	38	51	56
09-3/4	1.6	1.5	2.1	2.7
	41	38	53	69
08-1/4	1.4	1.5	1.9	2.4
	36	38	48	61
06-3/4	2.2	2.1	2.2	2.7
	56	53	56	69
04-1/2	1.6	1.6	1.9	1.8
	41	41	48	46
03-0/0	1.9	1.6	1.8	2.2
	48	41	46	56
01-1/2	1.9	1.8	1.8	2
	48	46	46	51
00-1/2	2.4	2.2	2.5	2.3
	61	56	64	58

Mean (mils / microns) - 1.9 (47)
Standard Deviation (mils / microns) - 0.5 (13)

Table A-3

Conductor Coating Thickness Data / Bushing 1.260 (3)
(mils / microns)

Degrees	0	90	180	270
Location				
12-1/2	2.6	2.1	1.8	1.9
	66	53	46	48
11-1/4	1.7	1.7	1.7	1.6
	43	43	43	41
09-3/4	1.7	1.7	1.6	1.8
	43	43	41	46
08-1/4	1.7	1.7	1.6	1.7
	43	43	41	43
06-3/4	1.6	1.1	1.1	1.2
	41	28	28	30
04-1/2	2.1	1.8	1.7	2.2
	53	46	43	56
03-0/0	1.9	1.9	1.4	1.7
	48	48	36	43
01-1/2	2	1.9	1	1.1
	51	48	25	28
00-1/2	1.2	1.1	1.2	1.7
	30	28	30	43

Mean (mils / microns) - 1.7 (42)
Standard Deviation (mils / microns) - 0.4 (10)

Table A-4

Conductor Coating Thickness Data / Bushing 1.262 (1)
(mils / microns)

Degrees	0	90	180	270
Location				
12-1/2	1.7	2.2	2.2	1.7
	43	56	56	43
11-1/4	1.4	2.3	2.4	1.1
	36	58	61	28
09-3/4	1.5	2.4	2.3	1.5
	38	61	58	38
08-1/4	1.5	2.4	2.3	1.5
	38	61	58	38
06-3/4	1.7	2.2	2.2	1.6
	43	56	56	41
04-1/2	1.8	2.5	2.5	1.7
	46	64	64	43
03-0/0	1.9	1.9	2.2	2.2
	48	48	56	56
01-1/2	1.8	1.5	2.4	2.4
	46	38	61	61
00-1/2	1.9	1.8	2	2
	48	46	51	51

Mean (mils / microns) - 2.0 (50)
Standard Deviation (mils / microns) - 0.4 (10)

Table A-5

Conductor Coating Thickness Data / Bushing 1.262 (2)
(mils / microns)

Degrees	0	90	180	270
Location				
12-1/2	2.0	2.0	2.3	2.1
	51	51	58	53
11-1/4	3.7	1.7	0.5	2.0
	94	43	13	51
09-3/4	3.5	1.9	1.2	2.5
	89	48	30	64
08-1/4	3.6	1.9	1.2	2.6
	91	48	30	66
06-3/4	3.1	1.7	1.5	2.3
	79	43	38	58
04-1/2	3.0	1.6	1.2	2.6
	76	41	30	66
03-0/0	3.0	2.1	1.2	2.1
	76	53	30	53
01-1/2	2.8	2.2	1.8	2.6
	71	56	46	66
00-1/2	1.4	0.9	2.6	2.8
	36	23	66	71

Mean (mils / microns) - 2.1 (54)
Standard Deviation (mils / microns) - 0.8 (20)

Table A-6

Conductor Coating Thickness Data / Bushing 1.262 (3)
(mils / microns)

Degrees	0	90	180	270
Location				
12-1/2	2.8	2.1	0.9	2.7
	71	53	23	69
11-1/4	1.6	2.4	2.2	2.0
	41	61	56	51
09-3/4	2.1	2.3	2.1	2.5
	53	58	53	64
08-1/4	2.0	2.3	2.2	2.6
	51	58	56	66
06-3/4	2.2	2.3	2.0	2.4
	56	58	51	61
04-1/2	2.2	1.9	2.1	2.9
	56	48	53	74
03-0/0	1.9	1.5	2.2	3.1
	48	38	56	79
01-1/2	1.8	2.2	2.5	2.5
	46	56	64	64
00-1/2	2.3	2.7	2.1	2.3
	58	69	53	58

Mean (mils / microns) - 2.2 (56)
Standard Deviation (mils / microns) - 0.4 (10)

Table A-7

Conductor Coating Thickness Data / Bushing 1.264 (1)
(mils / microns)

Degrees	0	90	180	270
Location				
12-1/2	2.2	3.0	2.8	2.1
	56	76	71	53
11-1/4	1.0	2.4	2.8	2.0
	25	61	71	51
09-3/4	1.9	2.5	2.6	2.5
	48	64	66	64
08-1/4	2.0	2.6	2.6	2.5
	51	66	66	64
06-3/4	2.1	2.6	2.7	2.5
	53	66	69	64
04-1/2	1.9	2.4	2.7	2.7
	48	61	69	69
03-0/0	1.9	2.4	3.2	2.7
	48	61	81	69
01-1/2	2.3	3.3	3.0	2.1
	58	84	76	53
00-1/2	2.8	3.4	2.6	2.2
	71	86	66	56

Mean (mils / microns) - 2.5 (63)
Standard Deviation (mils / microns) - 0.5 (13)

Table A-8

Conductor Coating Thickness Data / Bushing 1.264 (2)
(mils / microns)

Degrees	0	90	180	270
Location				
12-1/2	2.8	2.9	2.4	2.5
	71	74	61	64
11-1/4	2.3	2.4	2.3	2.5
	58	61	58	64
09-3/4	2.5	2.5	2.1	2.5
	64	64	53	64
08-1/4	2.6	2.6	2.2	2.7
	66	66	56	69
06-3/4	2.6	2.7	2.2	2.6
	66	69	56	66
04-1/2	2.3	2.6	2.4	2.5
	58	66	61	64
03-0/0	2.2	3.1	2.8	2.0
	56	79	71	51
01-1/2	3.0	2.9	2.2	2.5
	76	74	56	64
00-1/2	2.8	2.4	2.4	3.1
	71	61	61	79

Mean (mils / microns) - 2.5 (63)
Standard Deviation (mils / microns) - 0.3 (8)

Table A-9

Conductor Coating Thickness Data / Bushing 1.264 (3)
(mils / microns)

Degrees	0	90	180	270
Location				
12-1/2	2.5	2.9	2.4	2.0
	64	74	61	51
11-1/4	2.3	1.2	2.7	3.6
	58	30	69	91
09-3/4	2.4	2.5	2.7	2.5
	61	64	69	64
08-1/4	2.4	2.4	2.6	2.4
	61	61	66	61
06-3/4	2.5	2.9	2.5	2.4
	64	74	64	61
04-1/2	2.8	2.3	2.5	2.9
	71	58	64	74
03-0/0	3.0	1.5	2.2	3.7
	76	38	56	94
01-1/2	2.5	2.5	2.8	2.9
	64	64	71	74
00-1/2	2.9	2.6	2.3	2.6
	74	66	58	66

Mean (mils / microns) - 2.6 (65)
Standard Deviation (mils / microns) - 0.5 (13)

Table A-10

Conductor Coating Thickness Data / Bushing 1.266 (1)
(mils / microns)

Degrees	0	90	180	270
Location				
12-1/2	3.1	3.5	3.4	2.7
	79	89	86	69
11-1/4	2.1	2.7	3.6	2.5
	53	69	91	64
09-3/4	2.5	2.8	3.4	2.6
	64	71	86	66
08-1/4	2.6	2.8	3.2	2.8
	66	71	81	71
06-3/4	2.7	2.8	3.1	2.8
	69	71	79	71
04-1/2	2.9	3.1	3.4	2.6
	74	79	86	66
03-0/0	2.9	3.3	3.3	2.4
	74	84	84	61
01-1/2	3.2	2.5	3.0	3.2
	81	64	76	81
00-1/2	2.7	2.0	3.6	4.0
	69	51	91	102

Mean (mils / microns) - 2.9 (75)
Standard Deviation (mils / microns) - 0.4 (10)

Table A-11

Conductor Coating Thickness Data / Bushing 1.266 (2)
(mils / microns)

Degrees	0	90	180	270
Location				
12-1/2	4.2	2.8	2.3	3.5
	107	71	58	89
11-1/4	3.7	3.5	1.9	2.2
	94	89	48	56
09-3/4	3.4	3.7	2.4	2.7
	86	94	61	69
08-1/4	3.3	3.6	2.7	2.8
	84	91	69	71
06-3/4	3.2	3.7	2.9	2.8
	81	94	74	71
04-1/2	3.7	3.4	2.6	3.0
	94	86	66	76
03-0/0	4.1	3.4	2.0	3.2
	104	86	51	81
01-1/2	3.3	3.7	3.4	3.1
	84	94	86	79
00-1/2	2.0	4.2	4.5	2.3
	51	107	114	58

Mean (mils / microns) - 3.1 (80)
Standard Deviation (mils / microns) - 0.7 (18)

Table A-12

Conductor Coating Thickness Data / Bushing 1.266 (3)
(mils / microns)

Degrees	0	90	180	270
Location				
12-1/2	2.7	2.9	3.1	3.2
	69	74	79	81
11-1/4	3.0	3.2	2.5	2.2
	76	81	64	56
09-3/4	2.7	2.8	2.7	2.8
	69	71	69	71
08-1/4	2.7	2.8	2.4	2.8
	69	71	61	71
06-3/4	2.5	2.8	2.7	2.9
	64	71	69	74
04-1/2	2.5	3.1	2.8	2.5
	64	79	71	64
03-0/0	2.5	3.1	2.4	2.6
	64	79	61	66
01-1/2	3.1	2.9	2.8	3.0
	79	74	71	76
00-1/2	4.1	2.5	1.7	3.5
	104	64	43	89

Mean (mils / microns) - 2.8 (71)
Standard Deviation (mils / microns) - 0.4 (10)

Table A-13

Conductor Coating Thickness Data / Bushing 1.268 (1)
(mils / microns)

Degrees	0	90	180	270
Location				
12-1/2	2.8	3.2	3.7	3.1
	71	81	94	79
11-1/4	1.5	3.2	4.8	3.3
	38	81	122	84
09-3/4	1.7	2.9	4.1	3.5
	43	74	104	89
08-1/4	2.0	2.6	4.0	3.1
	51	66	102	79
06-3/4	3.1	3.0	3.5	3.4
	79	76	89	86
04-1/2	2.6	2.7	3.2	3.2
	66	69	81	81
03-0/0	3.1	2.5	2.8	3.2
	79	64	71	81
01-1/2	3.2	1.6	2.2	4.0
	81	41	56	102
00-1/2	2.7	3.8	3.7	2.8
	69	97	94	71

Mean (mils / microns) - 3.0 (77)
Standard Deviation (mils / microns) - 0.7 (18)

Table A-14

Conductor Coating Thickness Data / Bushing 1.268 (2)
(mils / microns)

Degrees	0	90	180	270
Location				
12-1/2	3.8	1.2	2.7	5.1
	97	30	69	130
11-1/4	4.4	1.8	2.1	5.0
	112	46	53	127
09-3/4	3.6	2.2	3.3	4.5
	91	56	84	114
08-1/4	3.3	1.9	3.1	3.6
	84	48	79	91
06-3/4	3.3	3.6	3.5	2.7
	84	91	89	69
04-1/2	3.3	2.9	2.9	3.2
	84	74	74	81
03-0/0	3.3	2.6	2.9	3.3
	84	66	74	84
01-1/2	3.2	2.6	3.1	4.3
	81	66	79	109
00-1/2	3.8	3.9	3.1	3.0
	97	99	79	76

Mean (mils / microns) - 3.2 (82)
Standard Deviation (mils / microns) - 0.8 (20)

Table A-15

Conductor Coating Thickness Data / Bushing 1.268 (3)
(mils / microns)

Degrees	0	90	180	270
Location				
12-1/2	3.2	3.8	3.5	3.0
	81	97	89	76
11-1/4	2.6	3.3	3.8	2.7
	66	84	97	69
09-3/4	3.3	3.6	3.3	2.8
	84	91	84	71
08-1/4	3.2	3.5	3.3	2.8
	81	89	84	71
06-3/4	3.2	3.8	3.2	2.5
	81	97	81	64
04-1/2	3.4	3.4	2.9	2.8
	86	86	74	71
03-0/0	4.0	3.8	3.1	2.8
	102	97	79	71
01-1/2	5.1	4.3	2.5	3.1
	130	109	64	79
00-1/2	4.9	4.9	2.0	1.9
	124	124	51	48

Mean (mils / microns) - 3.3 (84)
Standard Deviation (mils / microns) - 0.7 (18)

APPENDIX B

THERMAL CHAMBER TEST DATA

Although Chapter 3 gives the overall process and results of the thermal shock tests, it does not fully describe the thermal chamber cycles. The thermal tests were run over a period of three weeks with cycles being run on various dates. A total of nine bushings were formed with non-coated conductors. The seven 1201-625B2 bushings were designated NC (1), (2), (3), (4), (5), (6), (7) and the two 1203-1225B2 bushings were designated NCC (1), (2). Three bushings each were formed with conductors coated by sleeves 1.260, 1.262, 1.264, 1.266, and 1.268. They were designated 1.260 (1), (2), (3); 1.262 (1), (2), (3); 1.264 (1), (2), (3); 1.266 (1), (2), (3); and 1.268 (1), (2), (3).

The tables contained in this appendix give the actual time requirements for each temperature change during the cycles. The amount of time each test load of bushings was required to remain at a certain temperature was maintained at one hour throughout the tests. The amount of time required to change from one test temperature to another varied mainly with the number of bushings in the chamber and the need to change the liquid nitrogen bottles after they were depleted.

In addition to cycle time data, the bushings involved in each cycle and other pertinent data are given below each table.

Table B-1

Thermal Cycle Data Collected August 10, 1998

	BEGIN	END	ELAPSED TIME (minutes)
Start	8:08 AM	8:42AM	34
@ 250°F (121.1°C)	8:42AM	9:42AM	60
Cool	9:42AM	10:23AM	41
@ –50°F (-45.6°C)	10:23AM	11:23AM	60
Heat	11:23AM	11:55AM	32
@ 250°F (121.1°C)	11:55AM	12:55PM	60
Cool	1:16PM	2:00PM	44
@ - 100°F (-73.3°C)	2:00PM	3:00PM	60
Heat	3:00PM	3:40PM	40
@ 250°F (121.1°C)	3:40PM	4:40PM	60

Bushings Tested:

NC (1), (2), (3)
1.260 (1), (2), (3)
1.262 (1), (2), (3)
1.264 (1), (2), (3)
1.266 (1), (2), (3)
1.268 (1), (2), (3)

Table B-2

Thermal Cycle Data Collected August 11, 1998

	BEGIN	END	ELAPSED TIME (minutes)
Start	7:23AM	7:28AM	5
@ 250°F (121.1°C)	7:28AM	9:20AM	112
Cool	9:20AM	10:30AM	70
@ - 150°F (-101.1°C)	10:30AM	11:30AM	60
Heat	11:30AM	12:30PM	60
@ 250°F (121.1°C)	12:30PM	1:30PM	60

Bushings Tested:

NC (1), (2), (3)
1.260 (1), (2), (3)
1.262 (1), (2), (3)
1.264 (1), (2), (3)
1.266 (1), (2), (3)
1.268 (1), (2), (3)

Table B-3

Thermal Cycle Data Collected August 12, 1998

	BEGIN	END	ELAPSED TIME (minutes)
Start	8:15AM	8:20AM	5
@ 250°F (121.1°C)	8:20AM	9:30AM	70
Cool	9:30AM	9:54AM	24
@ - 100°F (-73.3°C)	9:54AM	10:54AM	60
Heat	10:54AM	11:18AM	24
@ 250°F (121.1°C)	11:18AM	12:18PM	60
Cool	12:23PM	12:55PM	32
@ - 150°F (-101.1°C)	12:55PM	1:55PM	60
Heat	1:55PM	2:23PM	28
@ 250°F (121.1°C)	2:23PM	3:23PM	60

Bushings Tested:

NC (3)
1.260 (1)
1.262 (1)
1.264 (1)
1.266 (3)
1.268 (1)

Table B-4

Thermal Cycle Data Collected August 13, 1998

	BEGIN	END	ELAPSED TIME (minutes)
Start	8:05AM	8:10AM	5
@ 250°F (121.1°C)	8:10AM	9:10AM	60
Cool	9:10AM	9:47AM	37
@ - 200°F (-128.9°C)	9:47AM	10:47AM*	60
Heat	10:47AM	11:08AM	21
@ 250°F (121.1°C)	11:08AM	12:08PM	60
Cool	12:12PM	1:05PM	53
@ - 250°F (-156.7°C)	1:05PM	2:05PM	60
Heat	2:05PM	2:37PM	32
@ 250°F (121.1°C)	2:37PM	3:37PM	60

Bushings Tested:

NC (3)
1.260 (1)
1.262 (1)
1.264 (1)
1.266 (3)
1.268 (1)

Table B-5

Thermal Cycle Data Collected August 14, 1998

	BEGIN	END	ELAPSED TIME (minutes)
Start	8:40AM	8:47AM	7
@ 250°F (121.1°C)	8:47AM	9:47AM	60
Cool	9:47AM	11:45AM*	118
@ - 300°F (-184.4°C)	11:45AM	12:45PM	60
Heat	12:45PM	1:15PM	30
@ 250°F (121.1°C)	1:15PM	2:15PM	60

Bushings Tested:

NC (3)
1.260 (1)
1.262 (1)
1.264 (1)
1.266 (3)
1.268 (1)

Table B-6

Thermal Cycle Data Collected August 18, 1998

	BEGIN	END	ELAPSED TIME (minutes)
Start	8:52AM	9:00AM	8
@ 250°F (121.1°C)	9:00AM	10:00AM	60
Cool	10:00AM	10:23AM	23
@ –50°F (-45.6°C)	10:23AM	11:23AM	60
Heat	11:23AM	11:47AM	24
@ 250°F (121.1°C)	11:47AM	12:47PM	60
Cool	12:53PM	1:25PM	33
@ - 100°F (-73.3°C)	1:25PM	2:40PM	75
Heat	2:40PM	3:08PM	28
@ 250°F (121.1°C)	3:08PM	4:08PM	60

Bushings Tested:

NC (1), (2), (3), (4), (5), (6), (7)
NCC (1), (2)

Bushing NCC (1) cracked during the - 100°F (-73.3°C) cycle and was removed from the chamber.

Table B-7

Thermal Cycle Data Collected August 19, 1998

	BEGIN	END	ELAPSED TIME (minutes)
Start	8:37AM	8:43AM	6
@ 250°F (121.1°C)	8:43AM	9:43AM	60
Cool	9:43AM	10:23AM	40
@ - 150°F (-101.1°C)	10:23AM	11:23AM	60
Heat	11:23AM	11:50AM	27
@ 250°F (121.1°C)	11:50AM	12:50PM	60

Bushings Tested:

NC (1), (2), (3), (4), (5), (6), (7)
NCC (2)

Table B-8

Thermal Cycle Data Collected August 20, 1998

	BEGIN	END	ELAPSED TIME (minutes)
Start	8:49AM	8:56AM	7
@ 250°F (121.1°C)	8:56AM	9:56AM	60
Cool	9:56AM	10:47AM	51
@ - 200°F (-128.9°C)	10:47AM	11:47AM	60
Heat	11:47AM	12:21PM	34
@ 250°F (121.1°C)	12:21PM	1:31PM	70

Bushings Tested:

NC (1), (2), (3), (4), (5), (6), (7)
NCC (2)

Table B-9

Thermal Cycle Data Collected August 21, 1998

	BEGIN	END	ELAPSED TIME (minutes)
Start	8:08AM	8:16AM	8
@ 250°F (121.1°C)	8:16AM	9:16AM	60
Cool	9:16AM	10:08AM	52
@ - 250°F (-156.7°C)	10:08AM	11:08AM	60
Heat	11:08AM	11:40AM	32
@ 250°F (121.1°C)	11:40AM	12:40PM	60
Cool	12:45PM	2:10PM	85
@ - 300°F (-184.4°C)	2:10PM	3:10PM	60
Heat	3:10PM	3:50	40
@ 250°F (121.1°C)	3:50PM	4:50PM	60

Bushings Tested:

NC (1), (2), (3), (4), (5), (6), (7)
NCC (2)

Bushings NC (2) and NC (7) cracked during the - 250°F (-156.7°C) cycle. Bushing NC (5) cracked during the - 300°F (-184.4°C) cycle. No further tests were run on bushings with non-coated conductors.

Table B-10

Thermal Cycle Data Collected August 25, 1998

	BEGIN	END	ELAPSED TIME (minutes)
Start	8:20AM	8:28AM	8
@ 250°F (121.1°C)	8:28AM	9:31AM	63
Cool	9:31AM	10:33AM	62
@ - 200°F (-128.9°C)	10:33AM	11:33AM	60
Heat	11:33AM	12:30AM	57
@ 250°F (121.1°C)	12:30PM	1:40PM	70

Bushings Tested:

1.260 (2), (3)
1.262 (2), (3)
1.264 (2), (3)
1.266 (1), (2)
1.268 (2), (3)

Table B-11

Thermal Cycle Data Collected August 26, 1998

	BEGIN	END	ELAPSED TIME (minutes)
Start	7:20AM	7:23AM	3
@ 250°F (121.1°C)	7:23AM	8:23AM	60
Cool	8:23AM	9:44AM	81
@ - 250°F (-156.7°C)	9:44AM	10:44AM	60
Heat	10:44AM	11:30AM	46
@ 250°F (121.1°C)	11:30AM	12:30PM	60
Cool	12:43PM	2:19PM	96
@ -300°F (-184.4°C)	2:19PM	3:19PM	60
Heat	3:19PM	4:40PM	81
@ 250°F (121.1°C)	4:40PM	5:40PM	60

Bushings Tested:

1.260 (2), (3)
1.262 (2), (3)
1.264 (2), (3)
1.266 (1), (2)
1.268 (2), (3)

After the tests run on this day, all bushings with coated conductors have passed the first -300°F (-184.4°C) cycle.

Table B-12

Thermal Cycle Data Collected August 27, 1998

	BEGIN	END	ELAPSED TIME (minutes)
Heat	10:30AM	10:40AM	10
@ 250°F (121.1°C)	10:40AM	11:40AM	60
Cool	11:40PM	1:40PM	120
@ -300°F (-184.4°C)	1:40PM	2:40PM	60
Heat	2:40PM	3:47PM	67
@ 250°F (121.1°C)	3:47PM	4:50PM	63

Bushings Tested:

1.260 (1), (2), (3)
1.262 (1), (2), (3)
1.264 (1), (2)
1.266 (1), (2)

This was the second –300°F (-184.4°C) cycle.

Table B-13

Thermal Cycle Data Collected September 3, 1998

	BEGIN	END	ELAPSED TIME (minutes)
Heat	8:35AM	8:45AM	10
@ 250°F (121.1°C)	8:45AM	9:45AM	60
Cool	9:45AM	12:20PM	155
@ -300°F (-184.4°C)	12:20PM	1:20PM	60
Heat	1:20PM	2:10PM	50
@ 250°F (121.1°C)	2:10PM	3:10PM	60

Bushings Tested:

1.260 (1), (2), (3)
1.262 (1), (2), (3)
1.264 (1), (2)
1.266 (1), (2)

This was the final –300°F (-184.4°C) cycle.

BIBLIOGRAPHY

1. ANSYS 5.4 Users Manuel. 1994. Swanson Analysis Systems. Houston, PA.

2. Boresi, Aurthur, and Omar Sidebottom.1985. Advanced Mechanics of Materials. 4th ed. New York: John Wiley and Sons.

3. Cylimold™ Liquid Injection Molding System.1984. Union Carbide Corporation Specialty Polymers and Composites Division. Product Data Bulletin F-50006. Danbury, CT.

4. Degarmo, Paul, J. Temple Black, and Ronald A. Kosher. 1984. Materials and Processes in Manufacturing. 6th ed. New York: McMillian Publishers.

5. Dieter, George. 1986. Mechanical Metallurgy. 3d ed. New York: McGraw Hill.

6. Dowling, Norman. 1999. Mechanical Behavior of Materials. 2d ed. New Jersey: Prentice Hall.

7. Elliott III, Kenneth C. 1986.Thermal Shock Induced Failures of Cycloaliphatic Epoxy Apparatus Bushings. Elliott Molding and Components Division. Elliott Industries. Bossier City, LA.

8. Elliott Molding and Components Product Catalog. 1984. Bossier City, LA

9. Fitzgerald, Robert. 1982. Mechanics of Materials. 2d ed. Massachusetts: Addison Wesley

10. High Performance Cycloaliphatic Epoxide Systems for Electrical Apparatus.1989. Union Carbide Solvents and Coatings Materials Division. Bound Brook, NJ.

11. Insulation Systems - Epoxy versus Porcelain.1975. Product Data Bulletin D-382. Square-D Corporation. Middleton, OH.

12. Logan, Daryl. 1989. Mechanics of Materials. New York: Harper-Collins

13. Separable Insulated Connector Systems for Power Distribution Systems Above 600V. 1985. ANSI / IEEE Std - 386-1985

14. Shigley, Joseph, and Larry Mitchell. 1983. Mechanical Engineering Design. 4th ed. New York: McGraw Hill.

15. "Stabil Therm LN2 Constant Temperature Environmental Chamber". 1984. Product Data Sheet Blue-M Corporation, Blue Island, IL.

16. Van Vlack, Lawrence. 1982. Materials for Engineering. Massachusetts: Addison Wesley.

17. Yamazaki, T, and Nobumits Kobayashi. 1979. Thermal Fatigue Strength of Epoxy Supporting Insulators with Embedded Electrodes. IEEE Transactions on Power Apparatus and Systems, Vol. PAS-104, No. 107, (July): 1910 - 1915.

IMAGE EVALUATION TEST TARGET (QA-3)

150mm

6"

APPLIED IMAGE . Inc
1653 East Main Street
Rochester, NY 14609 USA
Phone: 716/482-0300
Fax: 716/288-5989